SUPPLEMENTARY INFORMATION

Few Layer Phoshorene/Reduced Graphene Oxide/Graphitic Carbon Nitride Ternary Heterojunctions for Sustainable Photoredox C–H Functionalization of Heteroarenes

Zafer Eroglu[a,d#], Ozge Turbedaroglu[b#], Temirlan Kubanaliev[a], Sila Alemdar[a], Haydar Kilic[b*], Onder Metin[a,c*]

[a]*Department of Chemistry, College of Sciences, Koç University, 34450 Sarıyer, İstanbul, Türkiye*

[b]*Department of Chemistry, Faculty of Sciences, Atatürk University, 25240, Erzurum, Türkiye*

[c]*Koç University Surface Science and Technology Center (KUYTAM), 34450 Sarıyer, İstanbul, Türkiye*

[d] *Kocaeli University, Faculty of Arts and Sciences, Department of Chemistry, 41001, Kocaeli, Türkiye*

[#]The authors contributed equally to this work.

*To whom should be corresponded: Prof. Onder Metin; e-mail: ometin@ku.edu.tr;
Prof. Haydar Kilic; e-mail: hydk@atauni.edu.tr

1. Materials and Materials Characterizations

Materials

Red phosphorus (98.9%), tin (99.5%), and tin(IV) iodide (95%) were obtained from Alfa Aesar. Sigma-Aldrich supplied urea, thiophene (99%), furan (99%), tert-butyl nitrite (t-BuONO, 90%), tetrafluoroboric acid (HBF_4, 50 wt%), 2,2,6,6-tetramethylpiperidinoxyl (TEMPO, 98%) triethanolamine (TEOA, 99.0%), and 1,4-benzoquinone (BQ, 98.0%). Concentrated nitric acid (HNO_3, 67%) and sulfuric acid (H_2SO_4, 95–98%) were purchased from Merck. Tetrahydrofuran (THF, 99.9%), *N,N*-dimethylformamide (DMF, 99.0%), Acetonitrile (CH_3CN, 99.9%), isopropyl alcohol (IPA, 99.9%), ethyl acetate (EtOAc, ≥ 99.5%), dimethyl sulfoxide (DMSO, 99.9%) dichloromethane (DCM, ≥ 99.0%), hexane (99.8%) and ethyl alcohol (EtOH, 99.9%) were obtained from IsoLab Chemicals. All reagents and solvents were of analytical grade and used without further purification unless otherwise specified.

Characterization Techniques

X-ray diffraction (XRD) patterns were recorded using a Bruker D2 Phaser diffractometer equipped with Cu Kα radiation (λ = 1.54 Å). Raman spectra were collected on a Renishaw inVia Raman microscope employing a 532 nm excitation laser. X-ray photoelectron spectroscopy (XPS) analyses were carried out using a Thermo Scientific K-Alpha system with Al Kα radiation (1486.6 eV). Fourier-transform infrared (FT-IR) spectra were obtained with a Thermo Scientific iS10 FT-IR spectrometer fitted with an attenuated total reflectance (ATR) module. Morphological and structural features were examined by transmission electron microscopy (TEM), high-angle annular dark-field scanning transmission electron microscopy (HAADF-STEM), and energy-dispersive X-ray spectroscopy (EDS) elemental mapping using a Hitachi HT7800 microscope operated at an accelerating voltage of 120 kV. Diffuse reflectance spectroscopy (DRS) measurements were performed using a Shimadzu UV-3600 UV–vis–NIR spectrophotometer. Photoluminescence (PL) spectra were recorded on an Agilent Cary Eclipse spectrofluorometer with an excitation wavelength of 320 nm. Electrochemical measurements were conducted on a CHI 660E electrochemical workstation employing a three-electrode configuration, with Hg/Hg_2Cl_2 as the reference electrode and a platinum wire as the counter electrode. To fabricate the working electrodes, 2.50 mg of the material was dispersed in 5 mL of ethanol via sonication and subsequently spray-coated onto a 1 cm^2 indium tin oxide (ITO) substrate. All electrochemical tests were carried out in a 0.1 M Na_2SO_4 electrolyte. Mott-Schottky measurements were recorded at frequencies of 1.0, 1.5, and 2.0 kHz over a potential range from -1.2 to 1.0 V. Solid-state ^{13}C CP/MAS NMR experiments were performed at the

Koç University n^2STAR NMR facility using a Bruker Avance Neo Ascend 500 spectrometer operating at a spinning rate of 12,000 rpm, equipped with a 4 mm double-resonance BBO solid-state probe. Between 512 and 1024 scans were accumulated for each measurement. Spectral acquisition and processing were carried out using TopSpin 4.4 software. ^1H NMR and ^{13}C NMR spectra were recorded using a 400 MHz Varian and Bruker Avance II 400MHz instrument with tetramethylsilane (TMS) as an internal standard. The following abbreviations were used to describe peak patterns: s = singlet, d = doublet, dd = doublet of doublets, t = triplet, q = quartet and m = multiplet. High resolution mass spectra were recorded on Agilent QTOF (Quadrupole time-of-flight) spectrometry device. Thin layer chromatography (TLC) was used alumina plates precoated with silica gel (Merck silica gel, 60 F254).

Synthesis of BP Crystals

A quartz ampoule was loaded with 10 mg of tin (IV) iodide, 20 mg of metallic tin, and 500 mg of red phosphorus, then flame-sealed under vacuum. The sealed ampoule was placed in a muffle furnace and subjected to a controlled thermal process: heating to 620 °C over 5 hours, maintaining this temperature for 5 hours, followed by a gradual decrease to 485 °C over 6 hours, where it was held for 3 hours. The temperature was then lowered to 120 °C over 4 hours, and the system was allowed to cool naturally to room temperature. The ampoule was opened in anhydrous toluene to extract the BP crystals, which were subsequently washed with ethanol and subjected to sonication for 30 minutes to remove surface impurities. The ethanol was evaporated under vacuum, and larger BP crystals were ground into smaller fragments under an inert argon atmosphere before being stored under vacuum.

Synthesis of Reduced Graphene Oxide (rGO)

rGO was synthesized through a two-step process. First, graphene oxide (GO) was prepared via a modified Hummers'method. Natural graphite powder (20 g) was oxidized in a mixture of concentrated H_2SO_4 (50 mL), $K_2S_2O_8$ (10 g), and P_2O_5 (10 g) at 80 °C for 6 hours, followed by dilution, filtration, and drying. The pre-oxidized graphite was then subjected to further oxidation by dispersing 1 g of the material in concentrated H_2SO_4 (50 mL) with $NaNO_3$ (1 g) in an ice bath (0–3 °C), followed by the slow addition of $KMnO_4$ (3 g). After stirring for 30 minutes at low temperature, the reaction was maintained at 35 °C for 3 hours, and subsequently diluted with water while adding H_2O_2 (12 mL, 30%) under controlled conditions (<60 °C). The product was treated with HCl (27%, 100 mL) to remove metal ions, thoroughly washed with water, filtered, and dried at 80 °C to obtain GO. In the second step, GO was dispersed in DMF and reduced by refluxing at 150 °C for 6 hours. The reduced material was washed with ethanol, filtered, and dried via evaporation to obtain rGO.

Synthesis of g-CN

Finely ground urea (10 g) was placed in a ceramic crucible and heated in a muffle furnace. The temperature was initially set at 80 °C for 30 minutes, then ramped to 550 °C over 1 hour, followed by a 4-hour annealing at this temperature. The material was naturally cooled, washed sequentially with acid and distilled water to remove residual alkaline byproducts, and dried at 80 °C before storage.

Materials Characterizations

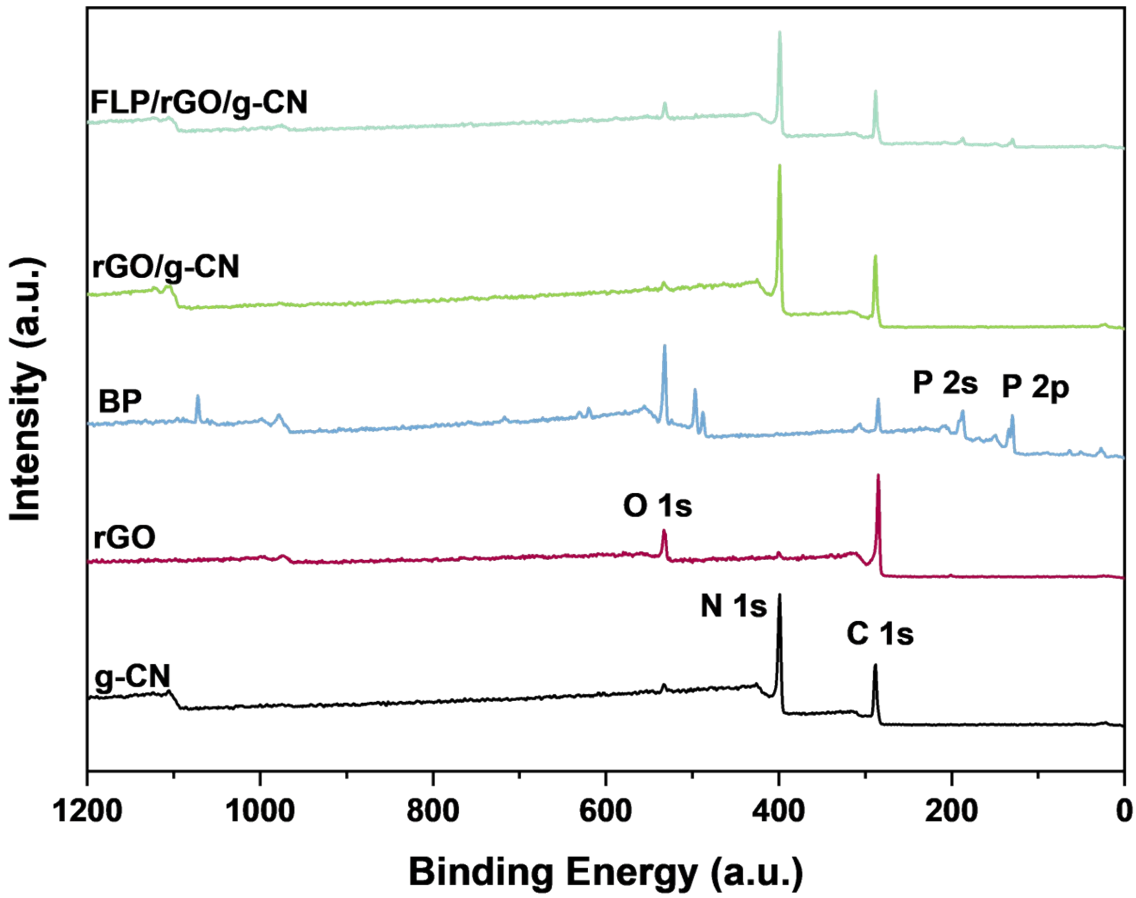

Figure S1. XPS survey spectra of all synthesized materials.

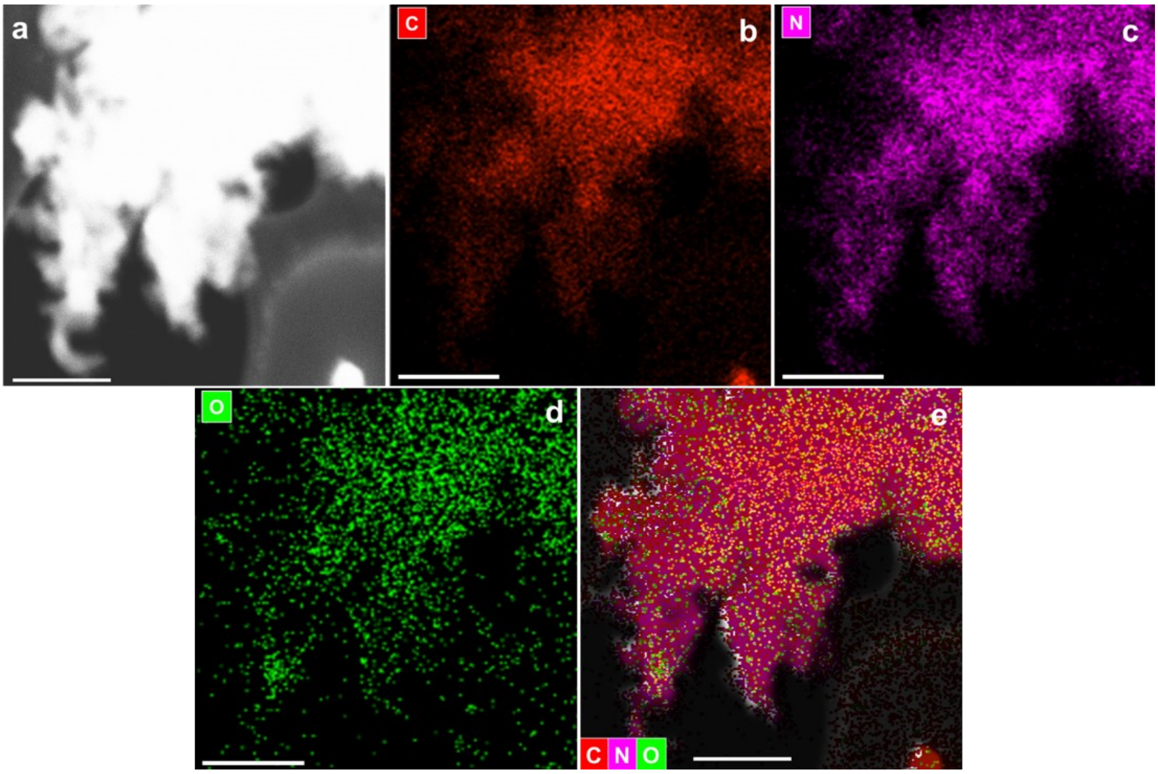

Figure S2. HAADF-STEM image and elemental mapping images of rGO/gCN (All scale bars are 500 nm).

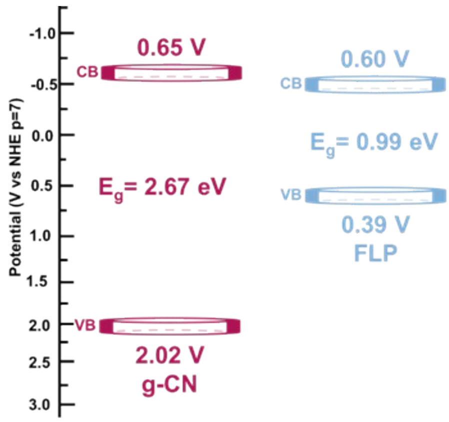

Figure S3. Schematic illustration of band potentials of g-CN and FLP.

Supplementary note 1. To this end, the valence band (VB) positions of g-CN and FLP were determined through linear extrapolation of the XPS-valence band (XPS-VB) spectra. The extrapolated VB onsets were found at 1.92 eV for g-CN and 0.29 eV for FLP (**Figure 4a**). These values were subsequently converted to the NHE scale using the equation:[16] $E_{NHE} = \Phi + E_{VB\text{-}XPS} - 4.44$ (work function of the XPS system used in this study) is 4.543 eV. Based on this conversion, the VB edges were calculated to be +2.02 V for g-CN and +0.32 V for FLP vs. NHE.

The conduction band (CB) positions were further assessed using Mott–Schottky (MS) analysis to estimate the flat-band potentials (V_{fb}), which approximate the Fermi level (E_F) in n-type semiconductors. The MS plots of g-CN (**Figure 4b**) and FLP (**Figure 4c**) exhibited positive slopes at all measured frequencies (1000, 1500, and 2000 Hz), confirming their n-type nature. The extracted V_{fb} values vs. the Hg/Hg_2Cl_2 reference electrode were −0.79 V for g-CN and −0.74 V for FLP, which correspond to −0.55 V and −0.50 V vs. NHE, respectively, after applying the conversion: E_{fb} (vs. NHE) = E_{fb} (vs. Hg/Hg_2Cl_2) + 0.24 V.[17]

Given that n-type semiconductors typically exhibit a CB edge located approximately 0.10–0.20 V more negative relative to the E_F, these data support the assignment of CB positions slightly above the measured flat-band values.[18] the corresponding CB levels were derived as −0.65 V and −0.60 V vs. NHE, respectively. Overall band diagram was shown in **Figure S3**.

Supplementary note 2. In addition to band-edge positions, understanding the direction of interfacial charge transfer is essential for elucidating the photocatalytic behavior of the system. The work functions of g-CN, FLP, rGO/g-CN, and FLP/rGO/g-CN were evaluated from VB-XPS spectra (**Figure 4c–f** and **Figure S4**), providing insight into the electronic equilibration at their interfaces.[19] Since a material with a larger work function possesses a deeper E_F relative to the vacuum level, it tends to accept electrons from a material with a lower work function. Electron transfer continues until their Fermi levels equilibrate, resulting in surface charge redistribution at the interface. Work function values were calculated using $\Delta V = \Phi - \varphi$ (where Φ is the measured work function and φ = 4.543 eV corresponds to the instrument parameter), with ΔV determined from the shift between inflection points (IP1 and IP2) of the VB onset. Based on this analysis, the work functions of g-CN, rGO/g-CN, and FLP were obtained as 6.83, 6.73 6.59, respectively. The decrease from 6.83 eV (g-CN) to 6.73 eV after coupling with rGO confirms that rGO behaves as an electron reservoir, shifting the Fermi level of g-CN closer to the vacuum level (**Figure 4d** and **f**). Following the incorporation of FLP into the rGO/g-CN binary system, electrons migrate from FLP, which possesses a lower E_F, to rGO/g-CN with a higher E_F until thermodynamic equilibrium is reached. This charge redistribution results in the formation of an intrinsic electric field (IEF) at the interface as the E_F align. Consequently, downward band bending occurs in rGO/g-CN, while upward band bending develops in FLP (**Figure 4g**). Under visible-light irradiation, this band alignment drives directional electron transfer from the CB of rGO/g-CN to the CB of FLP, opposing the built-in electric field. In contrast, holes generated in VB of rGO/g-CN remain localized rather than transferring to the VB of FLP due to the unfavorable band bending. This spatial separation of electrons and holes enhances charge separation and transport efficiency. Since photocatalytic oxidation dominates the reaction pathway, this electronic configuration supports interpreting the system as a non-classical type-I heterojunction.

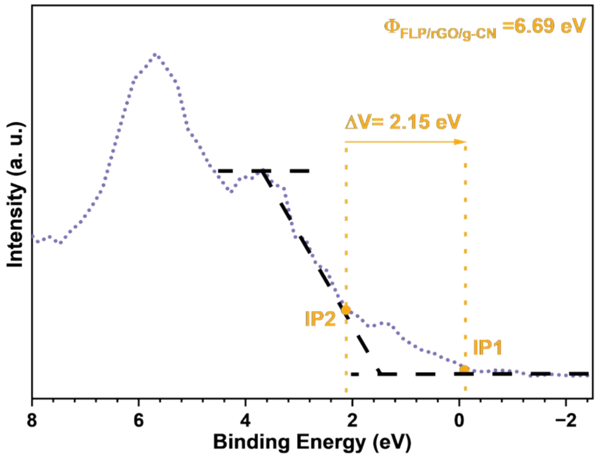

Figure S4. Work functions of FLP/rGO/g-CN.

Scavenger experiments

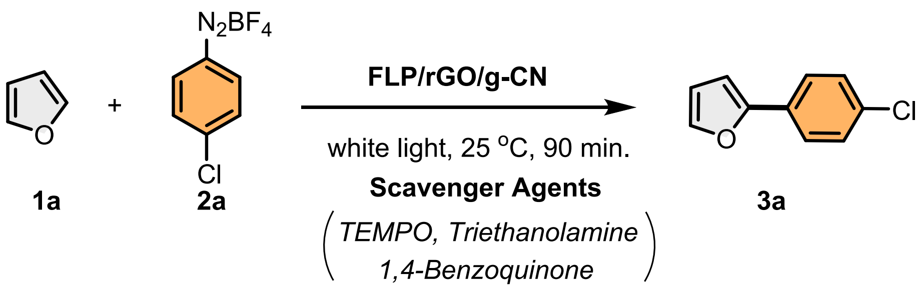

In scavenger experiments, aryl diazonium tetrafluoroborate (0.25 mmol), heteroarene (10 mmol), and scavenging agent (5.0 equiv., 0.5 mmol) were added to the reaction pot in dry DMSO (1 mL), then the reactions were carried out under the general experimental conditions.

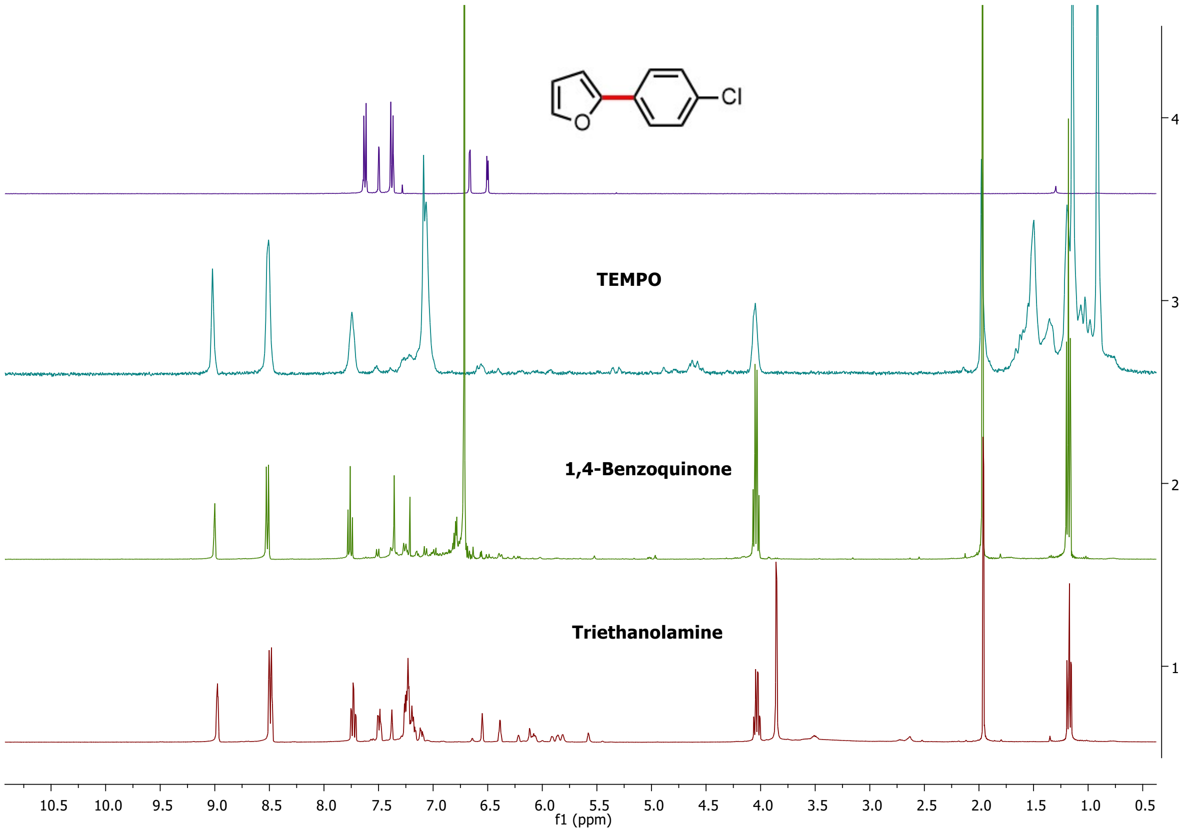

Figure S5a. NMR spectra for scavenger experiments

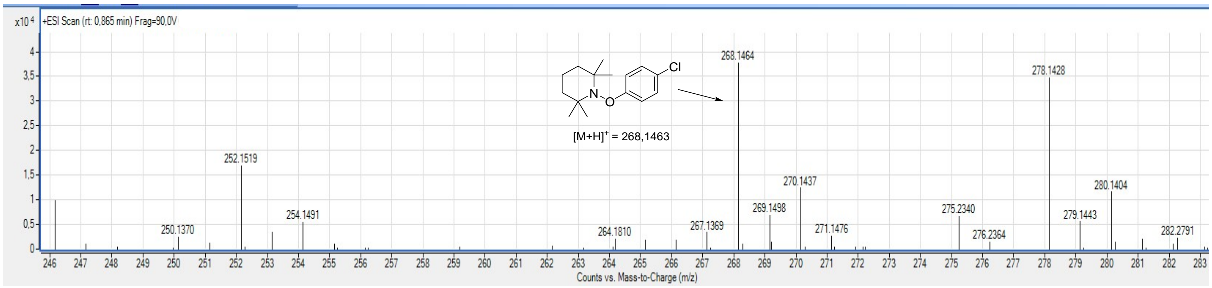

Figure S5b. Mass spectra of radical trapped compounds with TEMPO

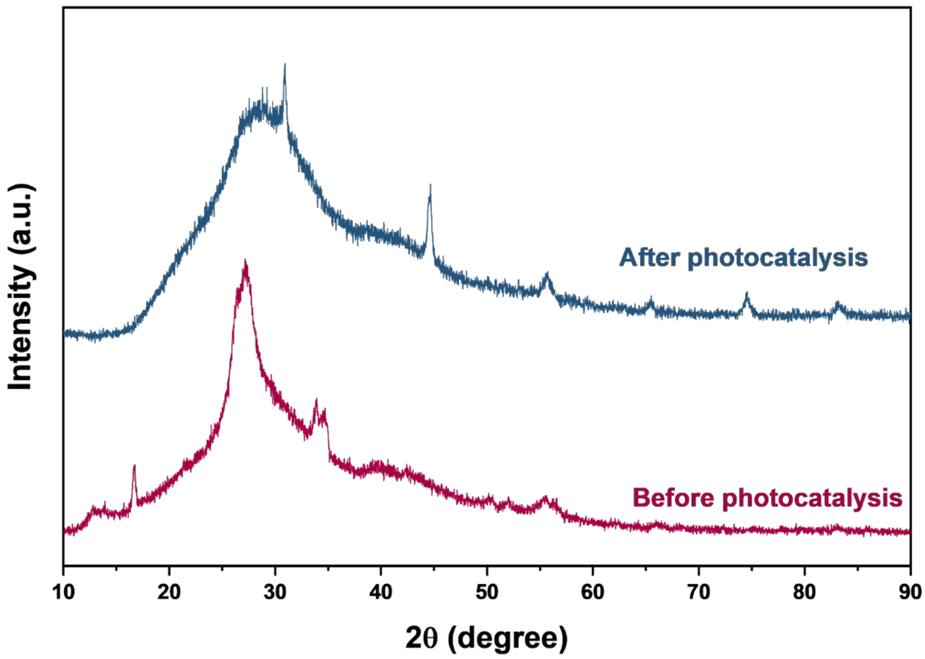

Figure S6. XRD pattern of materials before and after 5th run

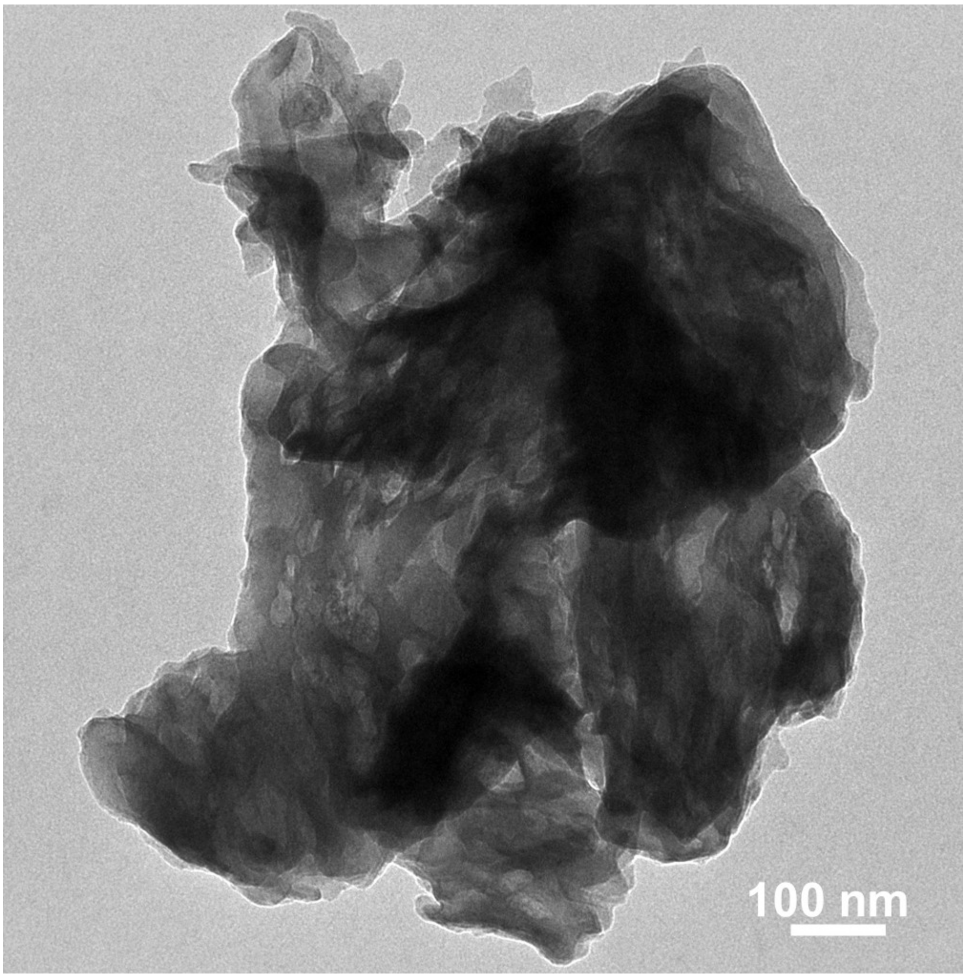

Figure S7. TEM image of FLP/rGO/gCN after the 5th run.

Comparison of C–H arylation performance with the literature

Table S1. Comparison of different photoredox C-H arylation conditions in the literature.

Entry	Photocatalyst	Catalyst mass (mg)	Time (h)	Light Source	Reusability (cycle times)	X- Substiued Diazonium Salts	Yield [%]	
1	Eosin B	< 5	2	CFL (20 W)	3	Cl	83	Ref[23]
2	PANI-g-C_3N_4-TiO_2	30		CFL (14 W)	10	Cl	87	Ref[24]
3	Bismuth(III) Oxide	10	15	CFL (23 W)	-	Br	86	Ref[25]
4	Cercosporin	≥ 1	16	Sunlight	-	CO_2Et	62	Ref[26]
5	Bi QDs	0.8 wt%		Blıe light	3	Cl	80	Ref[27]
6	MR-EosinY	77	2	Green LEDs (424 mW/cm^2)	3	Cl	75	Ref[28]
7	$CpMn(CO)_3$	< 5	0.5	Blue LED (24 W, λ = 450 nm)	-	CF_3	71	Ref[29]
8	Immobilized BODIPY	5	2	Green LED (λ = 495–555 nm)	5	Br	76	Ref[30]
9	Eosin Y	< 1	2	530 nm LED (1 W)	-	Cl	74	Ref[31]
10	mb-As	20	2	Red light	5	Cl	76	Ref[32]
11	$AcrH_2$	> 5	12	Blue LEDs (3 W)	-	Br	69	Ref[33]
12	Fe_3O_4@$Cu_{2-x}S$–MoS_2F	2	1	Xenon lamp ((λ = 700 nm)	6	Cl	98	Ref[34]
13	(BPY)CuII(O,O-PLY-Ph)Cl	3	24	Blue LEDs	-	Cl	91	Ref[35]
14	$CuInS_2$/K-C_3N_4	20	8	Blue LED 10 W	5	NO_2	91	Ref[36]

1. NMR characterization of the arylation products

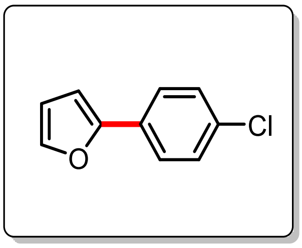	2-(4-Chlorophenyl)furan (**3a**)[1,2] **3a** was isolated by thin layer chromatography (hexane/EtOAc: 95/5) gave the product as white solid (94%). **^{1}H NMR (400 MHz, $CDCl_3$)** δ 7.60 (d, *J* = 8.6 Hz, 2H), 7.48 (s, 1H), 7.35 (d, *J* = 8.6 Hz, 2H), 6.64 (d, *J* = 3.3 Hz, 1H), 6.48 (dd, *J* = 3.3, 1.8 Hz, 1H). **^{13}C NMR (100 MHz, $CDCl_3$)** δ 153.12, 142.5, 133.2, 129.6, 129.1, 125.2, 112.0, 105.6. **HRMS (APCI-TOF) m/z:** $[M+H]^+$ calcd for $C_{10}H_8ClO$, 179.0258; found 179.0273.
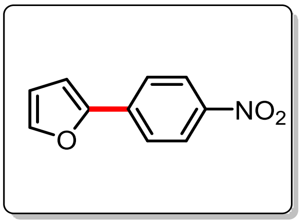	2-(4-Nitrophenyl)furan (**3b**)[1,2] **3b** was isolated by thin layer chromatography (hexane/EtOAc: 95/5) gave the product as yellow solid (76%). **^{1}H NMR (400 MHz, $CDCl_3$)** δ 8.24 (d, *J* = 8.9 Hz, 2H), 7.78 (d, *J* = 8.9 Hz, 2H), 7.57 (d, *J* = 1.5 Hz, 1H), 6.88 (d, *J* = 3.4 Hz, 1H), 6.55 (dd, *J* = 3.4, 1.7 Hz, 1H). **^{13}C NMR (100 MHz, $CDCl_3$)** δ 151.9, 146.6, 144.4, 136.7, 124.6, 124.2, 112.7, 109.2. **HRMS (APCI-TOF) m/z:** $[M+H]^+$ calcd for $C_{10}H_8NO_3$, 190.0499; found 190,0476.
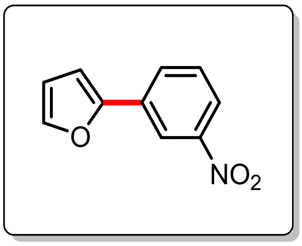	2-(3-Nitrophenyl)furan (**3c**)[1,2] **3c** was isolated by thin layer chromatography (hexane/EtOAc: 95/5) gave the product as orange solid (73%). **^{1}H NMR (400 MHz, $CDCl_3$)** δ 8.49 (t, *J* = 1.9 Hz, 1H), 8.15 – 8.02 (m, 1H), 7.96 (d, *J* = 7.9 Hz, 1H), 7.63 – 7.44 (m, 2H), 6.81 (d, *J* = 3.5 Hz, 1H), 6.53 (dd, *J* = 3.4, 1.8 Hz, 1H). **^{13}C NMR (100 MHz, $CDCl_3$)** δ 151.7, 149.0, 143.5, 132.6, 129.9, 129.4, 121.9, 118.7, 112.3, 107.5. **HRMS (APCI-TOF) m/z:** $[M+H]^+$ calcd for $C_{10}H_8NO_3$, 190.0499; found 190,0499.
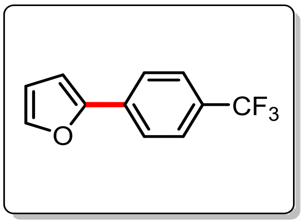	2-(4-(Trifluoromethyl)phenyl)furan (**3d**)[2,8,11] **3d** was isolated by thin layer chromatography (hexane/EtOAc: 95/5) gave the product as colorless oil (80%). **^{1}H NMR (400 MHz, $CDCl_3$)** δ 7.68 (d, *J* = 8.4 Hz, 2H), 7.55 (d, *J* = 8.4 Hz, 2H), 7.43 (d, *J* = 1.6 Hz, 1H), 6.68 (d, *J* = 3.4 Hz, 1H), 6.43 (dd, *J* = 3.4, 1.8 Hz, 1H). **^{13}C NMR (100 MHz, $CDCl_3$)** δ 152.7, 143.3, 134.2, 129.2 (q, *J* = 32.5 Hz), 125.9 (q, *J* = 3.9 Hz), 124.4 (q, *J* = 272.0 Hz), 124.0, 112.2, 107.2. **HRMS (APCI-TOF) m/z:** $[M+H]^+$ calcd for $C_{11}H_8F_3O$, 213.0522; found 213,0523.
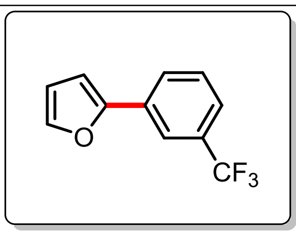	2-(3-(Trifluoromethyl)phenyl)furan (**3e**)[2,7,12] **3e** was isolated by thin layer chromatography (hexane/EtOAc: 95/5) gave the product as colorless oil (82%). **^{1}H NMR (400 MHz, $CDCl_3$)** δ 7.92 (s, 1H), 7.85 – 7.79 (m, 1H), 7.52 – 7.47 (m, 3H), 6.74 (dd, *J* = 3.4, 0.6 Hz, 1H), 6.51 (dd, *J* = 3.4, 1.8 Hz, 1H). **^{13}C NMR (100 MHz, $CDCl_3$)** δ 152.7, 143.0, 131.7, 131.4 (q, *J* = 34.5 Hz), 129.4, 126.9, 124.3 (q, *J* = 271.8 Hz), 124.0 (q, *J* = 3.9 Hz), 120.7 (q, *J* = 3.9 Hz), 112.1, 106.5. **HRMS (APCI-TOF) m/z:** $[M+H]^+$ calcd for $C_{11}H_8F_3O$, 213.0522; found 213.0523.

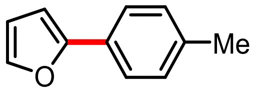	2-(4-Methylphenyl)furan (**3f**)[1,2] **3f** was isolated by thin layer chromatography (hexane/EtOAc: 95/5) gave the product as colorless oil (87%). **^{1}H NMR (400 MHz, $CDCl_3$)** δ 7.57 (d, *J* = 8.2 Hz, 2H), 7.45 (d, *J* = 1.6 Hz, 1H), 7.19 (d, *J* = 8.0 Hz, 2H), 6.59 (d, *J* = 3.3 Hz, 1H), 6.46 (dd, *J* = 3.3, 1.8 Hz, 1H), 2.37 (s, 3H). **^{13}C NMR (100 MHz, $CDCl_3$)** δ 154.1, 141.7, 137.2, 129.4, 128.2, 123.8, 111.6, 104.2, 21.3. **HRMS (APCI-TOF) m/z:** $[M+H]^+$ calcd for $C_{11}H_{11}O$, 159,0804; found 159,0833.
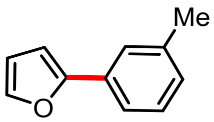	2-(3-Methylphenyl)furan (**3g**)[2,4] **3g** was isolated by thin layer chromatography (hexane/EtOAc: 95/5) gave the product as yellow oil (38%). **^{1}H NMR (400 MHz, $CDCl_3$)** δ 7.59 (d, *J* = 8.2 Hz, 2H), 7.46 (d, *J* = 1.6 Hz, 1H), 7.20 (d, *J* = 8.0 Hz, 2H), 6.61 (d, *J* = 3.3 Hz, 1H), 6.47 (dd, *J* = 3.3, 1.8 Hz, 1H), 2.38 (s, 3H). **^{13}C NMR (100 MHz, $CDCl_3$)** δ 154.2, 141.9, 138.3, 130.8, 128.6, 128.2, 124.5, 121.0, 111.6, 104.8, 21.5. **HRMS (APCI-TOF) m/z:** $[M+H]^+$ calcd for $C_{11}H_{11}O$, 159,0804; found 159,0815.
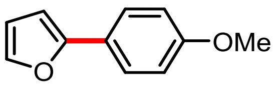	2-(4-Methoxyphenyl)furan (**3h**)[1,2] **3h** was isolated by thin layer chromatography (hexane/EtOAc: 95/5) gave the product as yellow oil (73%). **^{1}H NMR (400 MHz, $CDCl_3$)** δ 7.61 (d, *J* = 8.9 Hz, 2H), 7.43 (d, *J* = 1.5 Hz, 1H), 6.93 (d, *J* = 8.8 Hz, 2H), 6.52 (d, *J* = 3.2 Hz, 1H), 6.45 (dd, *J* = 3.3, 1.8 Hz, 1H), 3.84 (s, 3H). **^{13}C NMR (100 MHz, $CDCl_3$)** δ 159.2, 154.3, 141.6, 125.5, 124.3, 114.3, 111.7, 103.6, 55.5. **HRMS (APCI-TOF) m/z:** $[M+H]^+$ calcd for $C_{11}H_{11}O_2$, 175.0754; found 175,0761.
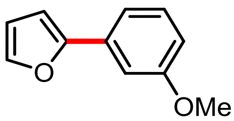	2-(3-Methoxyphenyl)furan (**3i**)[2,6] **3i** was isolated by thin layer chromatography (hexane/EtOAc: 95/5) gave the product as yellow solid (46%). **^{1}H NMR (400 MHz, $CDCl_3$)** δ 7.39 (s, 1H), 7.28 – 7.17 (m, 2H), 7.15 (d, *J* = 1.5 Hz, 1H), 6.77 – 6.70 (m, 1H), 6.58 (d, *J* = 3.4 Hz, 1H), 6.40 (dd, *J* = 3.2, 1.7 Hz, 1H), 3.78 (s, 3H). **^{13}C NMR (100 MHz, $CDCl_3$)** δ 159.9, 153.8, 142.1, 132.2, 129.8, 116.4, 113.2, 111.7, 109.1, 105.3, 55.3. **HRMS (APCI-TOF) m/z:** $[M+H]^+$ calcd for $C_{11}H_{11}O_2$, 175.0754; found 175,0773.
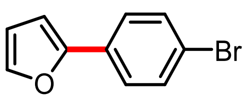	2-(4-Bromophenyl)furan (**3j**)[1,2] **3j** was isolated by thin layer chromatography (hexane/EtOAc: 95/5) gave the product as white solid (96%). **^{1}H NMR (400 MHz, $CDCl_3$)** δ 7.65 – 7.38 (m, 5H), 6.65 (d, *J* = 3.4 Hz, 1H), 6.47 (dd, *J* = 3.3, 1.8 Hz, 1H). **^{13}C NMR (100 MHz, $CDCl_3$)** δ 153.1, 142.6, 132.0, 130.0, 125.5, 121.3, 112.0, 105.8. **HRMS (APCI-TOF) m/z:** $[M+H]^+$ calcd for $C_{10}H_8BrO$, 222.9753; found 222,9765.
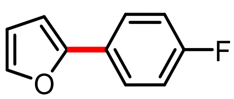	2-(4-Fluorophenyl)furan (**3k**)[2,3,12] **3k** was isolated by thin layer chromatography (hexane/EtOAc: 95/5) gave the product as white solid (92%). **^{1}H NMR (400 MHz, $CDCl_3$)** δ 7.71 – 7.57 (m, 2H), 7.45 (d, *J* = 1.1 Hz, 1H), 7.08 (t, *J* = 8.8 Hz, 2H), 6.58 (d, *J* = 3.3 Hz, 1H), 6.46 (dd, *J* = 3.3, 1.8 Hz, 1H). **^{13}C NMR (100 MHz, $CDCl_3$)** δ 162.3 (d, *J* = 246.5 Hz), 153.4, 142.2, 127.5 (d, *J* = 3.5 Hz), 125.7 (d, *J* = 8.2 Hz), 115.9 (d, *J* = 21.9 Hz). 111.9, 104.8.

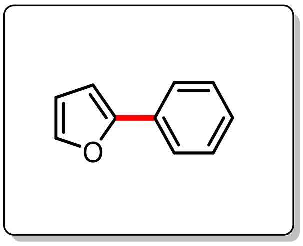	2-Phenylfuran (**3l**)[1,2] **3l** was isolated by thin layer chromatography (hexane/EtOAc: 95/5) gave the product as yellow oil (71%). **^{1}H NMR (400 MHz, CDCl$_3$)** δ 7.60 (dd, *J* = 8.3, 1.1 Hz, 2H), 7.39 (d, *J* = 1.6 Hz, 1H), 7.31 (t, *J* = 7.7 Hz, 2H), 7.21 – 7.13 (m, 1H), 6.58 (d, *J* = 3.1 Hz, 1H), 6.39 (dd, *J* = 3.3, 1.8 Hz, 1H). **^{13}C NMR (100 MHz, CDCl$_3$)** δ 154.2, 142.3, 131.1, 128.9, 127.6, 124.0, 111.9, 105.2. **HRMS (APCI-TOF) m/z:** $[M+H]^+$ calcd for $C_{10}H_9O$, 145.0648; found 145.0648.
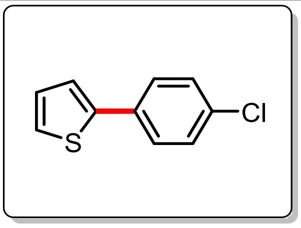	2-(4-Chlorophenyl)thiophene (**4a**)[2,3] **4a** was isolated by thin layer chromatography (hexane/EtOAc: 95/5) gave the product as white solid (77%). **^{1}H NMR (400 MHz, CDCl$_3$)** δ 7.57 (d, *J* = 8.5 Hz, 2H), 7.37 (d, *J* = 8.5 Hz, 2H), 7.33-7.30 (m, 2H), 7.11 (dd, *J* = 4.8, 3.9 Hz, 1H). **^{13}C NMR (100 MHz, CDCl$_3$)** δ 143.1, 133.2, 133.0, 129.1, 128.2, 127.1, 125.2, 123.5. **HRMS (APCI-TOF) m/z:** $[M+H]^+$ calcd for $C_{10}H_8ClS$, 195.0030; found 195,0048.
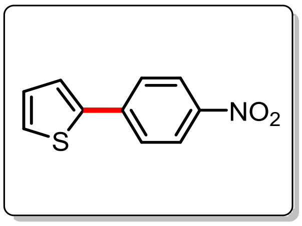	2-(4-Nitrophenyl)thiophene (**4b**)[1,2] **4b** was isolated by thin layer chromatography (hexane/EtOAc: 95/5) gave the product as yellow solid (77%). **^{1}H NMR (400 MHz, CDCl$_3$)** δ 8.16 (d, *J* = 8.9 Hz, 2H), 7.66 (d, *J* = 8.9 Hz, 2H), 7.40 (dd, *J* = 3.5, 0.9 Hz, 1H), 7.36 (dd, *J* = 5.1, 1.2 Hz, 1H), 7.08 (dd, *J* = 5.0, 3.6 Hz, 1H). **^{13}C NMR (100 MHz, CDCl$_3$)** δ 141.8, 140.8, 128.9, 127.9, 127.1, 126.3, 125.9, 124.6. **HRMS (APCI-TOF) m/z:** $[M+H]^+$ calcd for $C_{10}H_8NO_2S$, 206,0270; found 206,0281.
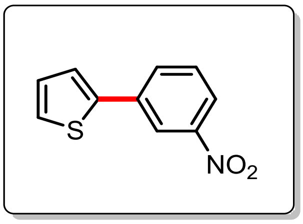	2-(3-Nitrophenyl)thiophene (**4c**)[2,5] **4c** was isolated by thin layer chromatography (hexane/EtOAc: 95/5) gave the product as yellow oil (76%). **^{1}H NMR (400 MHz, CDCl$_3$)** δ 8.35 (t, *J* = 1.9 Hz, 1H), 8.05 – 7.99 (m, 1H), 7.82 (d, *J* = 7.9 Hz, 1H), 7.46 (t, *J* = 8.0 Hz, 1H), 7.35 (dd, *J* = 3.5, 0.9 Hz, 1H), 7.30 (dd, *J* = 5.1, 0.9 Hz, 1H), 7.05 (dd, *J* = 5.0, 3.6 Hz, 1H). **HRMS (APCI-TOF) m/z:** $[M]^+$ calcd for $C_{10}H_7NO_2S$, 205,0192; found 205,0191.
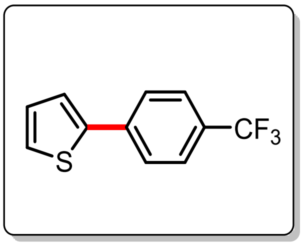	2-(4-(Trifluoromethyl)phenyl)thiophene (**4d**)[2,9,13] **4d** was isolated by thin layer chromatography (hexane/EtOAc: 99/1) gave the product as white solid (74%). **^{1}H NMR (400 MHz, DMSO)** δ 7.86 (d, *J* = 8.2 Hz, 2H), 7.74 (d, *J* = 8.2 Hz, 2H), 7.67 (dd, *J* = 5.6, 4.6 Hz, 2H), 7.18 (dd, *J* = 4.8, 3.9 Hz, 1H). **^{13}C NMR (100 MHz, DMSO)** δ 142.1, 138.2, 129.5, 128.2, 126.8, 126.7, 126.5, 126.3. **HRMS (APCI-TOF) m/z:** $[M+H]^+$ calcd for $C_{11}H_8F_3S$, 229,0293; found 229,0293.
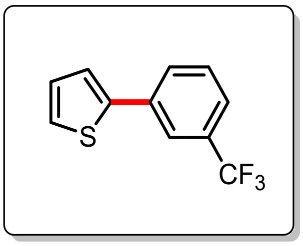	2-(3-(Trifluoromethyl)phenyl)thiophene (**4e**)[2,7] **4e** was isolated by thin layer chromatography (hexane/EtOAc: 99/1) gave the product as colorless oil (75%). **^{1}H NMR (400 MHz, CDCl$_3$)** δ 7.76 (s, 1H), 7.69 (d, *J* = 7.3 Hz, 1H), 7.46-7.39 (m, 2H), 7.29 (dd, *J* = 3.6, 1.0 Hz, 1H), 7.26 (dd, *J* = 5.3, 1.0 Hz, 1H), 7.03 (dd, *J* = 5.0, 3.7 Hz, 1H). **^{13}C NMR (100 MHz, CDCl$_3$)** δ 142.9, 135.4, 131.5 (q, *J* = 32.3 Hz), 129.6, 129.3, 128.5, 126.1, 124.2 (q, *J* = 3.7 Hz), 122.8 (q, *J* = 3.7 Hz), 121.6. **HRMS (APCI-TOF) m/z:** $[M]^+$ calcd for $C_{11}H_7F_3S$, 228,0215; found 228,0226.

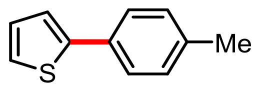	2-(4-Methylphenyl)furan (**4f**)[2,5] **4f** was isolated by thin layer chromatography (hexane/EtOAc: 99/1) gave the product as white solid (60%). **^{1}H NMR (400 MHz, $CDCl_3$)** δ 7.42 (d, *J* = 8.1 Hz, 2H), 7.17 (d, *J* = 3.6 Hz, 1H), 7.14 (d, *J* = 5.0 Hz, 1H), 7.09 (d, *J* = 8.0 Hz, 2H), 6.97 (dd, *J* = 5.0, 3.6 Hz, 1H), 2.27 (s, 3H). **^{13}C NMR (100 MHz, $CDCl_3$)** δ 144.6, 137.4, 131.7, 129.6, 128.0, 125.9, 124.3, 122.6, 21.2. **HRMS (APCI-TOF) m/z:** $[M]^+$ calcd for $C_{11}H_{10}S$, 174,0498; found 174,0515.
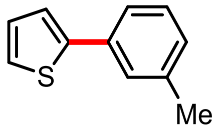	2-(3-Methylphenyl)furan (**4g**)[2,5] **4g** was isolated by thin layer chromatography (hexane/EtOAc: 99/1) gave the product as white solid (30%). **^{1}H NMR (400 MHz, $CDCl_3$)** δ 7.35 (m, 2H), 7.24 – 7.21 (m, 1H), 7.21 – 7.17 (m, 2H), 7.05 – 6.99 (m, 2H), 2.32 (s, 3H). **^{13}C NMR (100 MHz, $CDCl_3$)** δ 144.8, 138.8, 134.5, 129.0, 128.5, 128.2, 126.9, 124.9, 123.3, 123.2, 21.7. **HRMS (APCI-TOF) m/z:** $[M+H]^+$ calcd for $C_{11}H_{11}S$, 174,0576; found 175,0579.
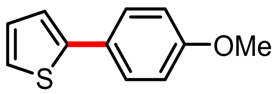	2-(4-Methoxyphenyl)thiophene (**4h**)[2,5] **4h** was isolated by thin layer chromatography (hexane/EtOAc: 99/1) gave the product as white solid (65%). **^{1}H NMR (400 MHz, $CDCl_3$)** δ 7.55 (d, *J* = 8.5 Hz, 2H), 7.22 (t, *J* = 4.9 Hz, 2H), 7.06 (dd, *J* = 4.6, 4.0 Hz, 1H), 6.92 (d, *J* = 8.5 Hz, 2H), 3.84 (s, 3H). **^{13}C NMR (100 MHz, $CDCl_3$)** δ 159.4, 144.6, 128.2, 127.8, 127.5, 124.1, 122.3, 114.5, 55.6. **HRMS (APCI-TOF) m/z:** $[M+H]^+$ calcd for $C_{11}H_{11}OS$, 191,0525; found 191,0544.
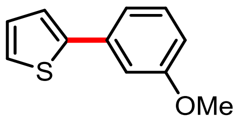	2-(3-Methoxyphenyl)thiophene (**4i**)[2,10] **4i** was isolated by thin layer chromatography (hexane/EtOAc: 99/1) gave the product as yellow oil (33%). **^{1}H NMR (400 MHz, $CDCl_3$)** δ 7.26 – 7.19 (m, 3H), 7.14 (d, *J* = 7.7 Hz, 1H), 7.10 – 7.05 (m, 1H), 7.01 (dd, *J* = 5.1, 3.6 Hz, 1H), 6.77 (dd, *J* = 8.3, 2.2 Hz, 1H), 3.78 (s, 3H). **^{13}C NMR (100 MHz, $CDCl_3$)** δ 159.9, 144.3, 135.7, 129.9, 128.0, 124.9, 123.3, 118.6, 112.9, 111.7, 55.3. **HRMS (APCI-TOF) m/z:** $[M+H]^+$ calcd for $C_{11}H_{11}OS$, 191,0525; found 191, 0546.
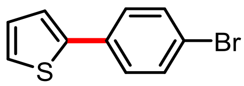	2-(4-Bromophenyl)thiophene (**4j**)[2,3] **4j** was isolated by thin layer chromatography (hexane/EtOAc: 95/5) gave the product as white solid (84%). **^{1}H NMR (400 MHz, $CDCl_3$)** δ 7.44 – 7.37 (m, 4H), 7.22 (d, *J* = 4.4 Hz, 2H), 7.00 (t, *J* = 4.4 Hz, 1H). **^{13}C NMR (100 MHz, $CDCl_3$)** δ 143.1, 133.4, 132.0, 128.2, 127.4, 125.3, 123.5, 121.3. **HRMS (APCI-TOF) m/z:** $[M]^+$ calcd for $C_{10}H_7BrS$, 237,9446; found 237,9448.
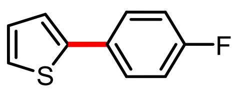	2-(4-Fluorophenyl)thiophene (**4k**)[2,3,13] **4k** was isolated by thin layer chromatography (hexane/EtOAc: 95/5) gave the product as light yellow solid (73%).**^{1}H NMR (400 MHz, $CDCl_3$)** δ 7.52 – 7.43 (m, 2H), 7.18 (dd, *J* = 5.0, 0.9 Hz, 1H), 7.15 (dd, *J* = 3.5, 0.9 Hz, 1H), 7.02 – 6.94 (m, 3H). **^{13}C NMR (100 MHz, $CDCl_3$)** δ 162.3 (d, *J* = 246.8 Hz), 143.3, 130.7 (d, *J* = 3.7 Hz), 128.1, 127.6 (d, *J* = 8.2 Hz), 124.8, 123.1, 115.8 (d, *J* = 21.7 Hz). **HRMS (APCI-TOF) m/z:** $[M+H]^+$ calcd for $C_{10}H_7FS$, 179,0325; found 179,0332.

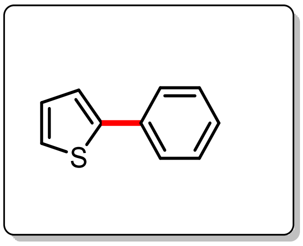	2-Phenylthiophene (**4l**)[2,5] **4l** was isolated by thin layer chromatography (hexane/EtOAc: 95/5) gave the product as light yellow solid (40%). **^{1}H NMR (400 MHz, CDCl$_3$)** δ 7.58 – 7.50 (m, 2H), 7.31 (t, *J* = 7.5 Hz, 2H), 7.26 – 7.16 (m, 3H), 7.01 (dd, *J* = 5.0, 3.6 Hz, 1H). **^{13}C NMR (100 MHz, CDCl$_3$)** δ 144.5, 134.4, 128.9, 128.0, 127.5, 126.0, 124.8, 123.1. **HRMS (APCI-TOF) m/z:** [M]$^+$ calcd for $C_{10}H_8S$, 160,0341; found 160,0342.
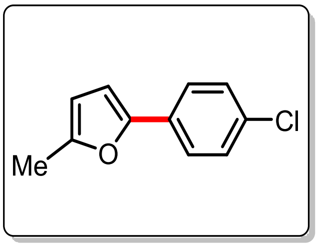	2-(4-Chlorophenyl)-5-methylfuran (**6aa**)[20] **6aa** was isolated by thin layer chromatography (hexane/EtOAc: 95/5) gave the product as white solid (42%). **^{1}H NMR (400 MHz, CDCl$_3$)** δ 7.47 (d, *J* = 8.6 Hz, 2H), 7.24 (d, *J* = 8.6 Hz, 2H), 6.45 (d, *J* = 3.2 Hz, 1H), 5.98 (d, *J* = 2.3 Hz, 1H), 2.29 (s, 3H). **^{13}C NMR (100 MHz, CDCl$_3$)** δ 152.3, 151.2, 132.3, 129.7, 128.8, 124.5, 107.9, 106.4, 13.7. **HRMS (APCI-TOF) m/z:** [M+H]$^+$ calcd for $C_{11}H_{10}ClO$, 193,0415; found 193,0433.
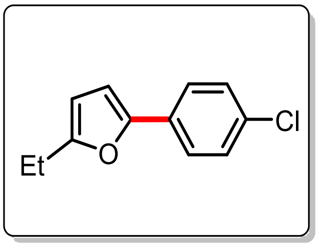	2-(4-Chlorophenyl)-5-ethylfuran (**6ab**)[20] **6ab** was isolated by thin layer chromatography (hexane/EtOAc: 95/5) gave the product as white solid (33%). **^{1}H NMR (400 MHz, CDCl$_3$)** δ 7.47 (d, *J* = 8.6 Hz, 2H), 7.23 (d, *J* = 8.6 Hz, 2H), 6.46 (d, *J* = 3.3 Hz, 1H), 5.98 (d, *J* = 3.3 Hz, 1H), 2.63 (q, *J* = 7.5 Hz, 2H), 1.20 (t, *J* = 7.6 Hz, 3H). **^{13}C NMR (100 MHz, CDCl$_3$)** δ 158.0, 151.1, 132.2, 129.7, 128.8, 124.5, 106.3, 106.2, 21.5, 12.2. **HRMS (APCI-TOF) m/z:** [M+H]$^+$ calcd for $C_{12}H_{12}ClO$, 207,0571; found 207,0573.
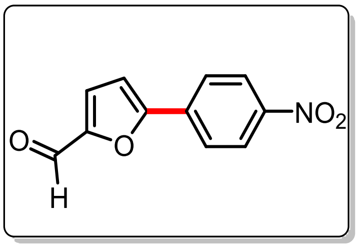	5-(4-Nitrophenyl)furan-2-carbaldehyde (**6ac**)[13] **6ac** was isolated by thin layer chromatography (hexane/EtOAc: 80/20) gave the product as brown solid (29%). **^{1}H NMR (400 MHz, CDCl$_3$)** δ 9.66 (s, 1H), 8.24 (d, *J* = 8.9 Hz, 2H), 7.91 (d, *J* = 8.9 Hz, 2H), 7.31 (d, *J* = 3.7 Hz, 1H), 6.98 (d, *J* = 3.8 Hz, 1H). **HRMS (APCI-TOF) m/z:** [M+H]$^+$ calcd for $C_{11}H_8NO_4$, 218,0448; found 218,0464.
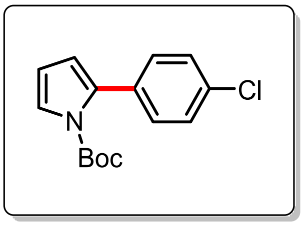	*tert*-Butyl 2-(4-chlorophenyl)-1*H*-pyrrole-1-carboxylate (**8aa**)[14] **8aa** was isolated by thin layer chromatography (hexane/EtOAc: 95/5) gave the product as orange solid (42%). **^{1}H NMR (400 MHz, CDCl$_3$)** δ 7.42 – 7.19 (m, 5H), 6.22 (t, *J* = 3.3 Hz, 1H), 6.18 (dd, *J* = 3.2, 1.8 Hz, 1H), 1.40 (s, 9H). **^{13}C NMR (100 MHz, CDCl$_3$)** δ 149.4, 134.0, 133.3, 133.0, 130.7, 128.0, 123.1, 115.0, 110.9, 84.1, 27.9. **HRMS (APCI-TOF) m/z:** [M+H]$^+$ calcd for $C_{15}H_{17}ClNO_2$, 278,0942; found 278,0969.
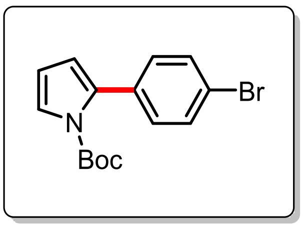	*tert*-Butyl 2-(4-bromophenyl)-1*H*-pyrrole-1-carboxylate (**8ab**)[15] **8ab** was isolated by thin layer chromatography (hexane/EtOAc: 95/5) gave the product as light yellow solid (49%). **^{1}H NMR (400 MHz, CDCl$_3$)** δ 7.47 (d, *J* = 8.3 Hz, 2H), 7.35 (dd, *J* = 3.3, 1.8 Hz, 1H), 7.22 (d, *J* = 8.3 Hz, 2H), 6.22 (t, *J* = 3.3 Hz, 1H), 6.18 (dd, *J* = 3.1, 1.9 Hz, 1H), 1.40 (s, 9H). **^{13}C NMR (100 MHz, CDCl$_3$)** δ 149.4, 134.0, 133.5, 131.0, 130.9, 123.1, 121.5, 115.0, 110.9, 84.1, 27.9. **HRMS (APCI-TOF) m/z:** [M+H]$^+$ calcd for $C_{15}H_{17}BrNO_2$, 322,0437; found 322,0458.

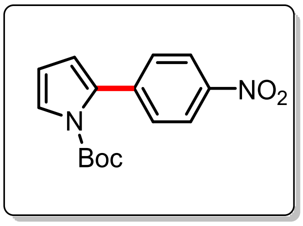	*tert*-Butyl 2-(4-nitrophenyl)-1*H*-pyrrole-1-carboxylate (**8ac**)[15] **8ac** was isolated by thin layer chromatography (hexane/EtOAc: 95/5) gave the product as yellow solid (35%). **^{1}H NMR (400 MHz, CDCl$_3$)** δ 8.21 (d, *J* = 8.9 Hz, 2H), 7.51 (d, *J* = 8.9 Hz, 2H), 7.40 (dd, *J* = 3.3, 1.8 Hz, 1H), 6.32 (dd, *J* = 3.4, 1.7 Hz, 1H), 6.27 (t, *J* = 3.3 Hz, 1H), 1.43 (s, 9H). **^{13}C NMR (100 MHz, CDCl$_3$)** δ 149.1, 146.8, 140.9, 133.0, 129.8, 124.5, 123.2, 116.8, 111.4, 84.8, 27.9. **HRMS (APCI-TOF) m/z:** [M+H]$^+$ calcd for $C_{15}H_{17}N_2O_4$, 289,1183; found 289,1196.
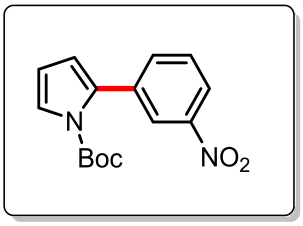	*tert*-Butyl 2-(3-nitrophenyl)-1*H*-pyrrole-1-carboxylate (**8ad**)[15] **8ad** was isolated by thin layer chromatography (hexane/EtOAc: 95/5) gave the product as orange solid (48%). **^{1}H NMR (400 MHz, CDCl$_3$)** δ 8.22 (t, *J* = 1.9 Hz, 1H), 8.17 – 8.13 (m, 1H), 7.68 (d, *J* = 7.7 Hz, 1H), 7.51 (t, *J* = 8.0 Hz, 1H), 7.40 (dd, *J* = 3.0, 1.6 Hz, 1H), 6.30 – 6.25 (m, 2H), 1.40 (s, 9H). **^{13}C NMR (100 MHz, CDCl$_3$)** δ 136.0, 135.3, 128.7, 124.4, 123.9, 123.9, 122.1, 116.3, 116.1, 111.3, 111.1, 84.6, 27.9. **HRMS (APCI-TOF) m/z:** [M+K]$^+$ calcd for $C_{15}H_{16}N_2O_4K$, 327,0742; found 327,0752.
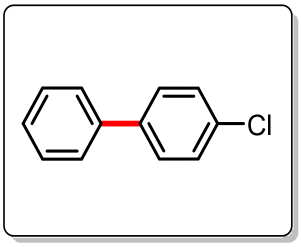	4-Chloro-1,1'-biphenyl (**8ba**)[13,15] **8ba** was isolated by thin layer chromatography (hexane/EtOAc: 95/5) gave the product as yellow solid (52%). **^{1}H NMR (400 MHz, CDCl$_3$)** δ 7.60 – 7.50 (m, 4H), 7.48 – 7.35 (m, 5H). **^{13}C NMR (100 MHz, CDCl$_3$)** δ 140.2, 139.9, 133.6, 129.1, 129.1, 128.6, 127.8, 127.2. **HRMS (APCI-TOF) m/z:** [M+H]$^+$ calcd for $C_{12}H_{10}Cl$, 189,0466; found 189,0481.
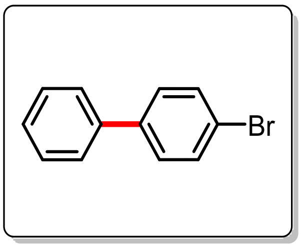	4-Bromo-1,1'-biphenyl (**8bb**)[15] **8bb** was isolated by thin layer chromatography (hexane/EtOAc: 95/5) gave the product as yellow solid (53%). **^{1}H NMR (400 MHz, CDCl$_3$)** δ 7.62 – 7.50 (m, 4H), 7.51 – 7.41 (m, 4H), 7.40 – 7.34 (m, 1H). **^{13}C NMR (100 MHz, CDCl$_3$)** δ 140.4, 140.2, 132.1, 129.1, 129.0, 127.9, 127.2, 121.8. **HRMS (APCI-TOF) m/z:** [M+H]$^+$ calcd for $C_{12}H_{10}Br$, 232,9960; found 232,9983.
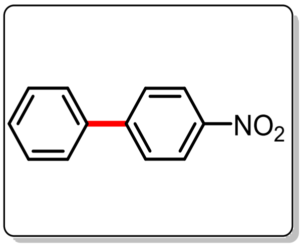	4-Nitro-1,1'-biphenyl (**8bc**)[13] **8bc** was isolated by thin layer chromatography (hexane/EtOAc: 95/5) gave the product as yellow solid (80%). **^{1}H NMR (400 MHz, CDCl$_3$)** δ 8.30 (d, *J* = 8.5 Hz, 2H), 7.74 (d, *J* = 8.5 Hz, 2H), 7.68 – 7.59 (m, 2H), 7.56 – 7.40 (m, 3H). **^{13}C NMR (100 MHz, CDCl$_3$)** δ 147.9, 139.7, 139.0, 129.4, 129.2, 128.0, 127.6, 124.3. **HRMS (APCI-TOF) m/z:** [M+H]$^+$ calcd for $C_{12}H_{10}NO_2$, 200,0706; found 200,0707.
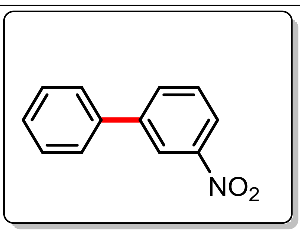	3-Nitro-1,1'-biphenyl (**8bd**)[15] **8bd** was isolated by thin layer chromatography (hexane/EtOAc: 95/5) gave the product as light yellow solid (84%). **^{1}H NMR (400 MHz, CDCl$_3$)** δ 8.45 (t, *J* = 2.0 Hz, 1H), 8.20 (dd, *J* = 8.2, 2.3 Hz, 1H), 7.95 – 7.87 (m, 1H), 7.65 – 7.58 (m, 3H), 7.50 (t, *J* = 7.6 Hz, 2H), 7.47 – 7.41 (m, 1H). **^{13}C NMR (100 MHz, CDCl$_3$)** δ 148.9, 143.1, 138.9, 133.3, 130.0, 129.4, 128.8, 127.4, 122.3, 122.2. **HRMS (APCI-TOF) m/z:** [M+H]$^+$ calcd for $C_{12}H_{10}NO_2$,

	200,0706; found 200,0724.
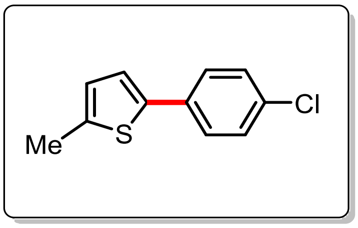	2-(4-Chlorophenyl)-5-methylthiophene (**6ba**)[21] The product could not be isolated. The yield was detected to be 8% by ^{1}H NMR analysis using 1,3-dinitrobenzene as an internal standard. **HRMS (APCI-TOF) m/z:** $[M+H]^+$ calcd for $C_{11}H_{10}ClS$, 209,0186; found 209,0171.
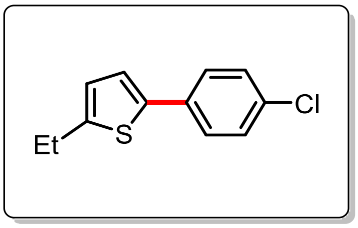	2-(4-Chlorophenyl)-5-ethylthiophene (**6bb**) The product could not be isolated. The yield was detected to be 17% by ^{1}H NMR analysis using 1,3-dinitrobenzene as an internal standard. **HRMS (APCI-TOF) m/z:** $[M]^+$ calcd for $C_{12}H_{11}ClS$, 222,0270; found 222,0272.
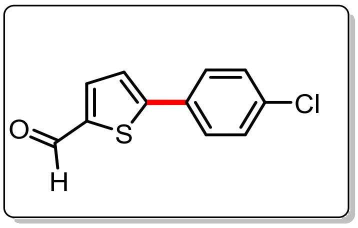	5-(4-Chlorophenyl)thiophene-2-carbaldehyde (**6bc**)[22] The product could not be isolated. The yield was detected to be trace by ^{1}H NMR analysis using 1,3-dinitrobenzene as an internal standard. **HRMS (APCI-TOF) m/z:** $[M+H]^+$ calcd for $C_{11}H_8ClOS$, 222,9979; found 222,9979.

Potential byproducts detected by HRMS for the related products

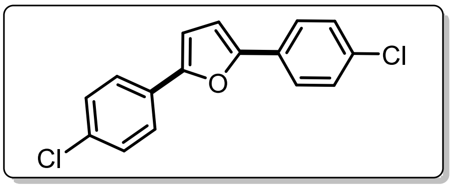	2,5-Bis(4-chlorophenyl)furan Potential byproducts were analyzed in trace yields and detected by mass spectroscopy. **HRMS (APCI-TOF) m/z:** $[M+H]^+$ calcd for $C_{16}H_{11}Cl_2O$, 289,0181; found 289,0215.
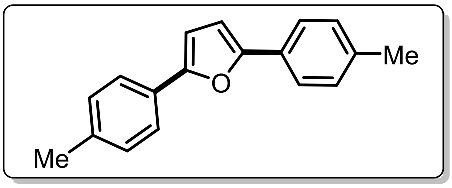	2,5-Di-*p*-tolylfuran Potential byproducts were analyzed in trace yields and detected by mass spectroscopy. **HRMS (APCI-TOF) m/z:** $[M+H]^+$ calcd for $C_{18}H_{17}O$, 249,1274; found 249,1264.
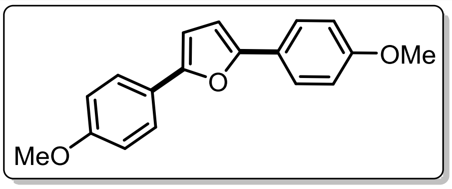	2,5-Bis(4-methoxyphenyl)furan Potential byproducts were analyzed in trace yields and detected by mass spectroscopy. **HRMS (APCI-TOF) m/z:** $[M+H]^+$ calcd for $C_{18}H_{17}O_3$, 281,1172; found 281,1172.
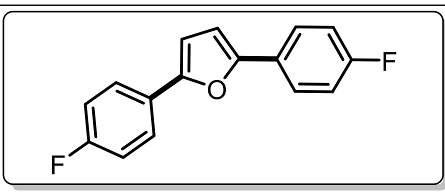	2,5-Bis(4-fluorophenyl)furan Potential byproducts were analyzed in trace yields and detected by mass spectroscopy. **HRMS (APCI-TOF) m/z:** $[M+H]^+$ calcd for $C_{16}H_{11}F_2O$, 257,0772; found 257,0803.
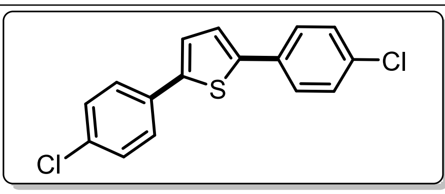	2,5-Bis(4-chlorophenyl)thiophene Potential byproducts were analyzed in trace yields and detected by mass spectroscopy. **HRMS (APCI-TOF) m/z:** $[M]^+$ calcd for $C_{16}H_{10}Cl_2S$, 303,9875; found 303,9895.

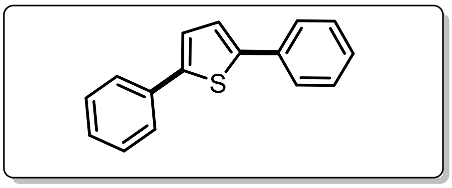	2,5-Diphenylthiophene Potential byproducts were analyzed in trace yields and detected by mass spectroscopy. **HRMS (APCI-TOF) m/z:** $[M+H]^+$ calcd for $C_{16}H_{13}S$, 237,0732; found 237,0732.
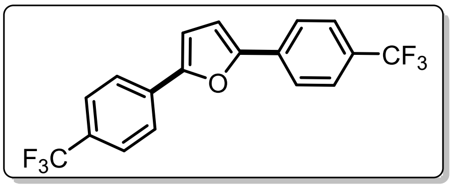	2,5-Bis(4-(trifluoromethyl)phenyl)furan Potential byproducts were analyzed in trace yields and detected by mass spectroscopy. **HRMS (APCI-TOF) m/z:** $[M]^+$ calcd for $C_{18}H_{10}F_6S$, 372,0402; found 372,0437.

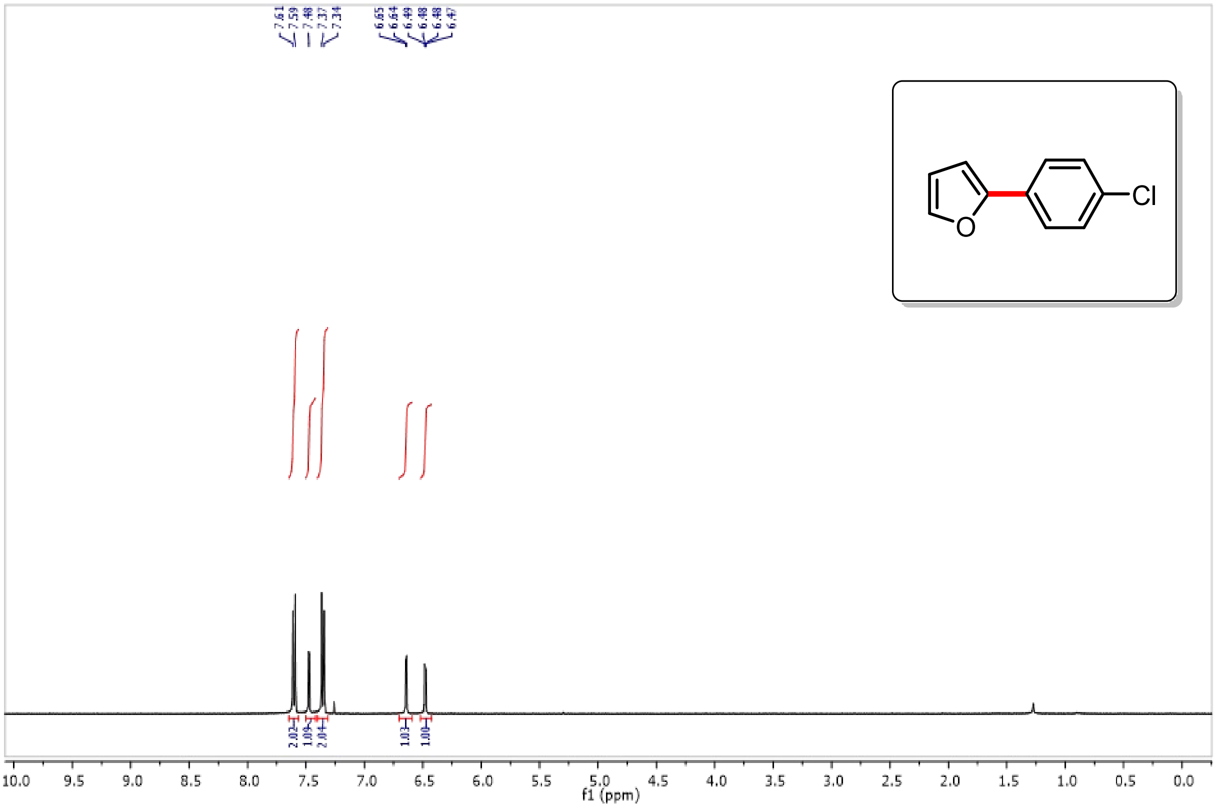

2. NMR spectral data for the arylation products

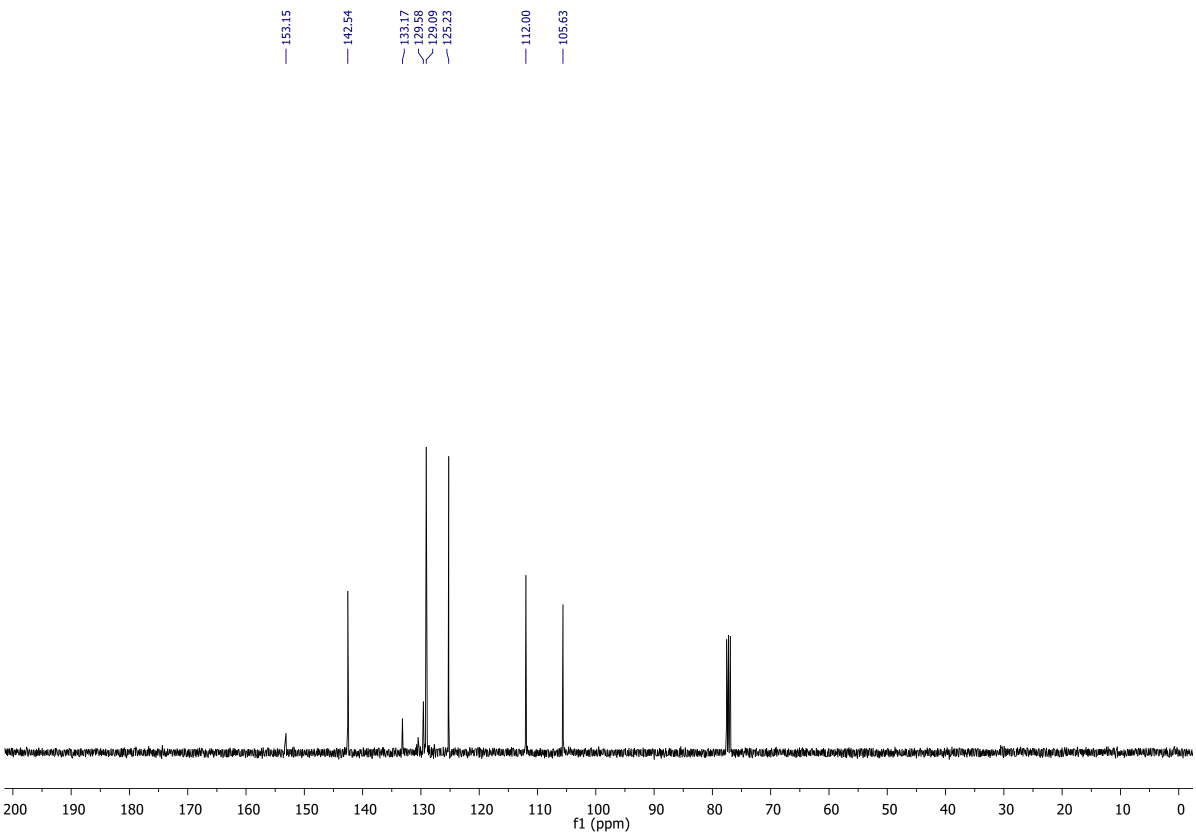

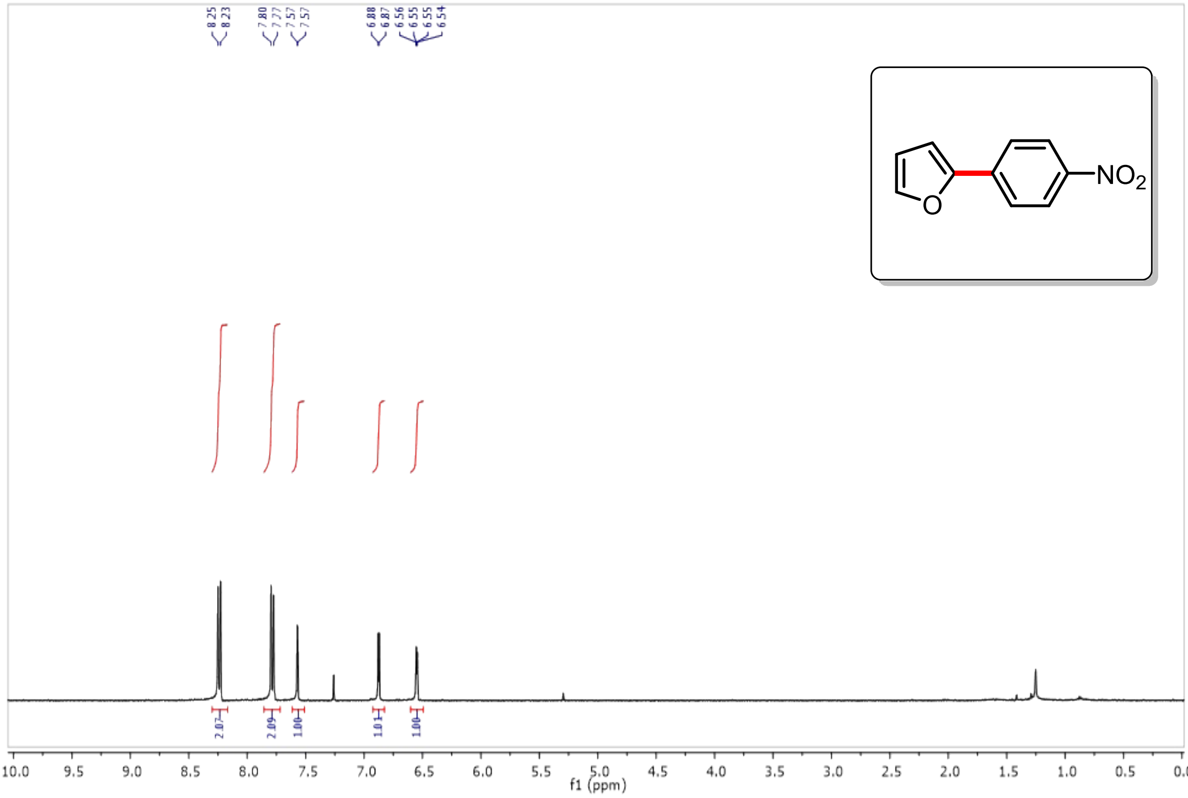
8.25
8.23
7.80
7.77
7.57
7.57
6.88
6.87
6.56
6.55
6.55
6.54
NO2
O
2.07
2.09
1.00
1.01
1.00
10.0 9.5 9.0 8.5 8.0 7.5 7.0 6.5 6.0 5.5 5.0 4.5 4.0 3.5 3.0 2.5 2.0 1.5 1.0 0.5 0.0
f1 (ppm)

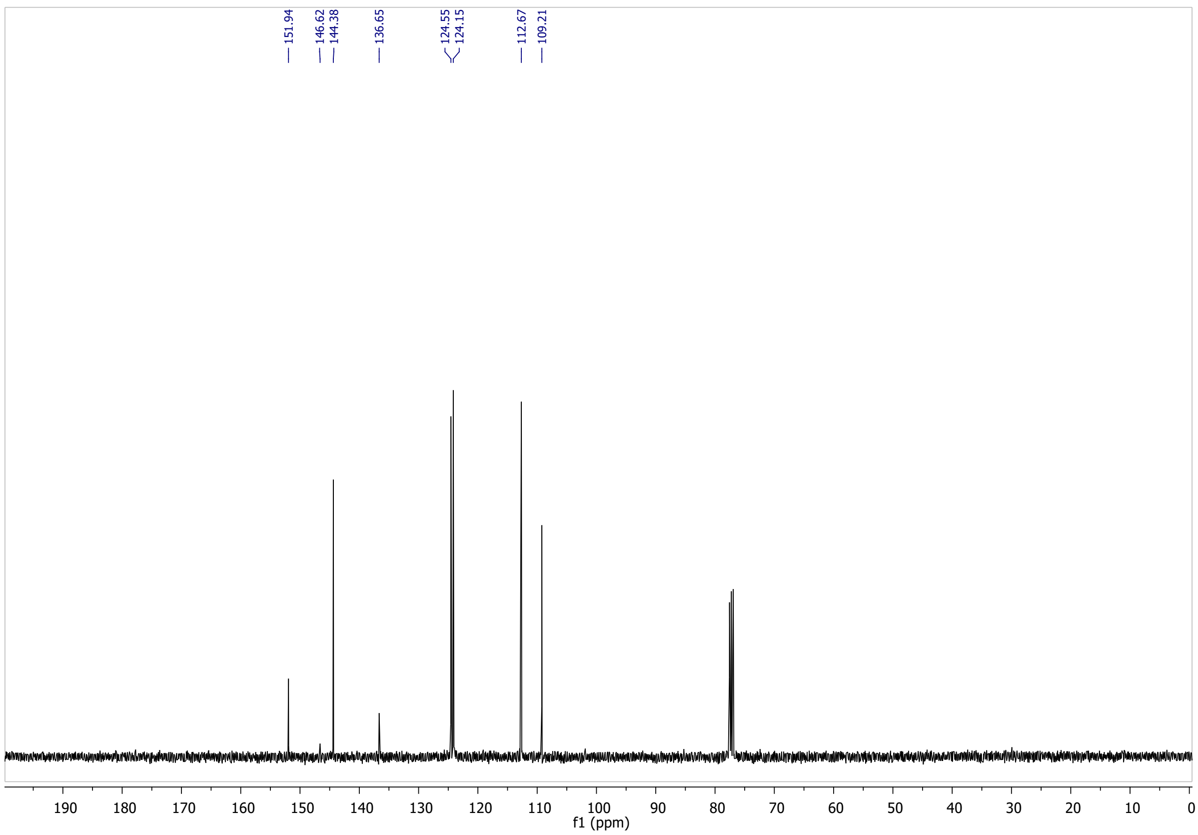
151.94
146.62
144.38
136.65
124.55
124.15
112.67
109.21
190 180 170 160 150 140 130 120 110 100 90 80 70 60 50 40 30 20 10 0
f1 (ppm)

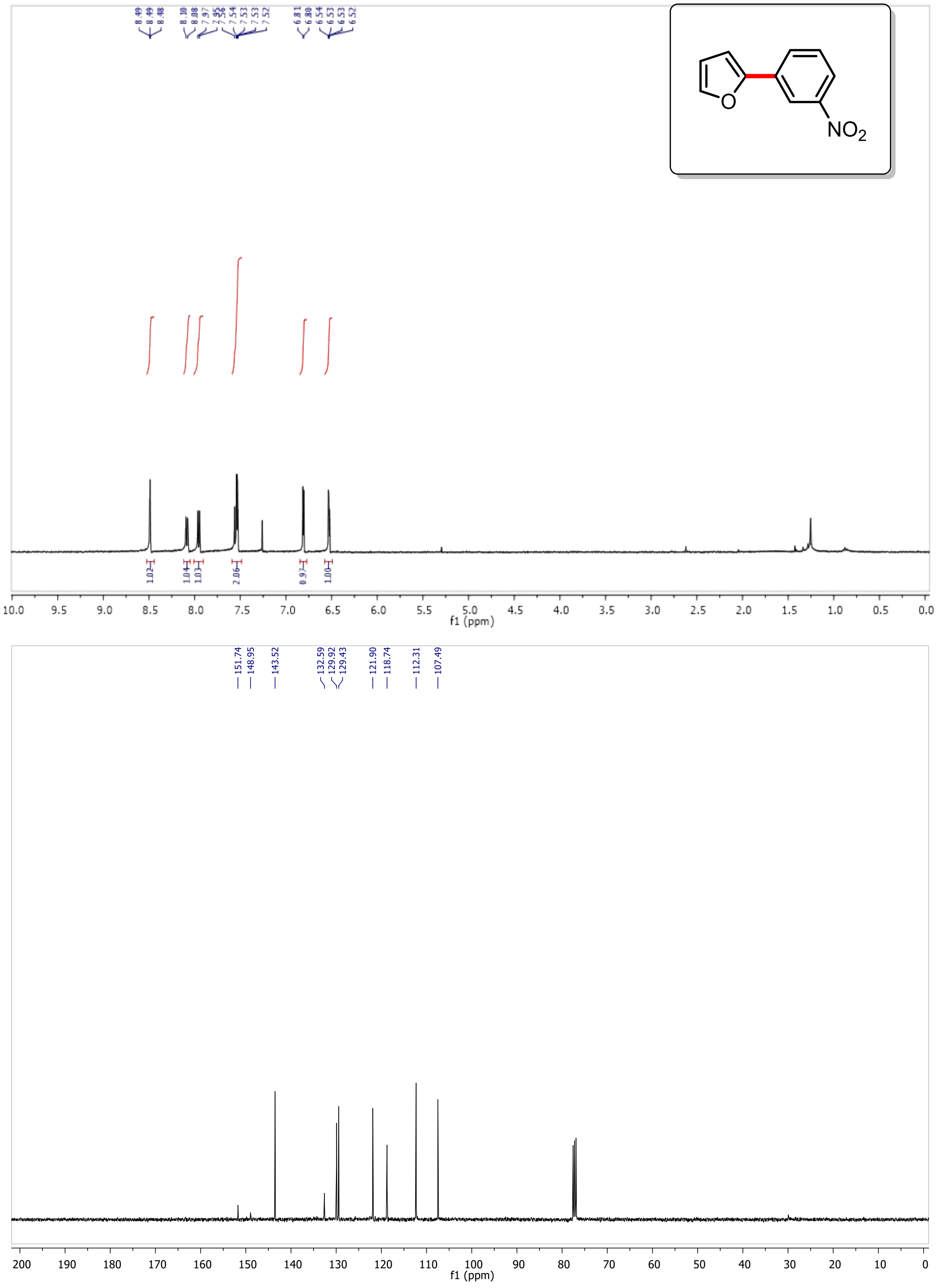
8.49
8.49
8.48
8.10
8.08
7.97
7.95
7.56
7.54
7.53
7.53
7.52
6.81
6.80
6.54
6.53
6.53
6.52
NO2
O
1.02
1.04
1.03
2.06
0.97
1.00
f1 (ppm)
151.74
148.95
143.52
132.59
129.92
129.43
121.90
118.74
112.31
107.49
f1 (ppm)

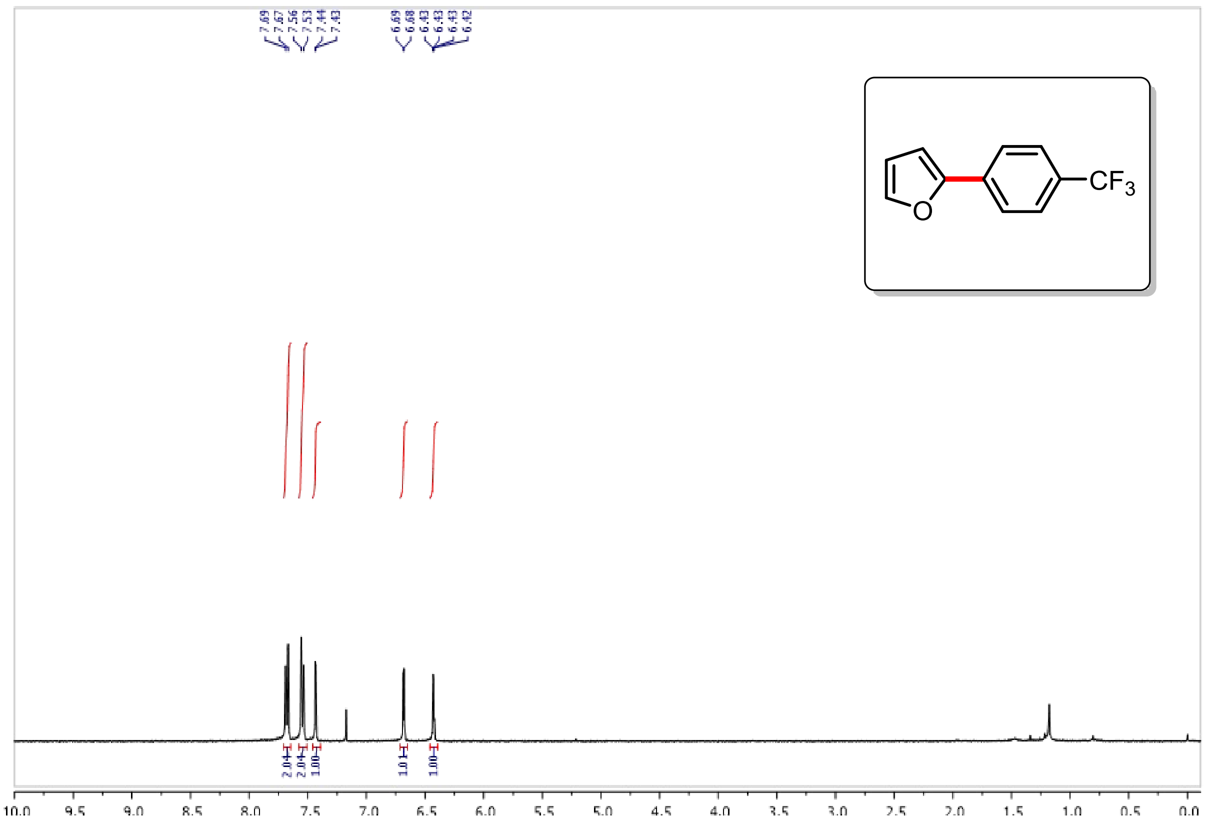

7.69
7.67
7.56
7.53
7.44
7.43
6.69
6.68
6.43
6.43
6.43
6.42
CF3
O
2.04
2.04
1.00
1.01
1.00
10.0 9.5 9.0 8.5 8.0 7.5 7.0 6.5 6.0 5.5 5.0 4.5 4.0 3.5 3.0 2.5 2.0 1.5 1.0 0.5 0.0

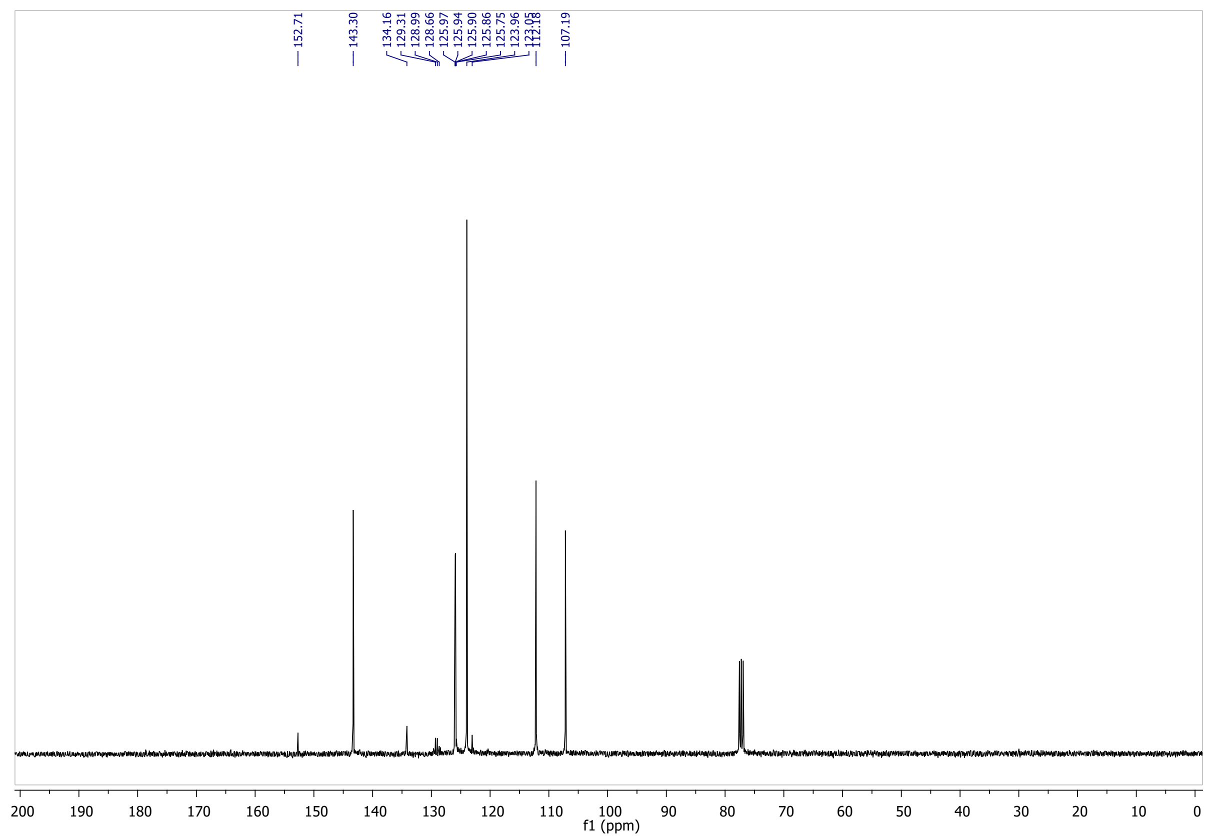

152.71
143.30
134.16
129.31
128.99
128.66
125.97
125.94
125.90
125.86
125.75
123.96
123.05
112.18
107.19
200 190 180 170 160 150 140 130 120 110 100 90 80 70 60 50 40 30 20 10 0
f1 (ppm)

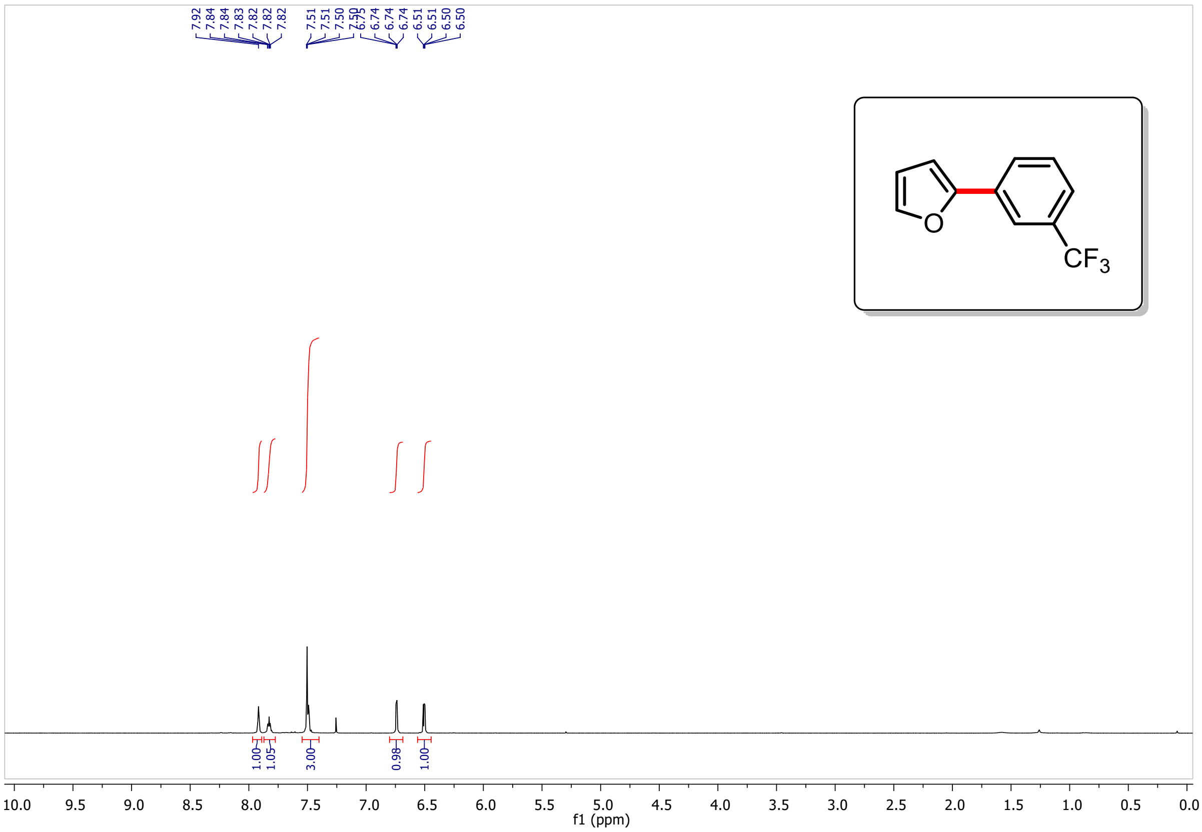
7.92
7.84
7.84
7.83
7.82
7.82
7.82
7.51
7.51
7.50
7.50
6.75
6.74
6.74
6.74
6.51
6.51
6.50
6.50
CF_3
O
1.00
1.05
3.00
0.98
1.00
f1 (ppm)

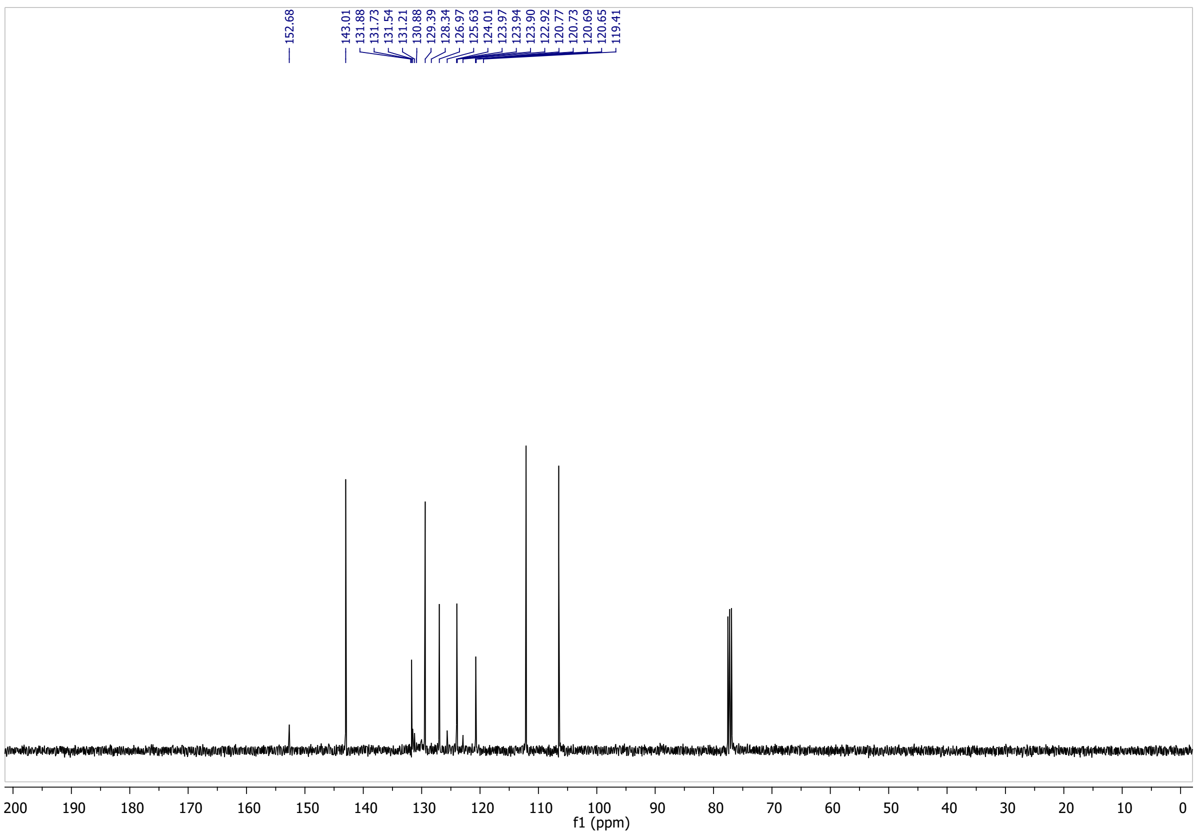
152.68
143.01
131.88
131.73
131.54
131.21
130.88
129.39
128.34
126.97
125.63
124.01
123.97
123.94
123.90
122.92
120.77
120.73
120.69
120.65
119.41
f1 (ppm)

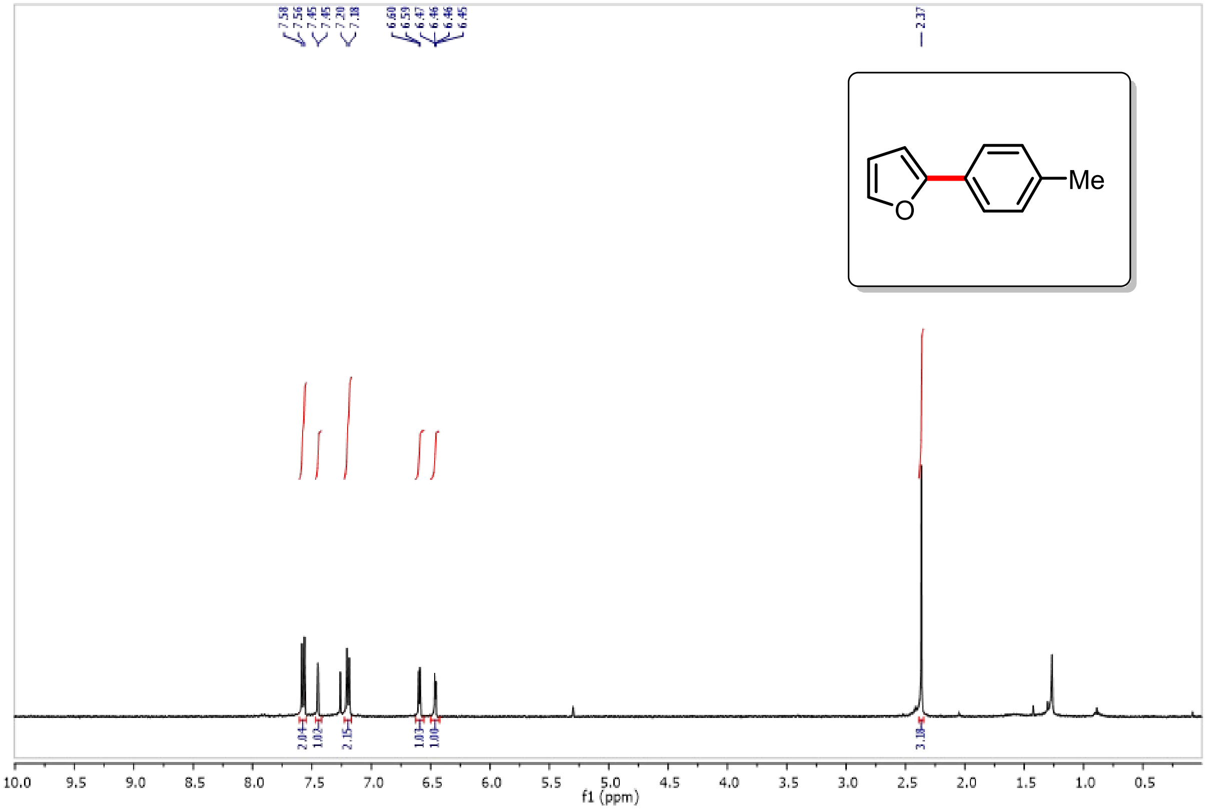
7.58
7.56
7.45
7.45
7.20
7.18
6.60
6.59
6.47
6.46
6.46
6.45
2.37
Me
O
2.04
1.02
2.15
1.03
1.00
3.18
10.0
9.5
9.0
8.5
8.0
7.5
7.0
6.5
6.0
5.5
5.0
4.5
4.0
3.5
3.0
2.5
2.0
1.5
1.0
0.5
f1 (ppm)

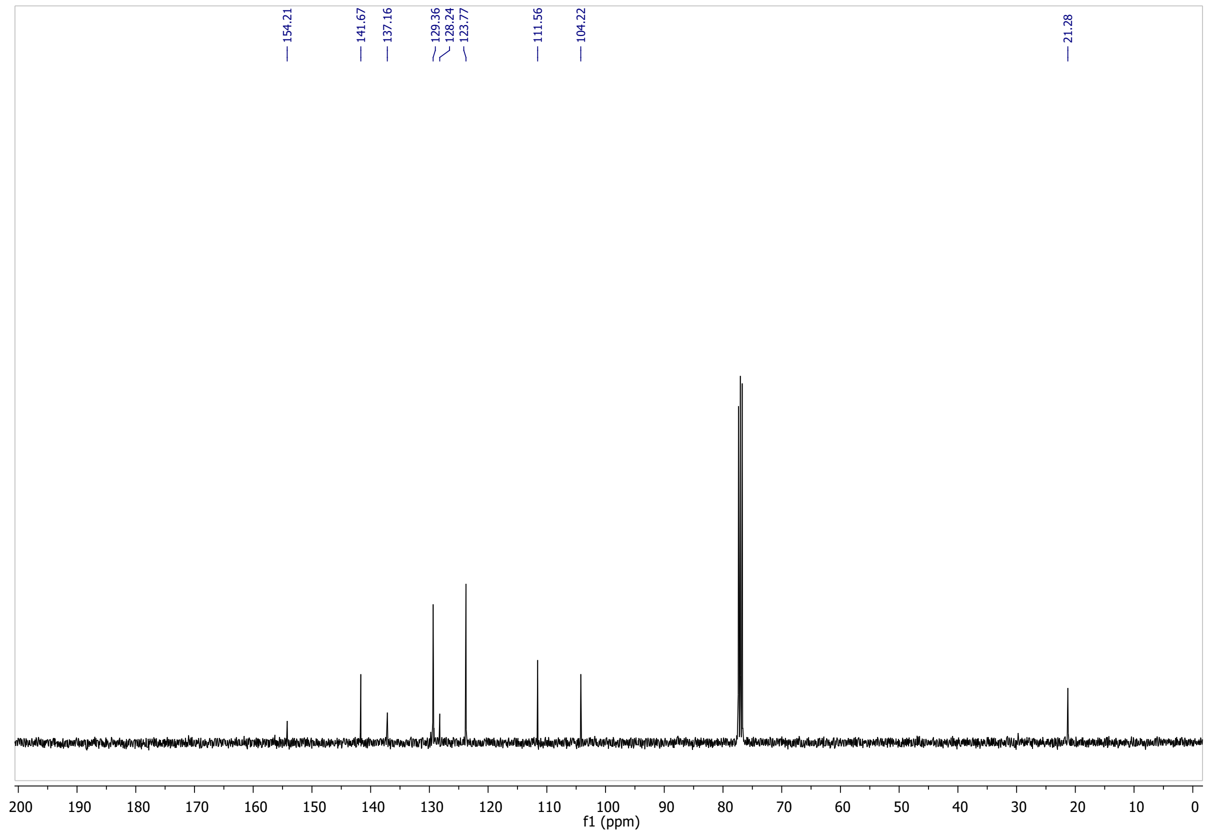
154.21
141.67
137.16
129.36
128.24
123.77
111.56
104.22
21.28
200
190
180
170
160
150
140
130
120
110
100
90
80
70
60
50
40
30
20
10
0
f1 (ppm)

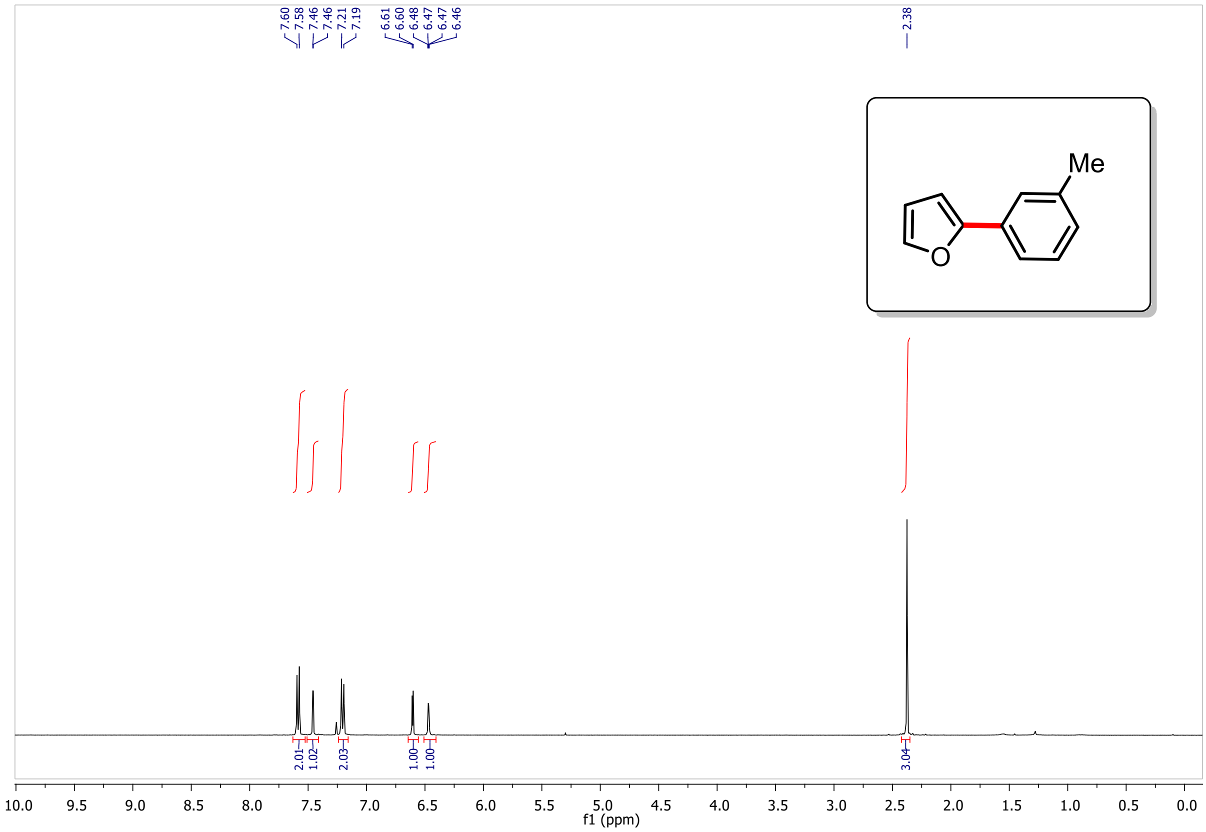
7.60
7.58
7.46
7.46
7.21
7.19
6.61
6.60
6.48
6.47
6.47
6.46
2.38
Me
O
2.01
1.02
2.03
1.00
1.00
3.04
f1 (ppm)

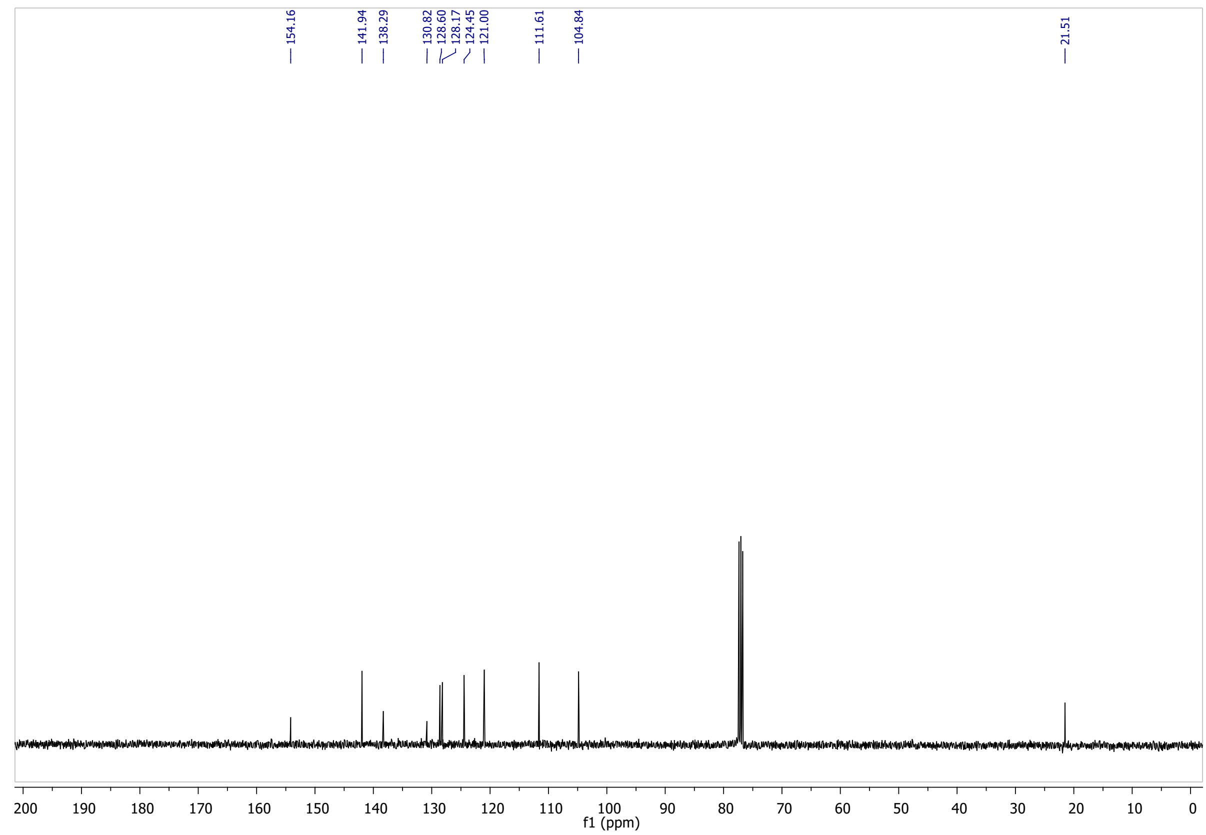
154.16
141.94
138.29
130.82
128.60
128.17
124.45
121.00
111.61
104.84
21.51
f1 (ppm)

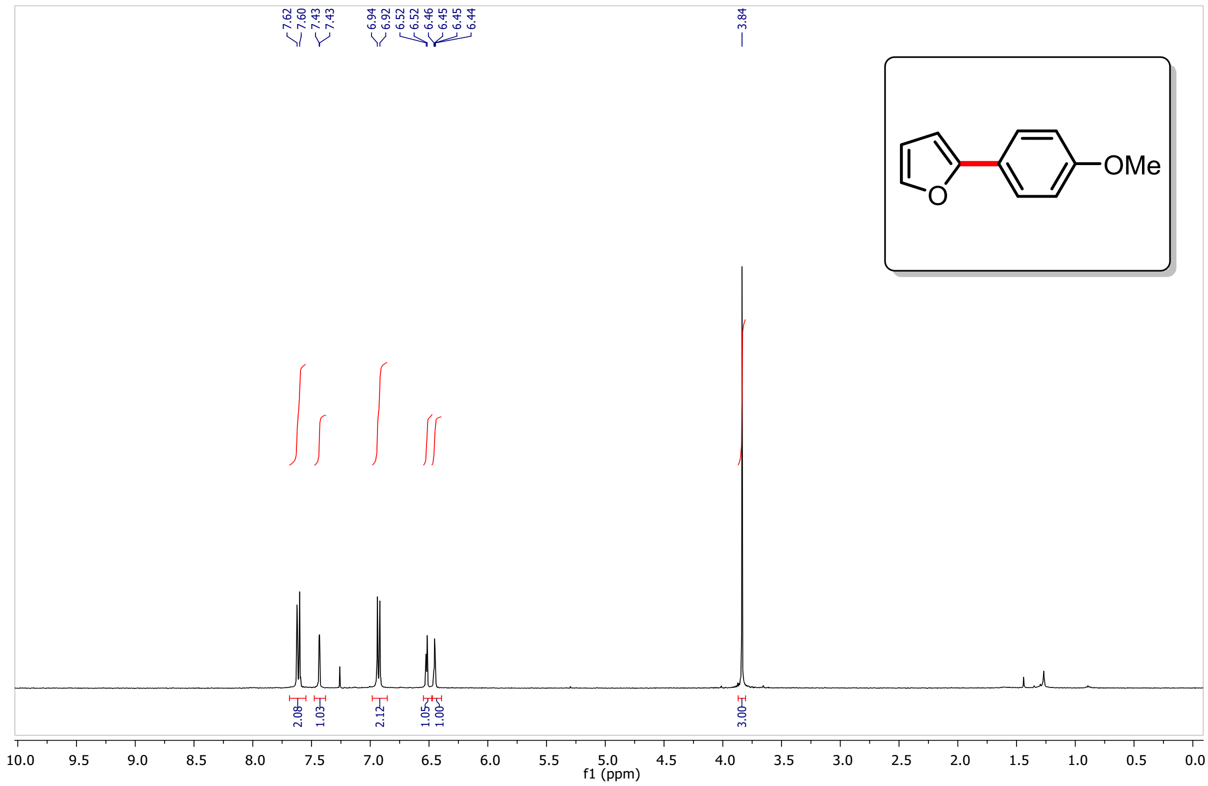
7.62
7.60
7.43
7.43
6.94
6.92
6.52
6.52
6.46
6.45
6.45
6.44
3.84
OMe
O
2.08
1.03
2.12
1.05
1.00
3.00
10.0 9.5 9.0 8.5 8.0 7.5 7.0 6.5 6.0 5.5 5.0 4.5 4.0 3.5 3.0 2.5 2.0 1.5 1.0 0.5 0.0
f1 (ppm)

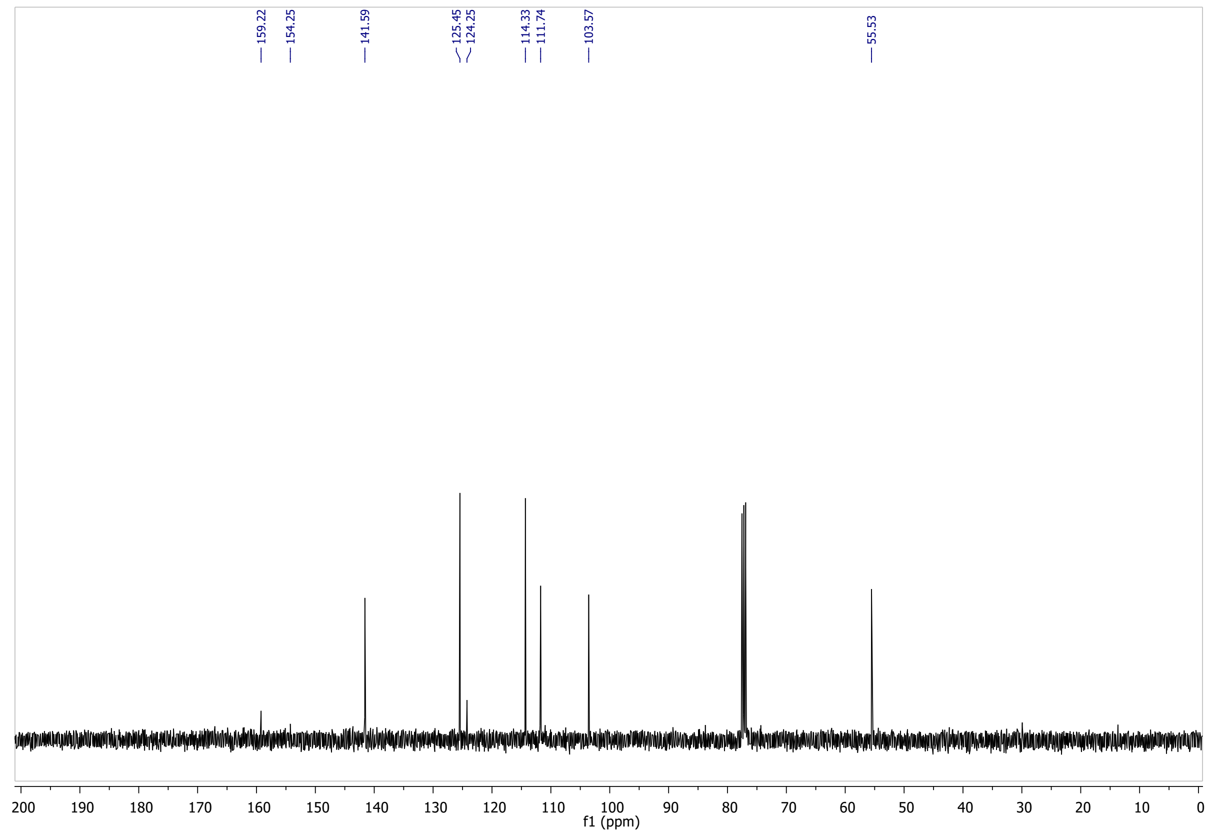
159.22
154.25
141.59
125.45
124.25
114.33
111.74
103.57
55.53
200 190 180 170 160 150 140 130 120 110 100 90 80 70 60 50 40 30 20 10 0
f1 (ppm)

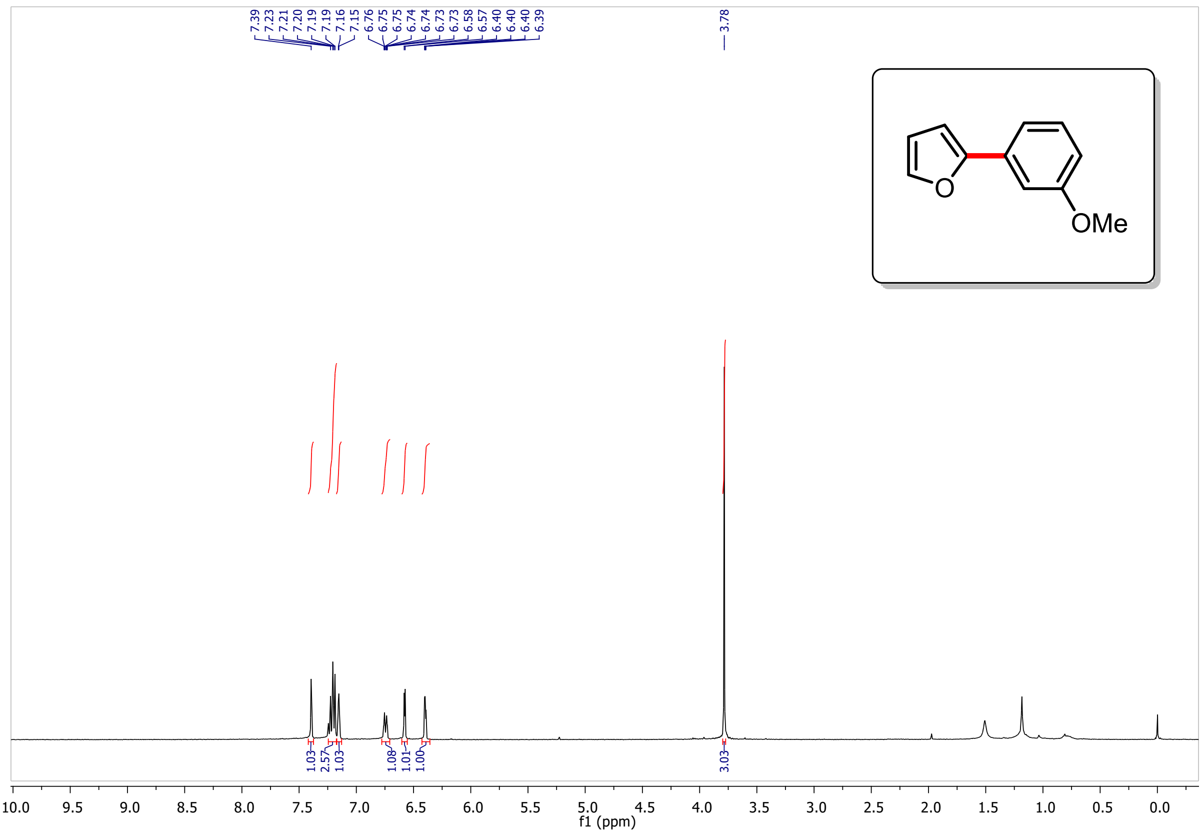

7.39
7.23
7.21
7.20
7.19
7.19
7.16
7.15
6.76
6.75
6.75
6.74
6.74
6.73
6.73
6.58
6.57
6.40
6.40
6.40
6.39
3.78
OMe
1.03
2.57
1.03
1.08
1.01
1.00
3.03
10.0
9.5
9.0
8.5
8.0
7.5
7.0
6.5
6.0
5.5
5.0
4.5
4.0
3.5
3.0
2.5
2.0
1.5
1.0
0.5
0.0
f1 (ppm)

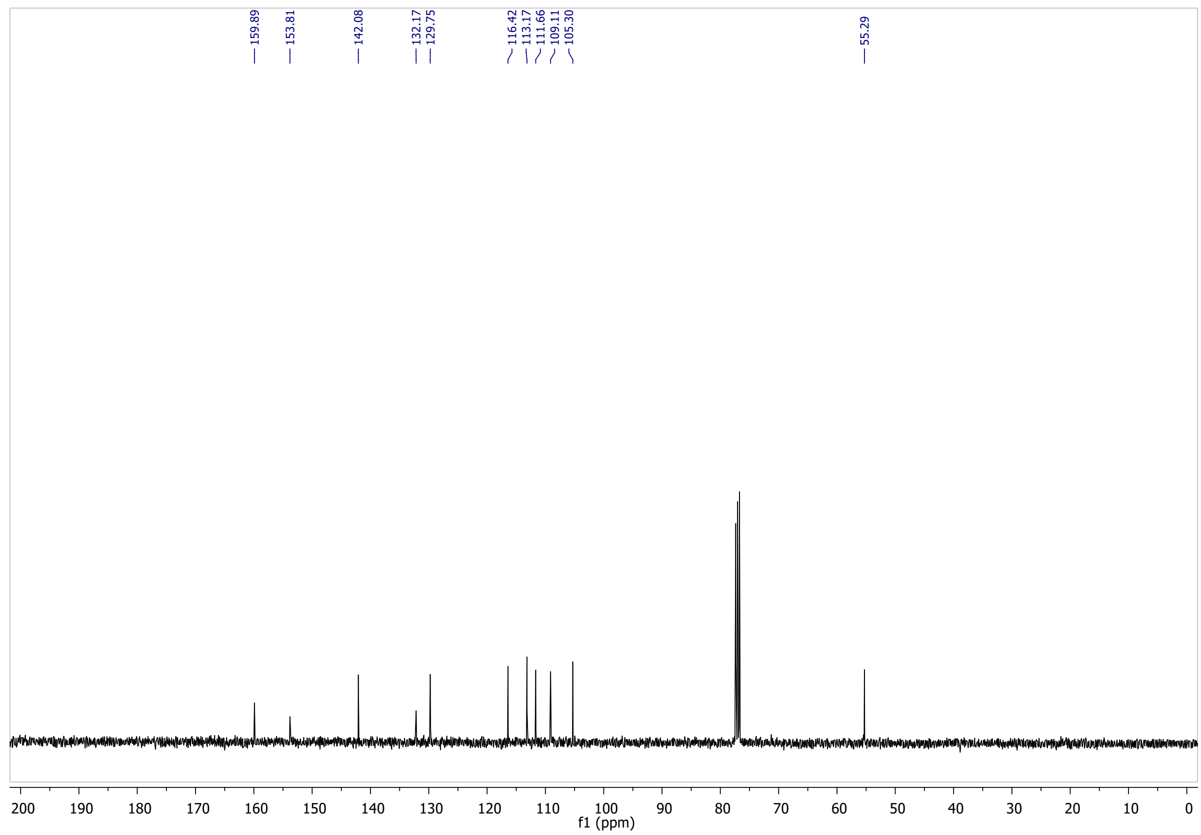

159.89
153.81
142.08
132.17
129.75
116.42
113.17
111.66
109.11
105.30
55.29
200
190
180
170
160
150
140
130
120
110
100
90
80
70
60
50
40
30
20
10
0
f1 (ppm)

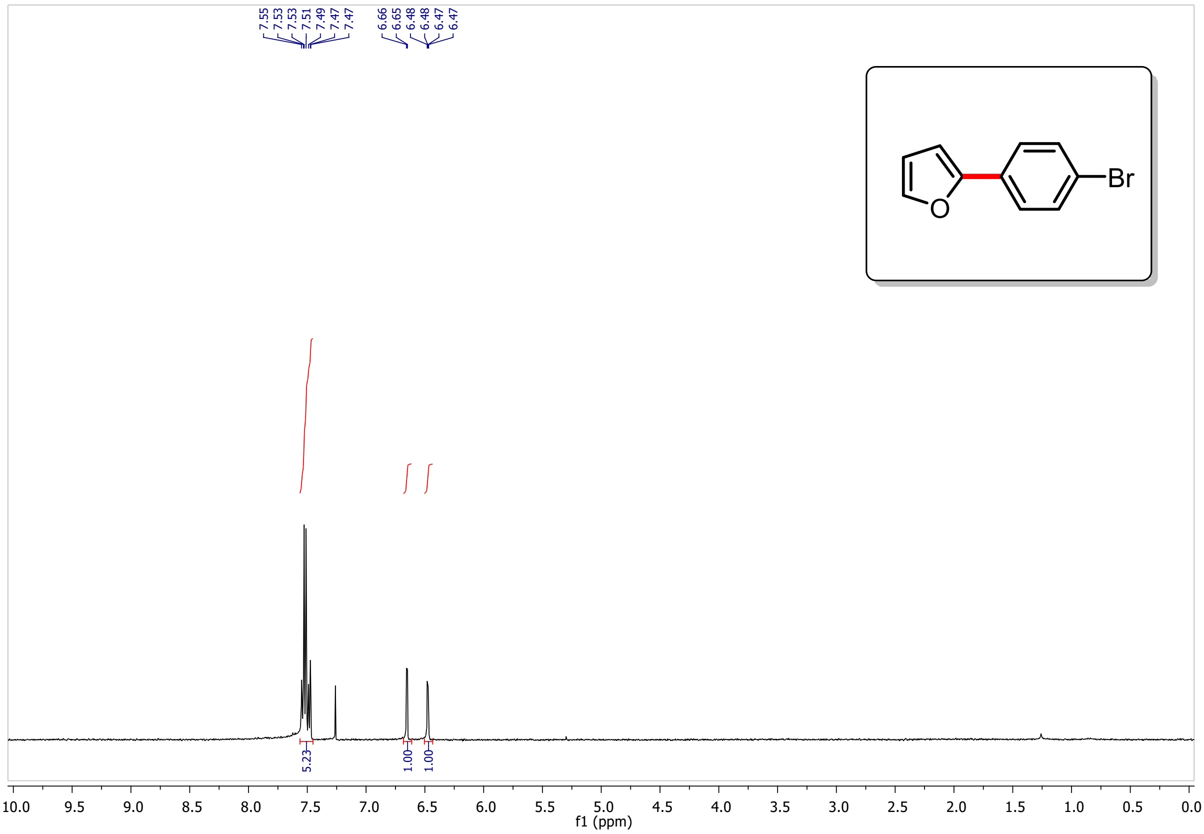
7.55
7.53
7.53
7.51
7.49
7.47
7.47
6.66
6.65
6.48
6.48
6.47
6.47
Br
O
5.23
1.00
1.00
10.0
9.5
9.0
8.5
8.0
7.5
7.0
6.5
6.0
5.5
5.0
4.5
4.0
3.5
3.0
2.5
2.0
1.5
1.0
0.5
0.0
f1 (ppm)

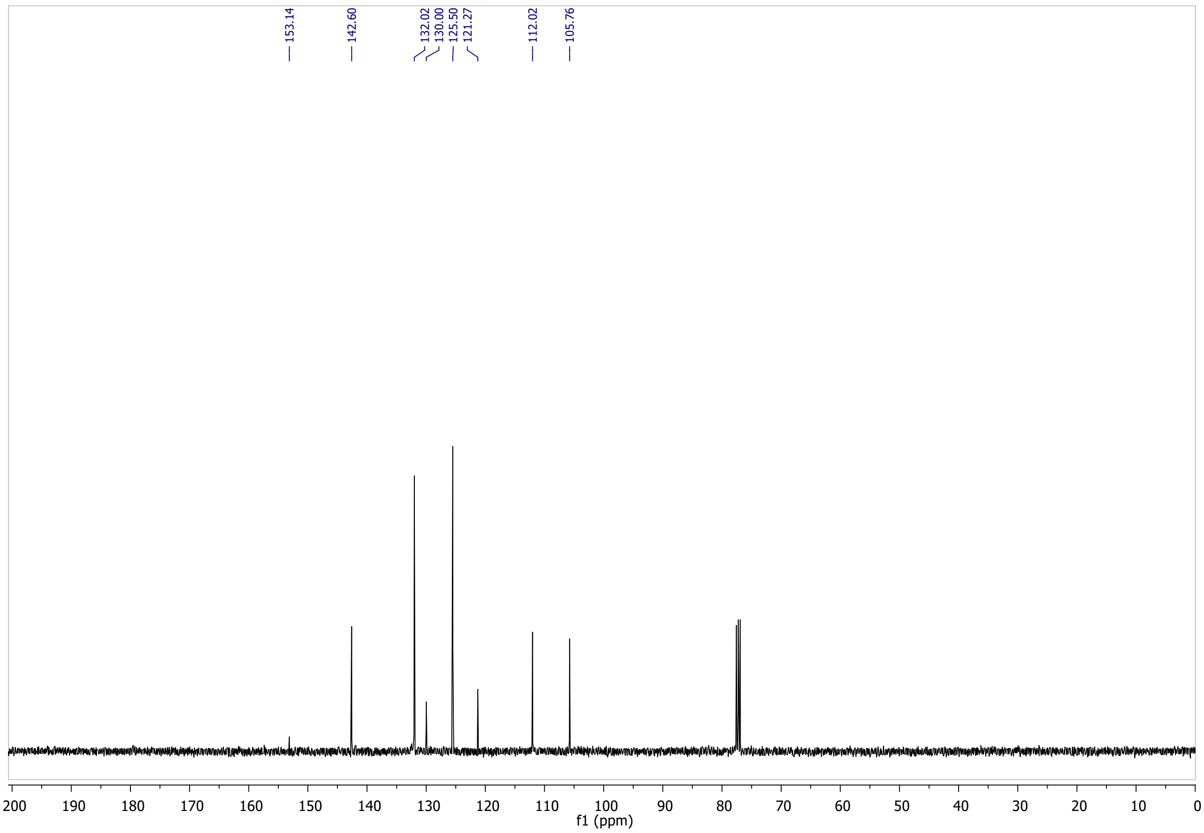
153.14
142.60
132.02
130.00
125.50
121.27
112.02
105.76
200
190
180
170
160
150
140
130
120
110
100
90
80
70
60
50
40
30
20
10
0
f1 (ppm)

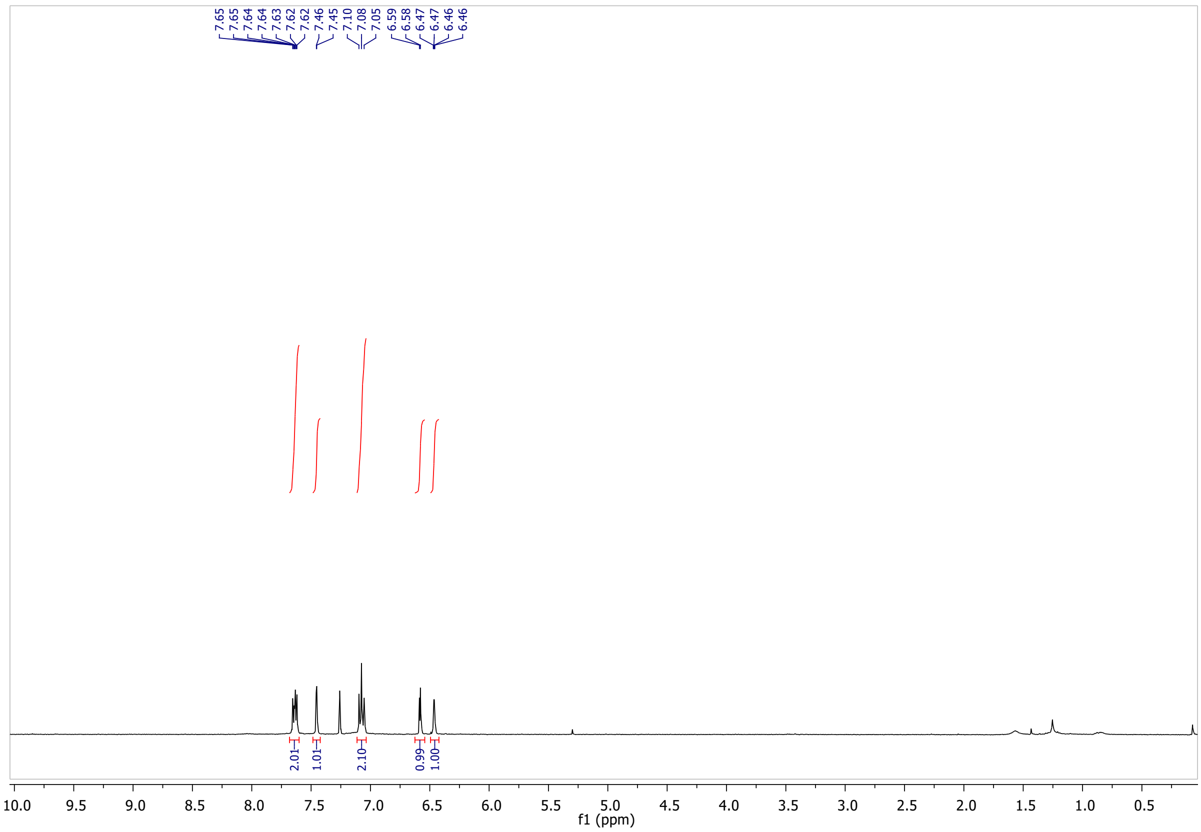
7.65
7.65
7.64
7.64
7.63
7.62
7.62
7.46
7.45
7.10
7.08
7.05
6.59
6.58
6.47
6.47
6.46
6.46
2.01
1.01
2.10
0.99
1.00
10.0
9.5
9.0
8.5
8.0
7.5
7.0
6.5
6.0
5.5
5.0
4.5
4.0
3.5
3.0
2.5
2.0
1.5
1.0
0.5
f1 (ppm)

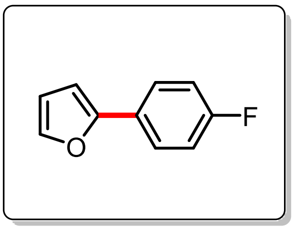
O
F

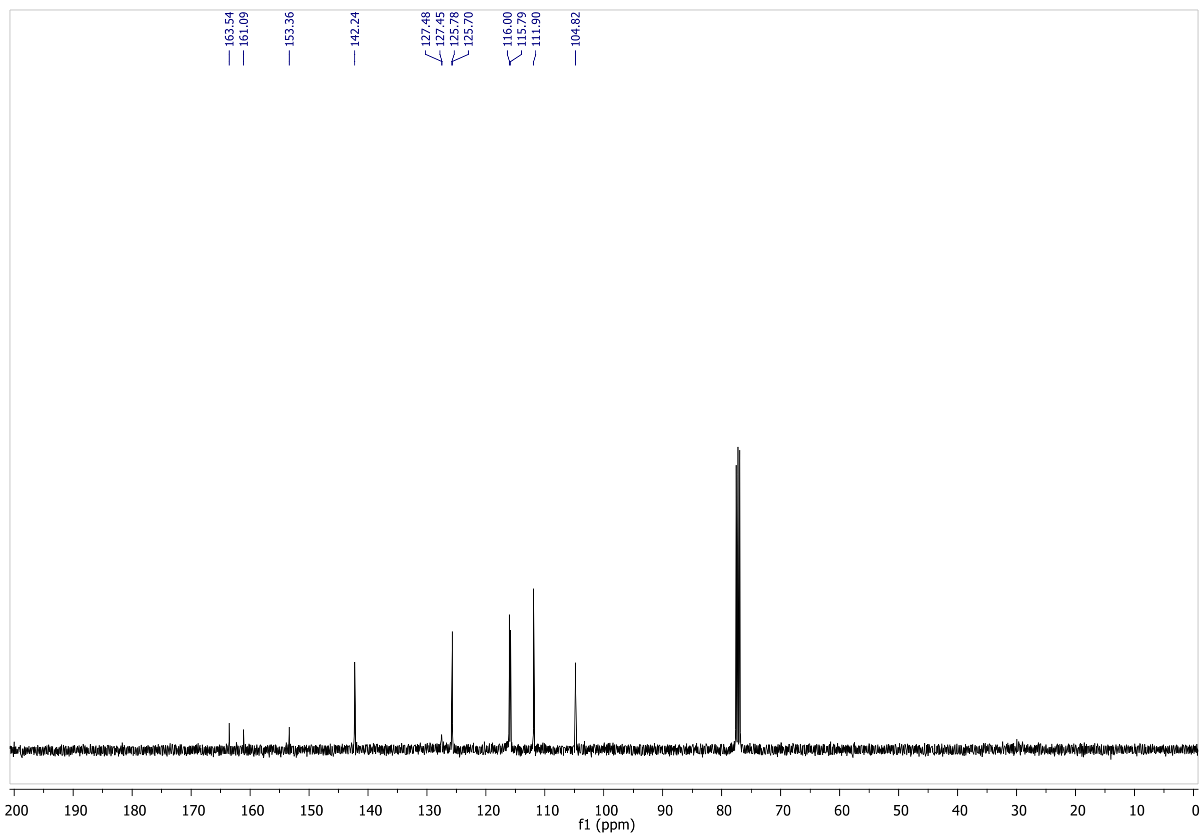
163.54
161.09
153.36
142.24
127.48
127.45
125.78
125.70
116.00
115.79
111.90
104.82
f1 (ppm)

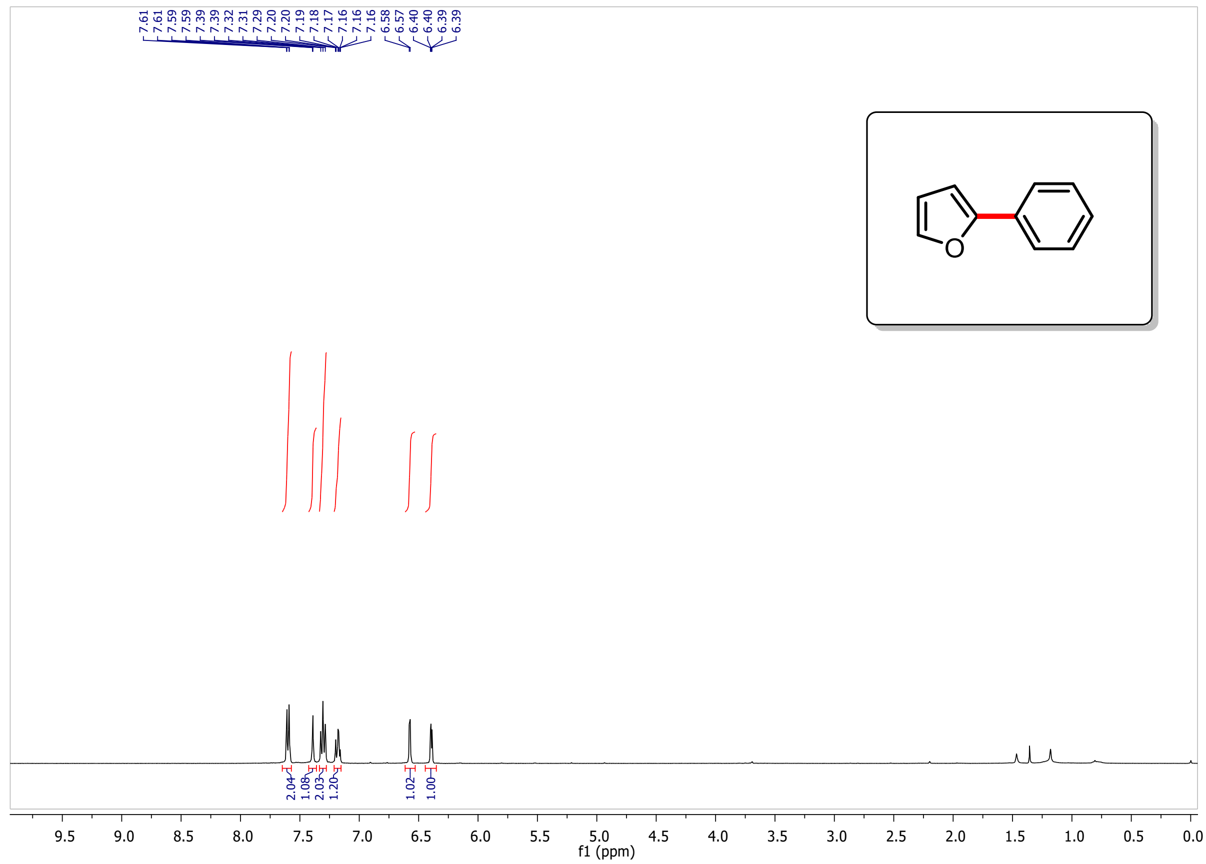
7.61
7.61
7.59
7.59
7.39
7.39
7.32
7.31
7.29
7.20
7.20
7.19
7.18
7.17
7.16
7.16
6.58
6.57
6.40
6.40
6.39
6.39
2.04
1.08
2.03
1.20
1.02
1.00
O
f1 (ppm)

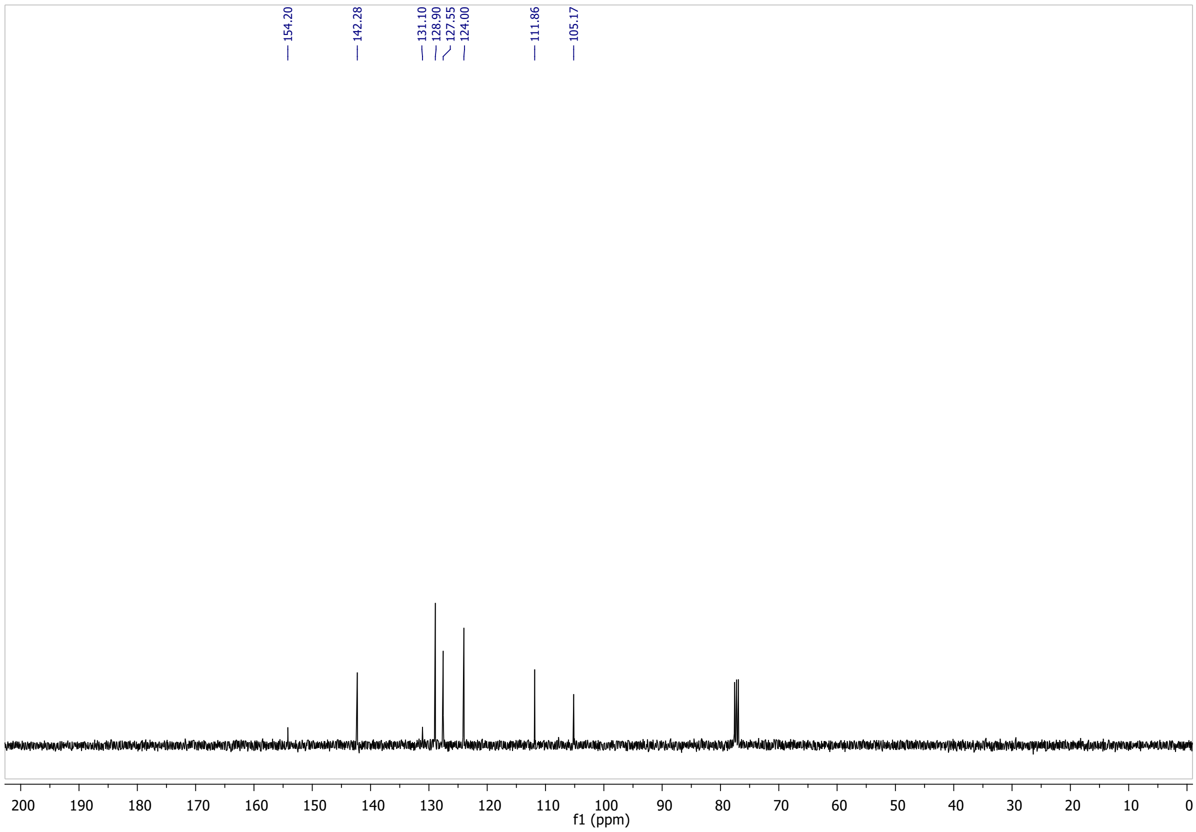
154.20
142.28
131.10
128.90
127.55
124.00
111.86
105.17
f1 (ppm)

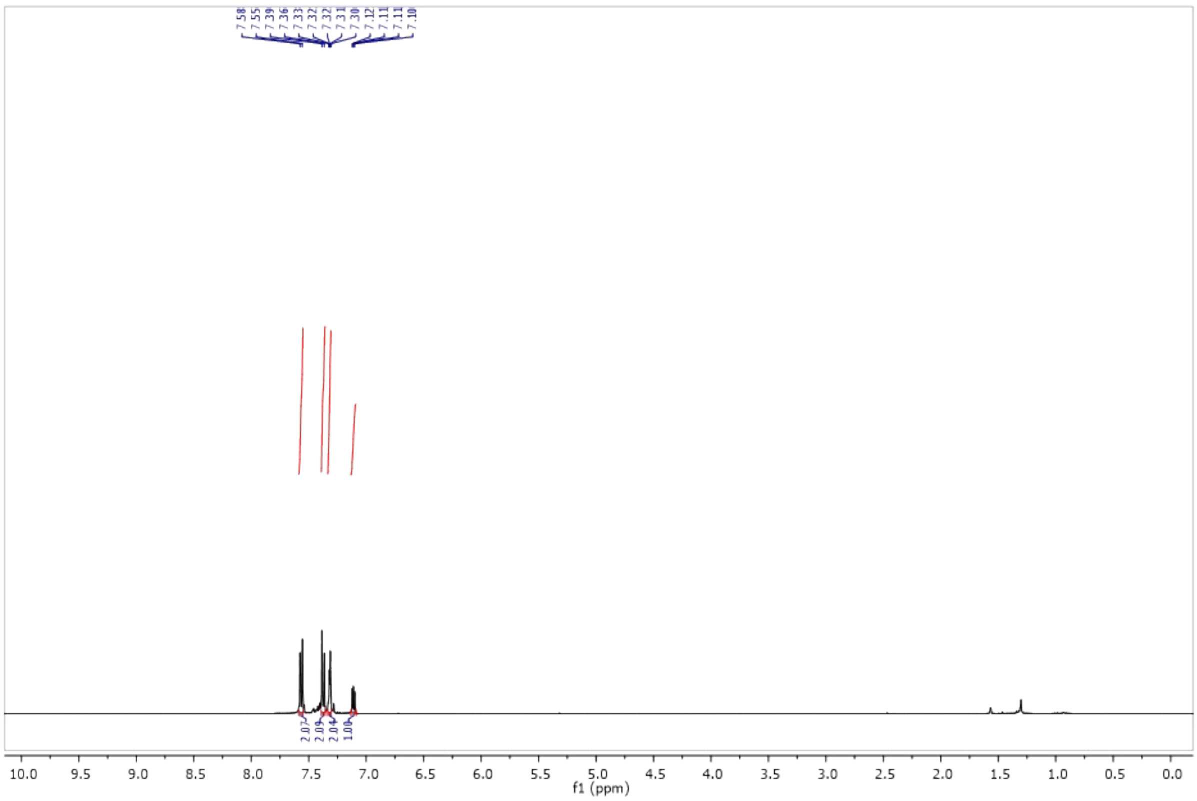
7.58
7.55
7.39
7.36
7.33
7.32
7.32
7.31
7.30
7.12
7.11
7.11
7.10
2.07
2.09
2.04
1.00
f1 (ppm)

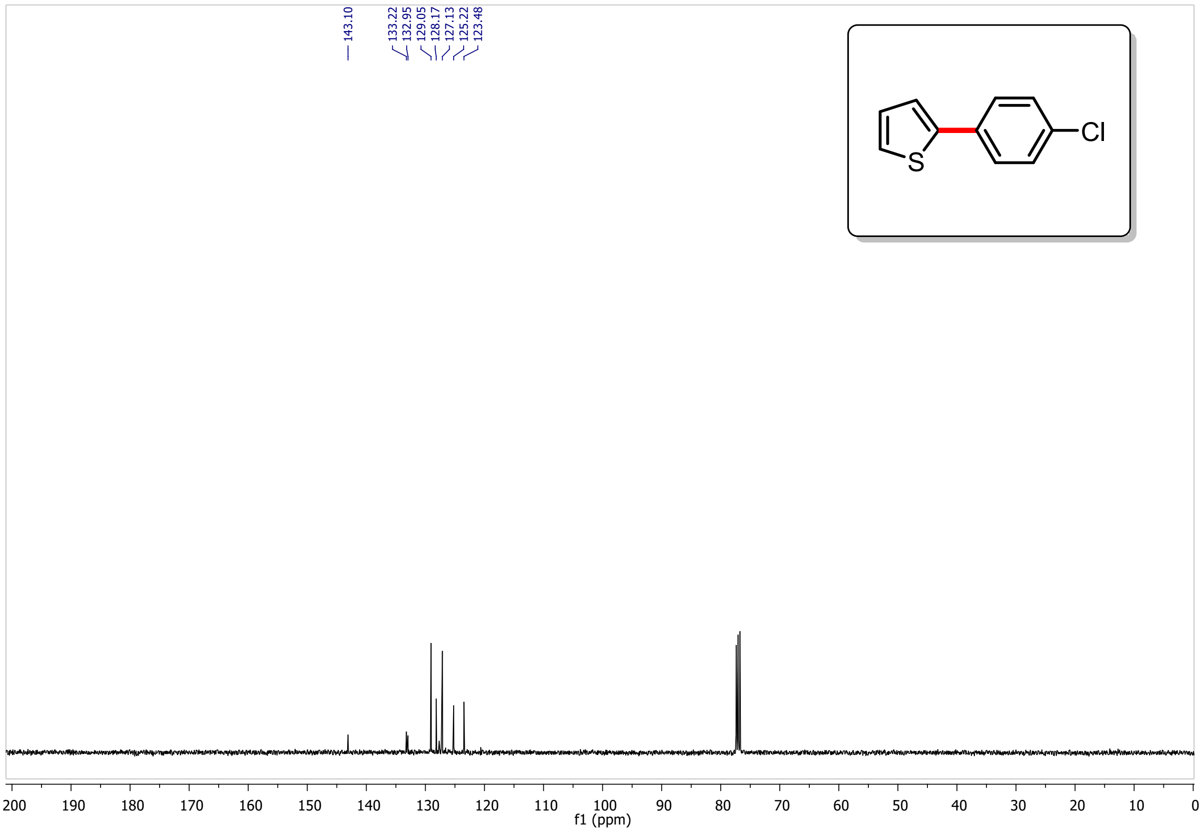

143.10
133.22
132.95
129.05
128.17
127.13
125.22
123.48
Cl
S
200 190 180 170 160 150 140 130 120 110 100 90 80 70 60 50 40 30 20 10 0
f1 (ppm)

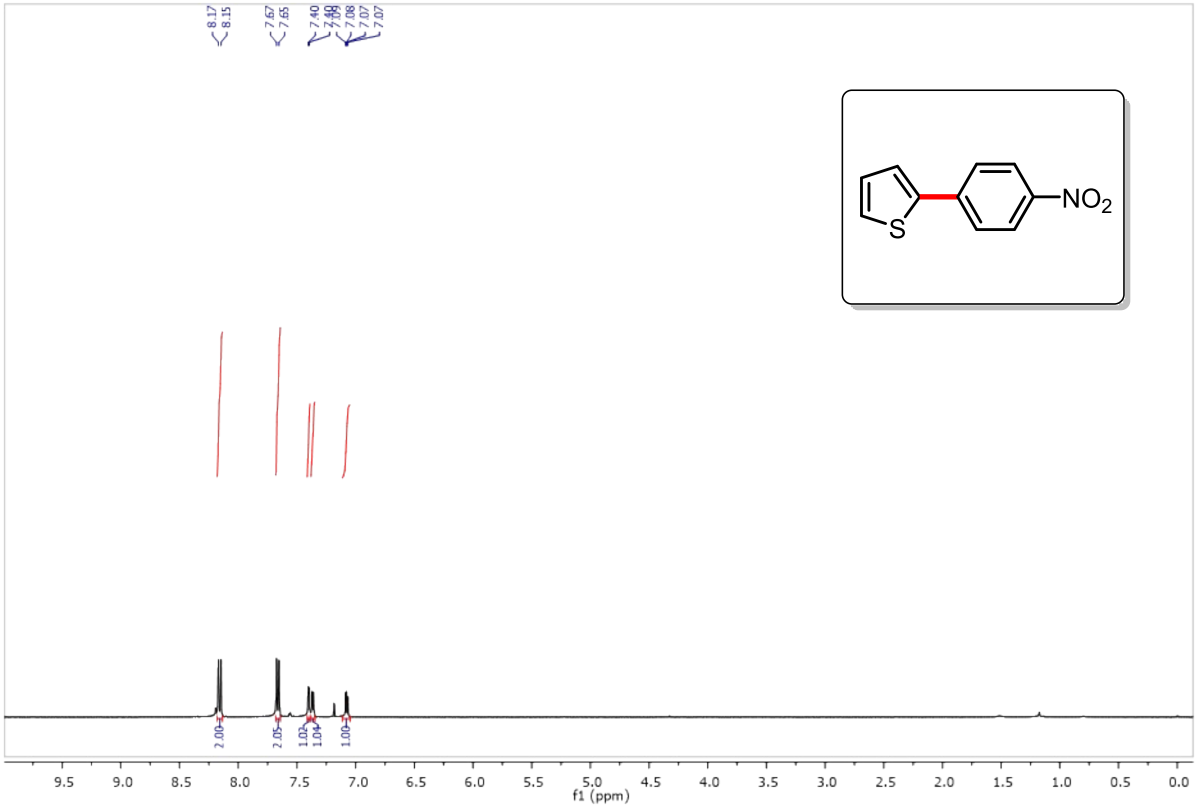
8.17
8.15
7.67
7.65
7.40
7.08
7.07
7.07
2.00
2.05
1.02
1.04
1.00
NO2
S
f1 (ppm)

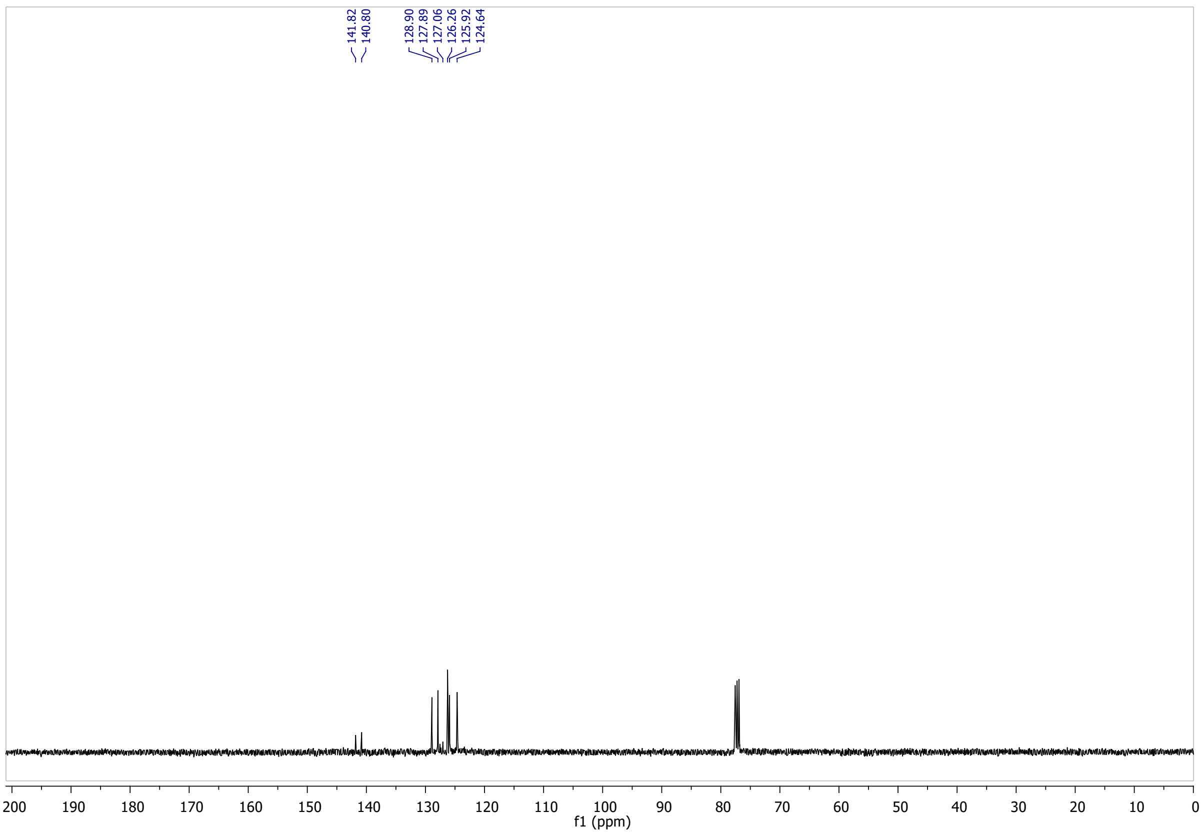
141.82
140.80
128.90
127.89
127.06
126.26
125.92
124.64
f1 (ppm)

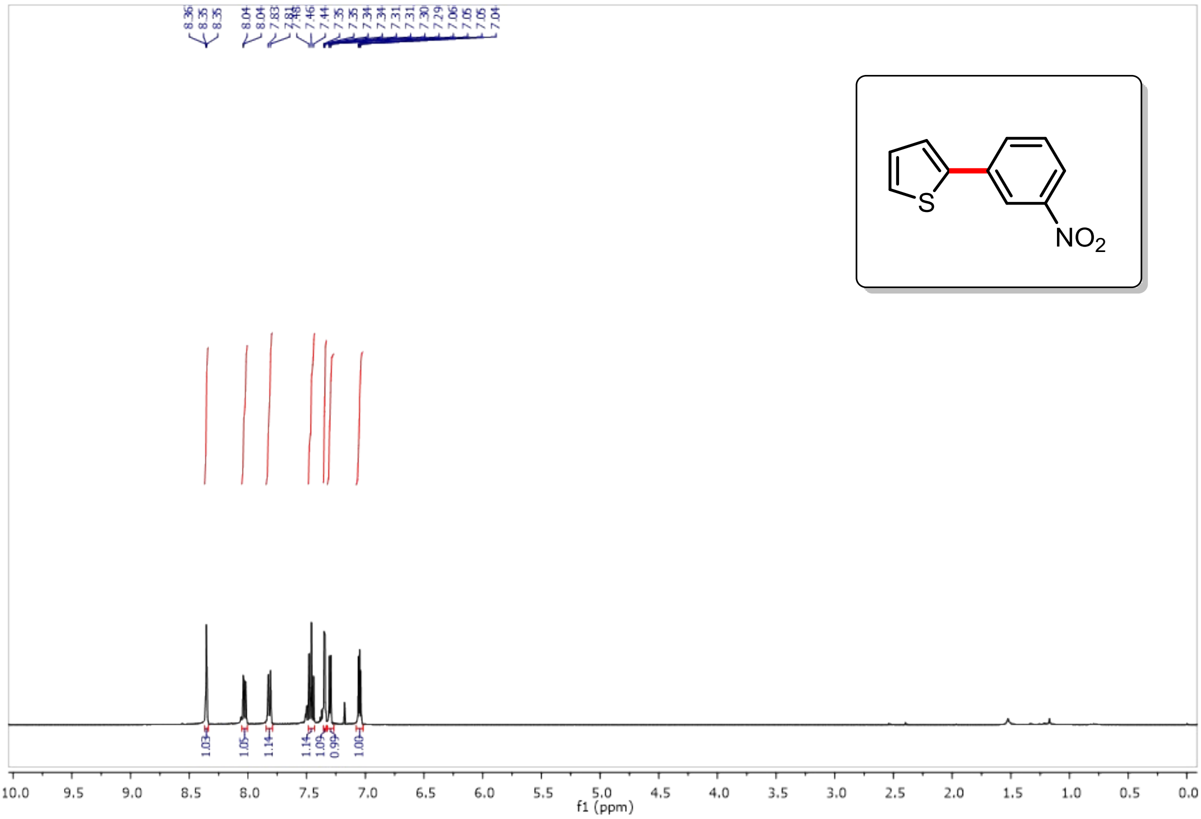
8.36
8.35
8.35
8.04
8.04
7.83
7.81
7.48
7.46
7.44
7.35
7.35
7.34
7.34
7.31
7.31
7.30
7.29
7.06
7.05
7.05
7.04
NO2
S
1.03
1.05
1.14
1.14
1.09
0.99
1.00
f1 (ppm)

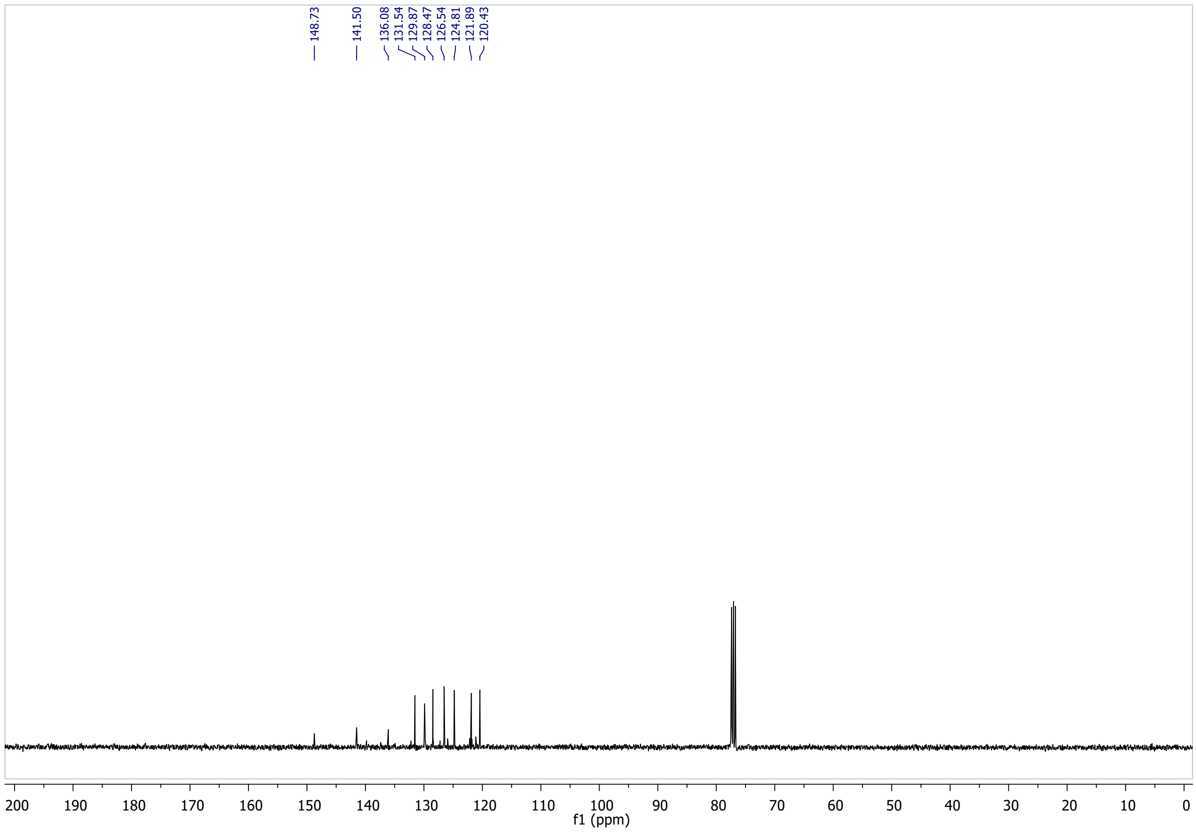
148.73
141.50
136.08
131.54
129.87
128.47
126.54
124.81
121.89
120.43
200
190
180
170
160
150
140
130
120
110
100
90
80
70
60
50
40
30
20
10
0
f1 (ppm)

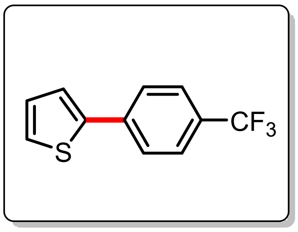
S
CF3

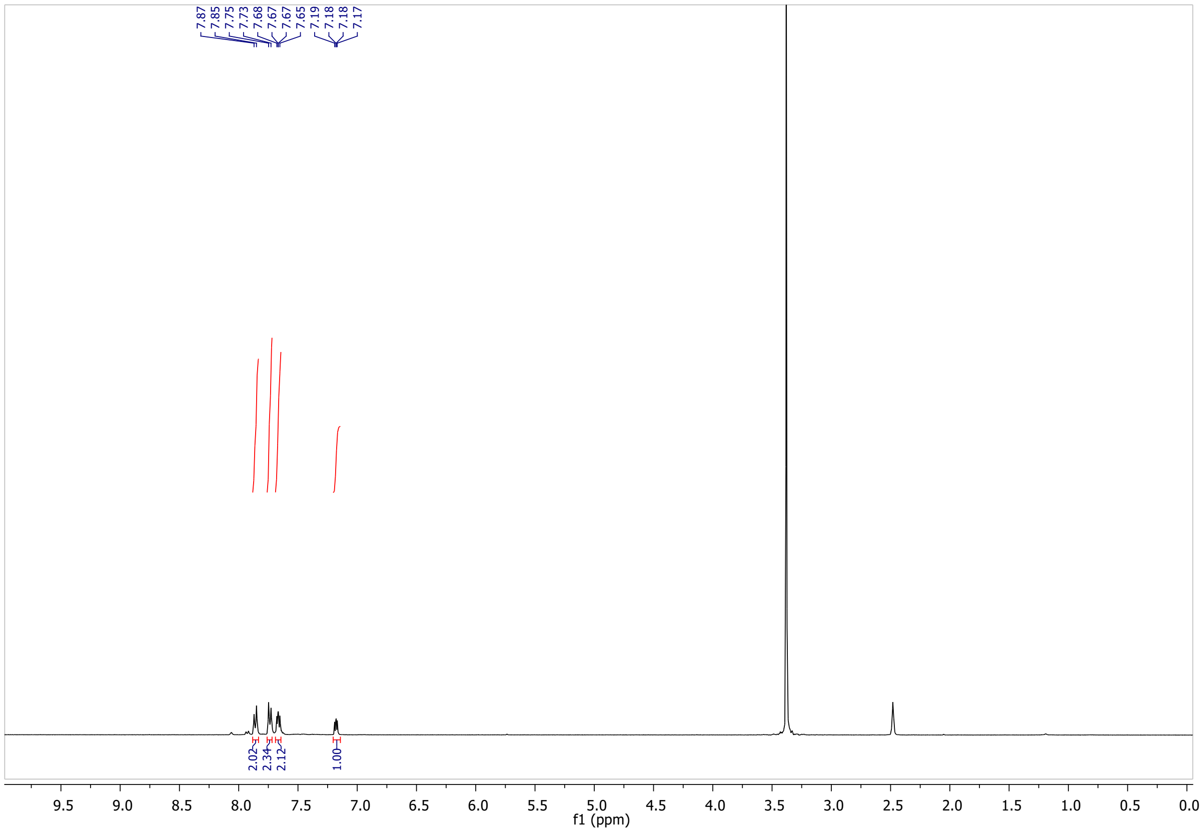
7.87
7.85
7.75
7.73
7.68
7.67
7.67
7.65
7.19
7.18
7.18
7.17
2.02
2.34
2.12
1.00
9.5
9.0
8.5
8.0
7.5
7.0
6.5
6.0
5.5
5.0
4.5
4.0
3.5
3.0
2.5
2.0
1.5
1.0
0.5
0.0
f1 (ppm)

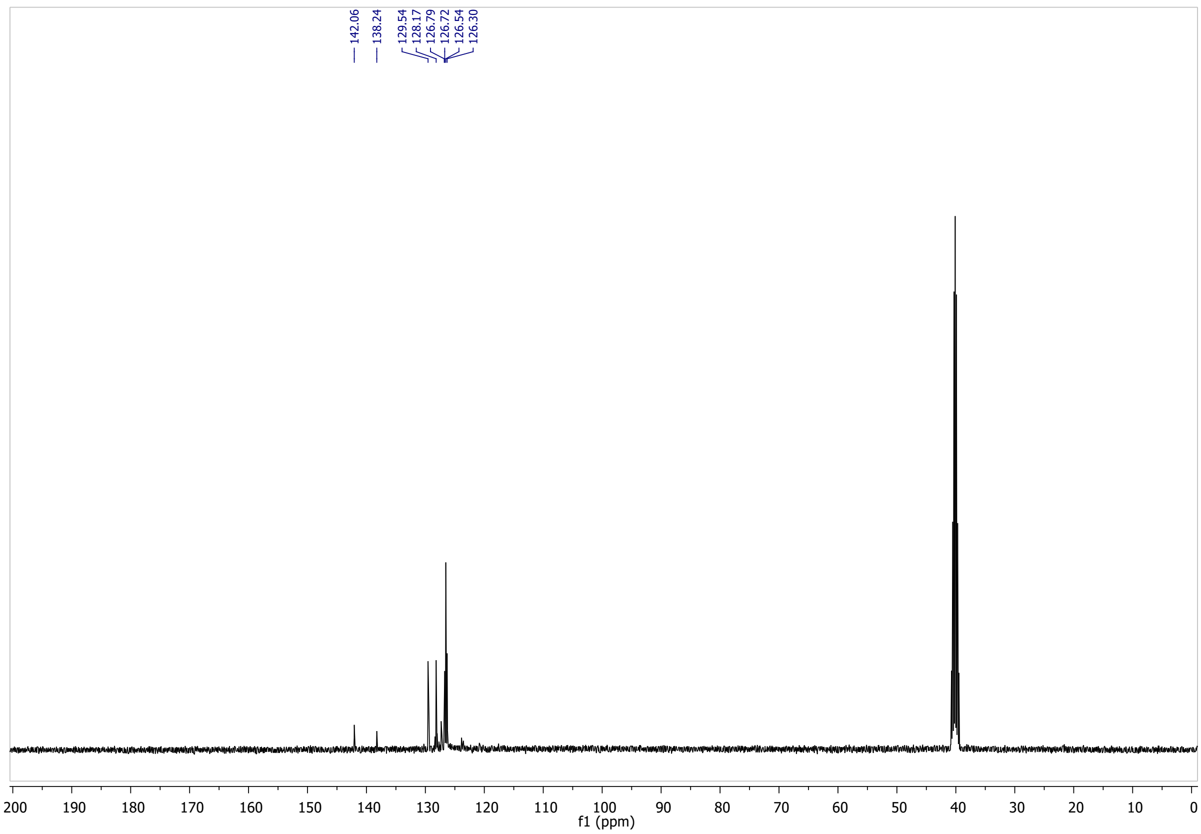
142.06
138.24
129.54
128.17
126.79
126.72
126.54
126.30
200
190
180
170
160
150
140
130
120
110
100
90
80
70
60
50
40
30
20
10
0
f1 (ppm)

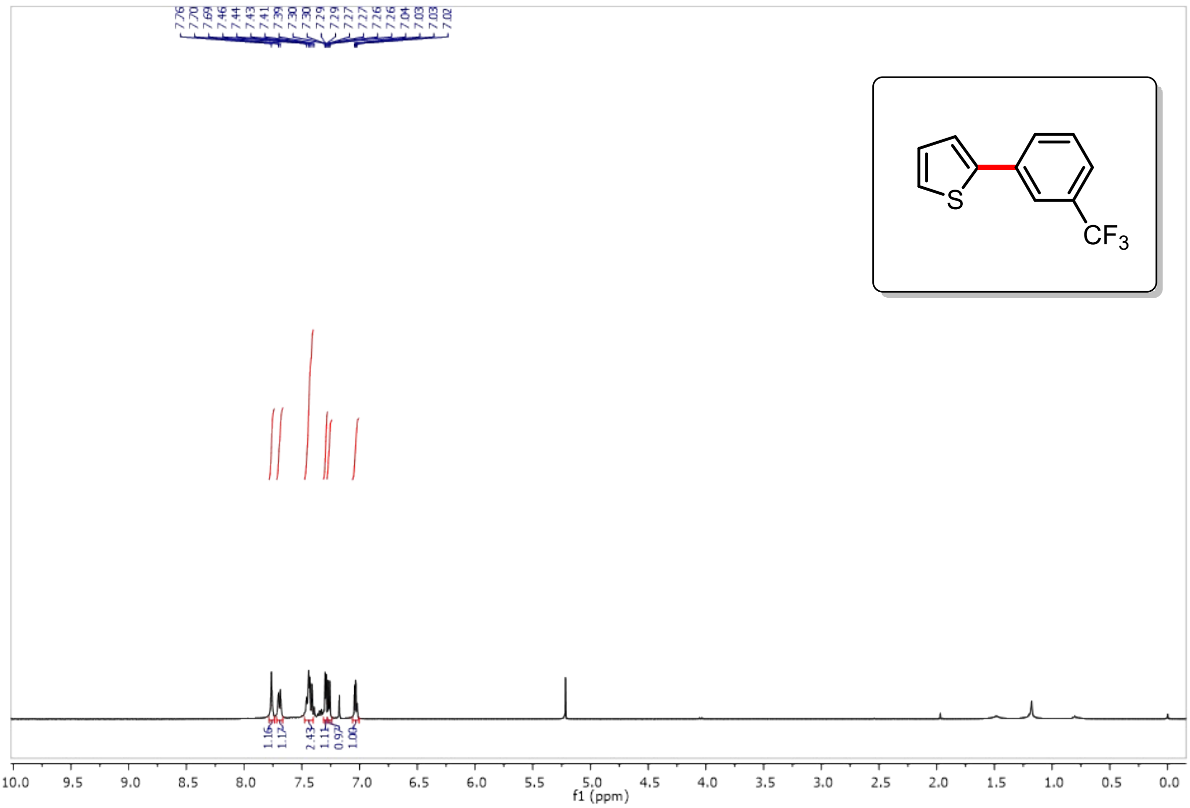
7.76
7.70
7.69
7.46
7.44
7.43
7.41
7.39
7.30
7.30
7.30
7.29
7.29
7.27
7.27
7.26
7.26
7.04
7.03
7.02
S
CF3
1.16
1.12
2.43
1.11
0.97
1.00
f1 (ppm)

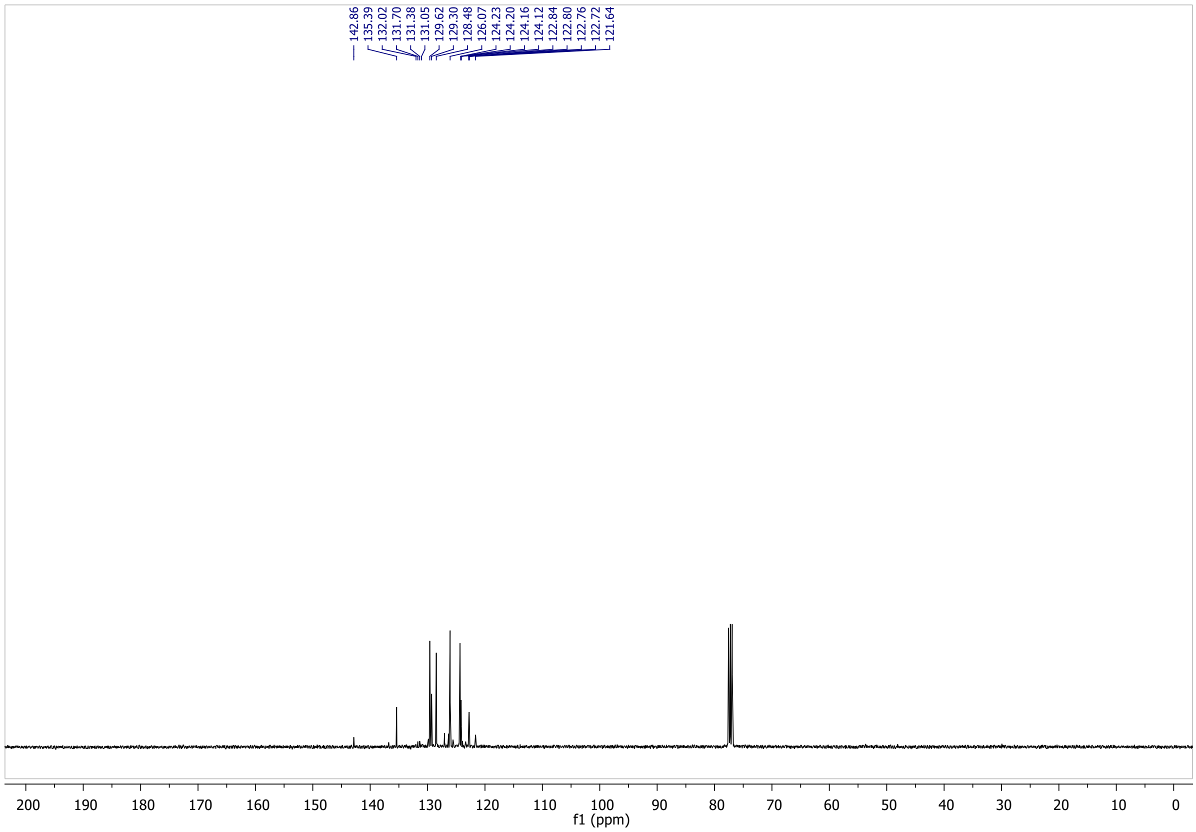
142.86
135.39
132.02
131.70
131.38
131.05
129.62
129.30
128.48
126.07
124.23
124.20
124.16
124.12
122.84
122.80
122.76
122.72
121.64
f1 (ppm)

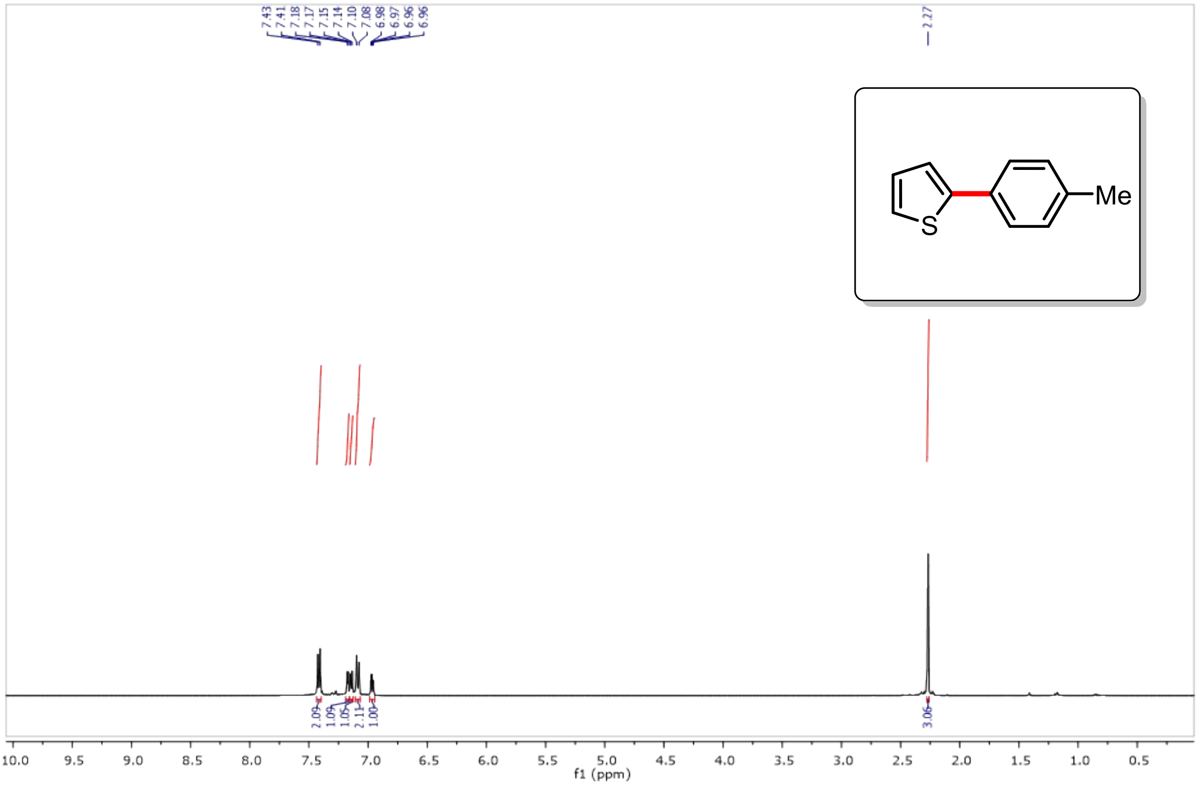
7.43
7.41
7.18
7.17
7.15
7.14
7.10
7.08
6.98
6.97
6.96
6.96
2.27
Me
S
2.09
1.09
1.05
2.11
1.00
3.06
f1 (ppm)

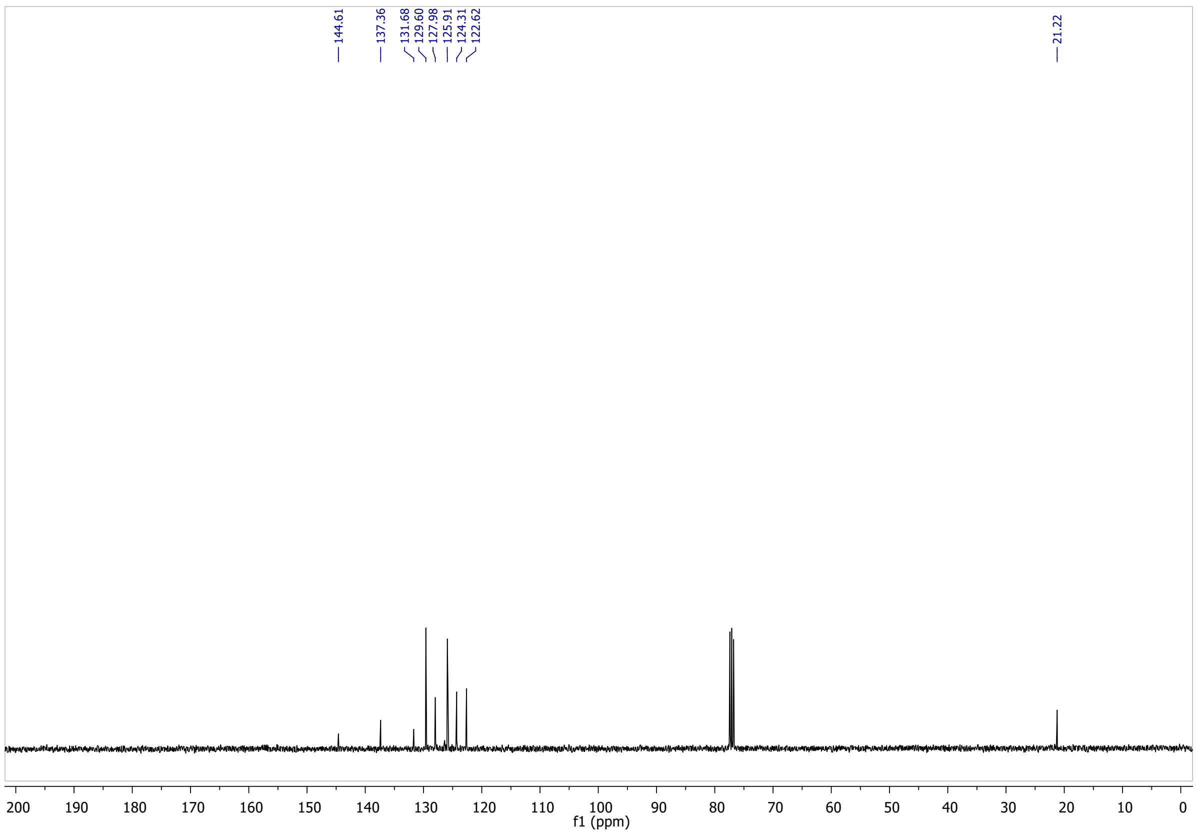
144.61
137.36
131.68
129.60
127.98
125.91
124.31
122.62
21.22
f1 (ppm)

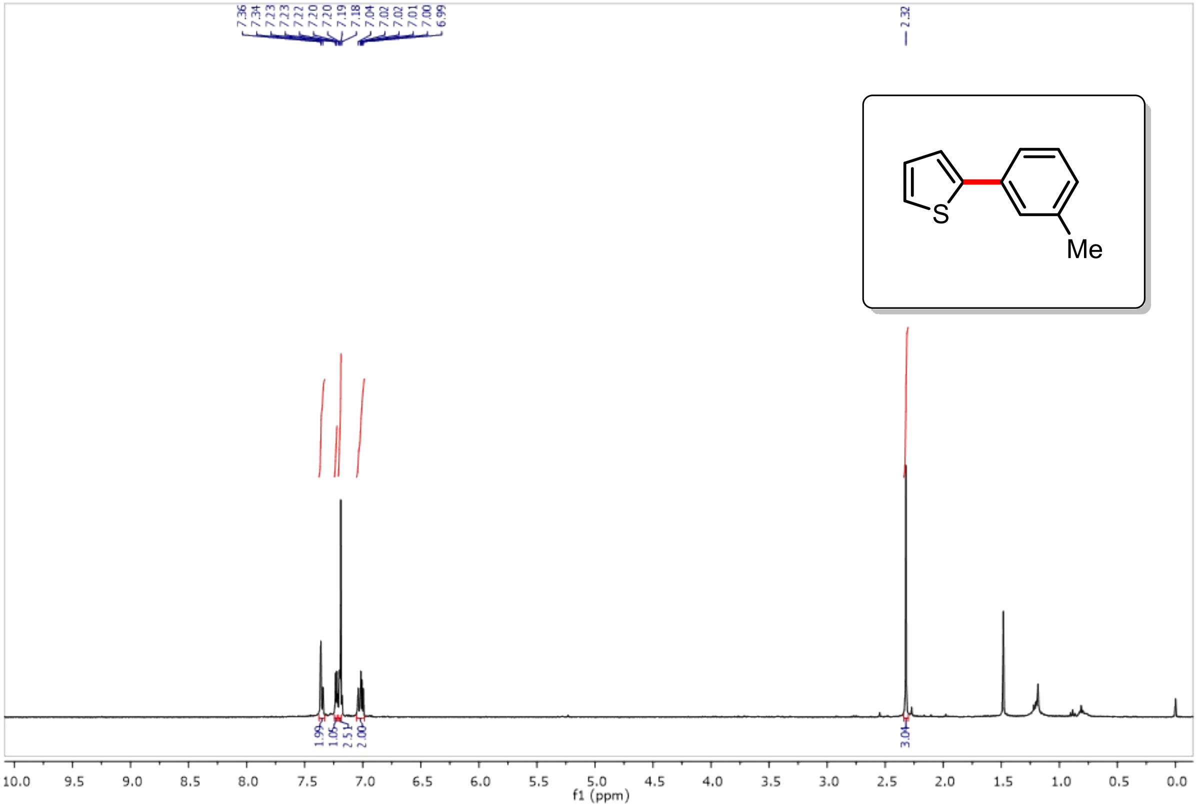
7.36
7.34
7.23
7.23
7.22
7.20
7.20
7.19
7.18
7.04
7.02
7.02
7.01
7.00
6.99
2.32
S
Me
1.99
1.05
2.51
2.00
3.04
10.0
9.5
9.0
8.5
8.0
7.5
7.0
6.5
6.0
5.5
5.0
4.5
4.0
3.5
3.0
2.5
2.0
1.5
1.0
0.5
0.0
f1 (ppm)

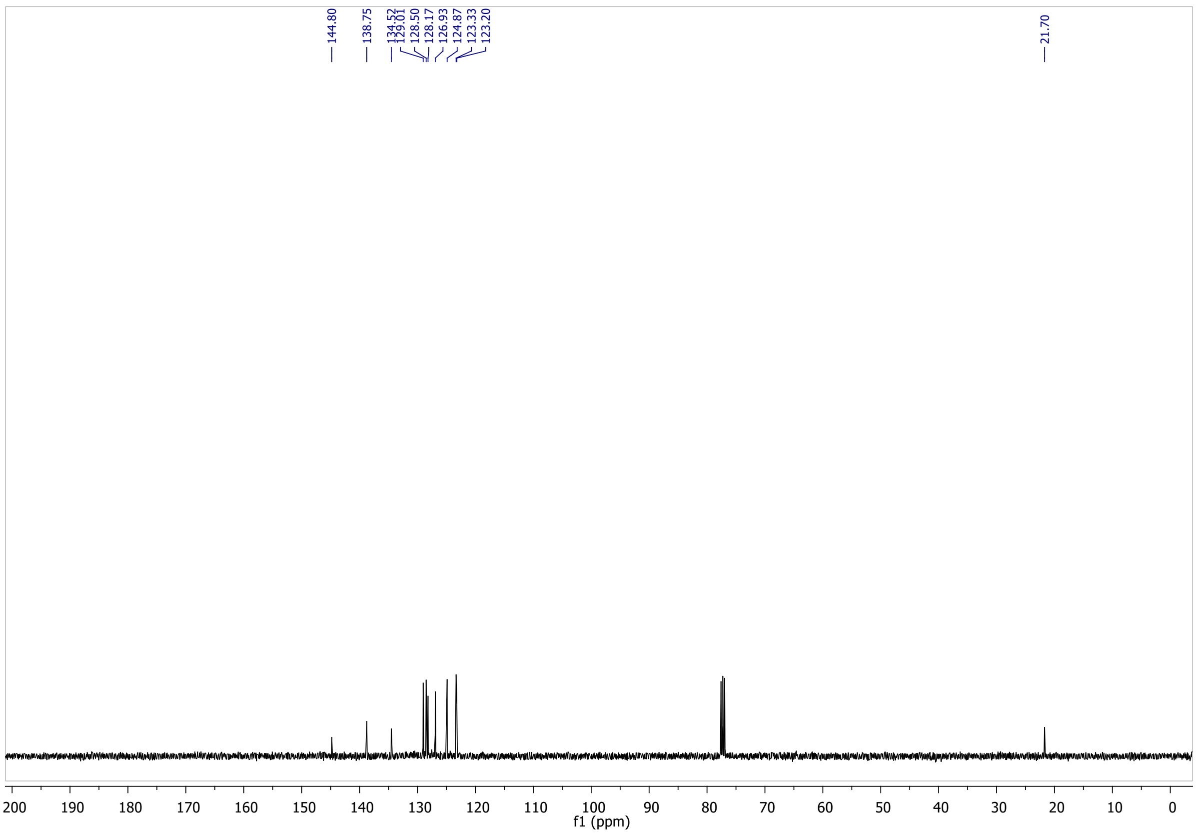
144.80
138.75
134.52
129.01
128.50
128.17
126.93
124.87
123.33
123.20
21.70
200
190
180
170
160
150
140
130
120
110
100
90
80
70
60
50
40
30
20
10
0
f1 (ppm)

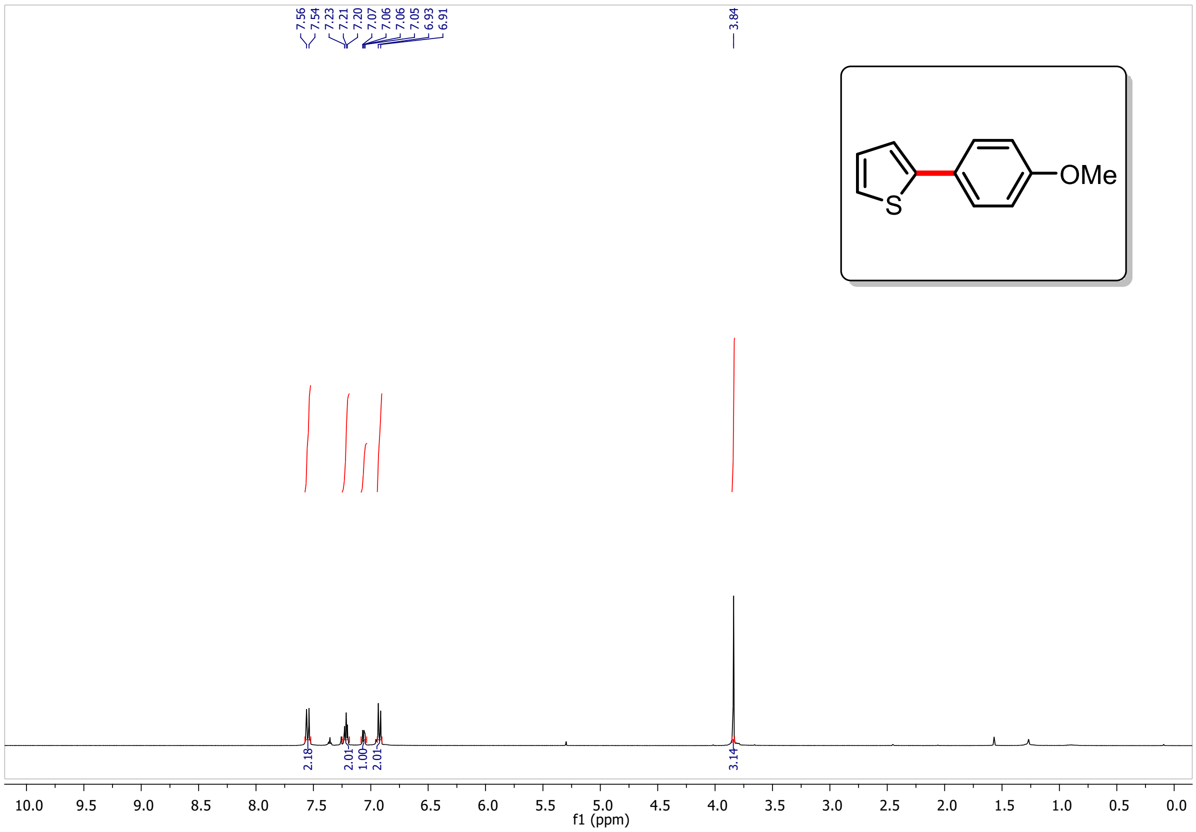
OMe
S
f1 (ppm)

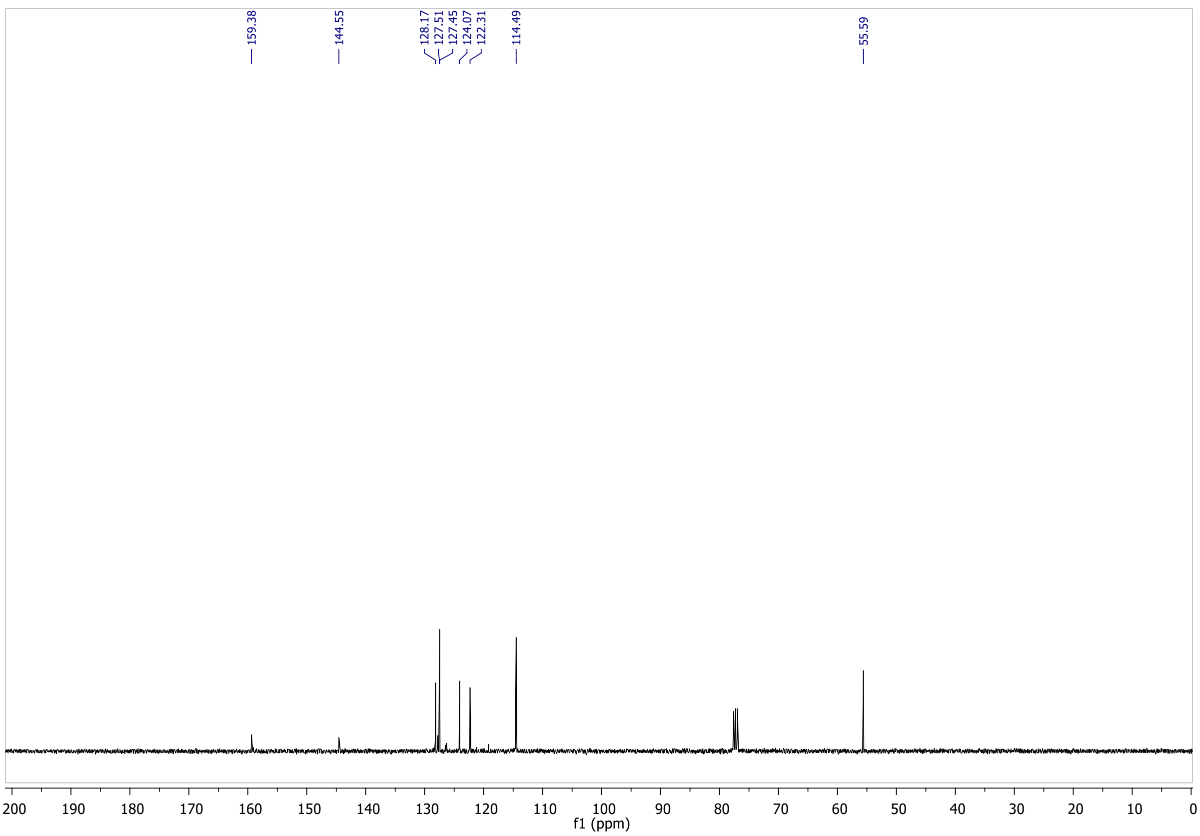
f1 (ppm)

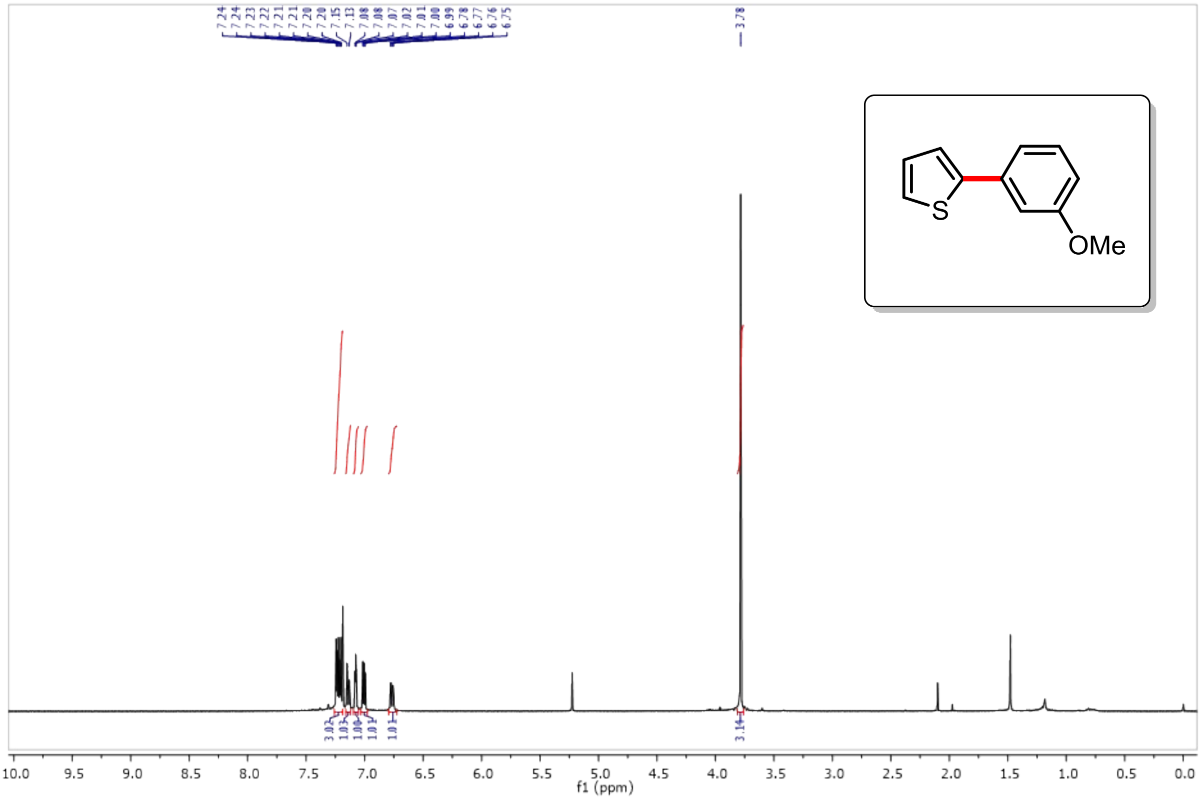

S
OMe
f1 (ppm)

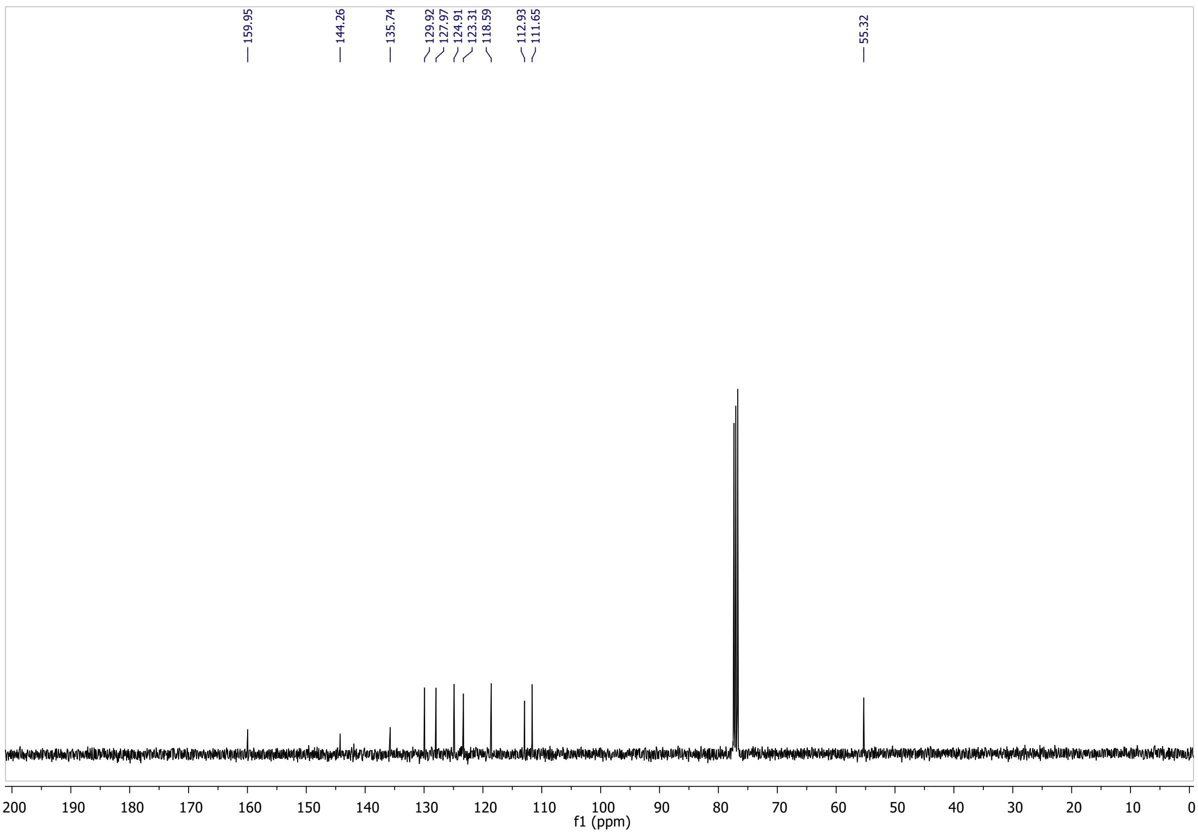

159.95
144.26
135.74
129.92
127.97
124.91
123.31
118.59
112.93
111.65
55.32
f1 (ppm)

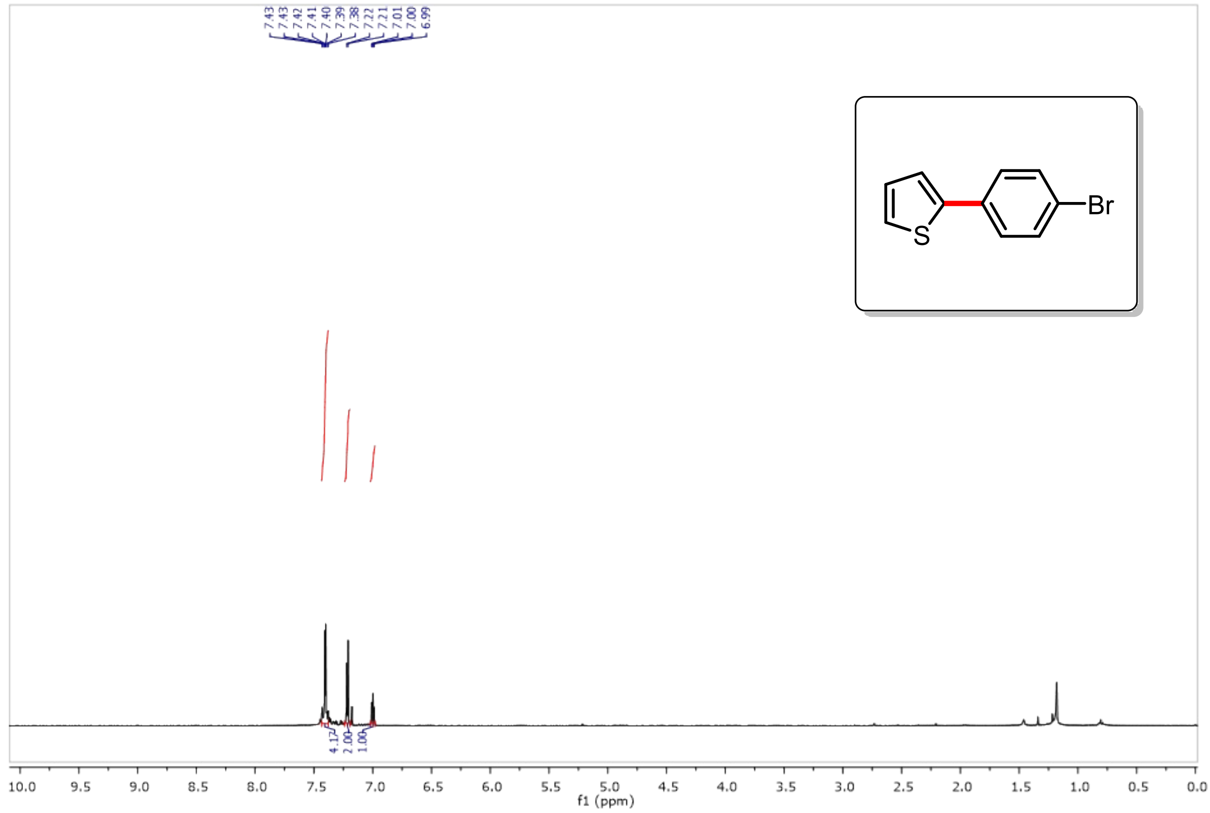
7.43
7.43
7.42
7.41
7.40
7.39
7.38
7.22
7.21
7.01
7.00
6.99
Br
S
4.17
2.00
1.00
10.0 9.5 9.0 8.5 8.0 7.5 7.0 6.5 6.0 5.5 5.0 4.5 4.0 3.5 3.0 2.5 2.0 1.5 1.0 0.5 0.0
f1 (ppm)

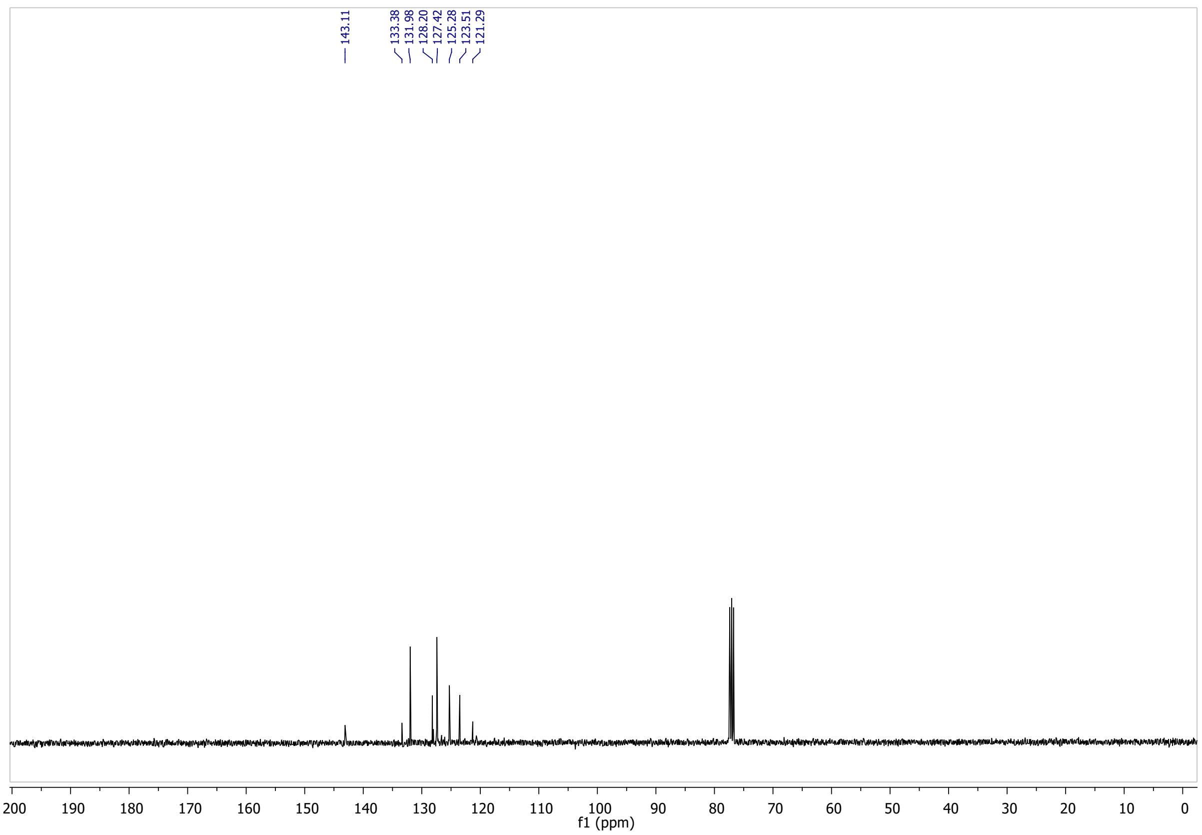
143.11
133.38
131.98
128.20
127.42
125.28
123.51
121.29
200 190 180 170 160 150 140 130 120 110 100 90 80 70 60 50 40 30 20 10 0
f1 (ppm)

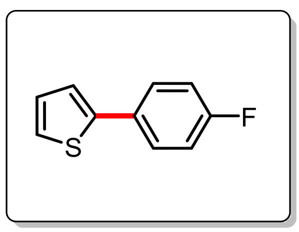
S
F

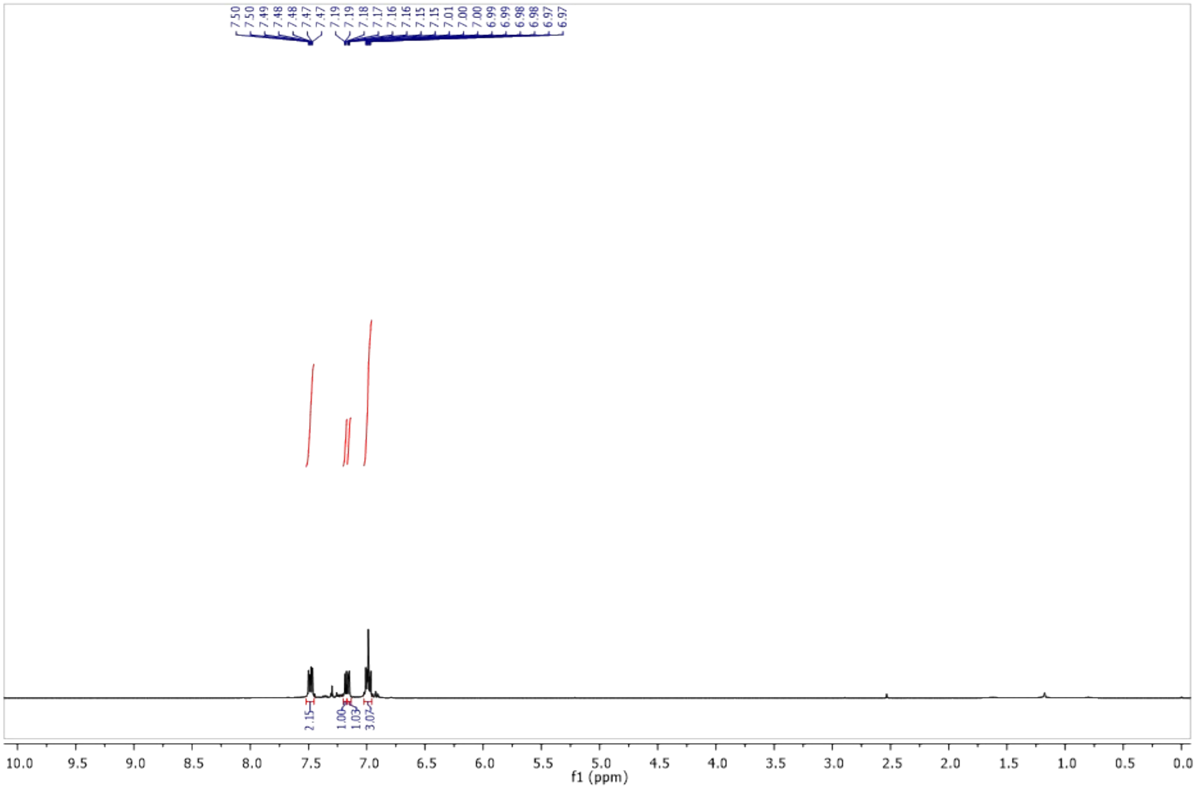

7.50
7.50
7.49
7.48
7.48
7.47
7.47
7.19
7.19
7.18
7.17
7.16
7.15
7.15
7.01
7.00
7.00
6.99
6.99
6.98
6.98
6.97
6.97
2.15
1.00
1.03
3.07
10.0
9.5
9.0
8.5
8.0
7.5
7.0
6.5
6.0
5.5
5.0
4.5
4.0
3.5
3.0
2.5
2.0
1.5
1.0
0.5
0.0
f1 (ppm)

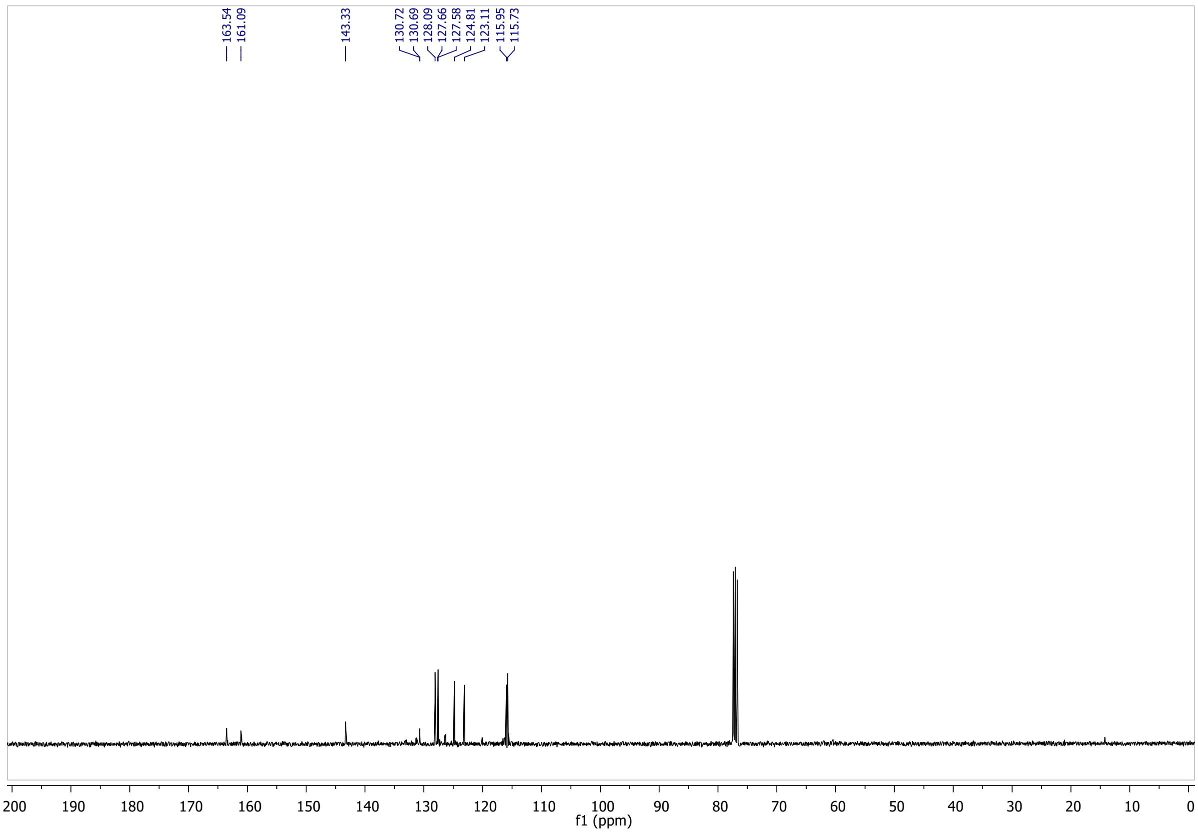

163.54
161.09
143.33
130.72
130.69
128.09
127.66
127.58
124.81
123.11
115.95
115.73
200
190
180
170
160
150
140
130
120
110
100
90
80
70
60
50
40
30
20
10
0
f1 (ppm)

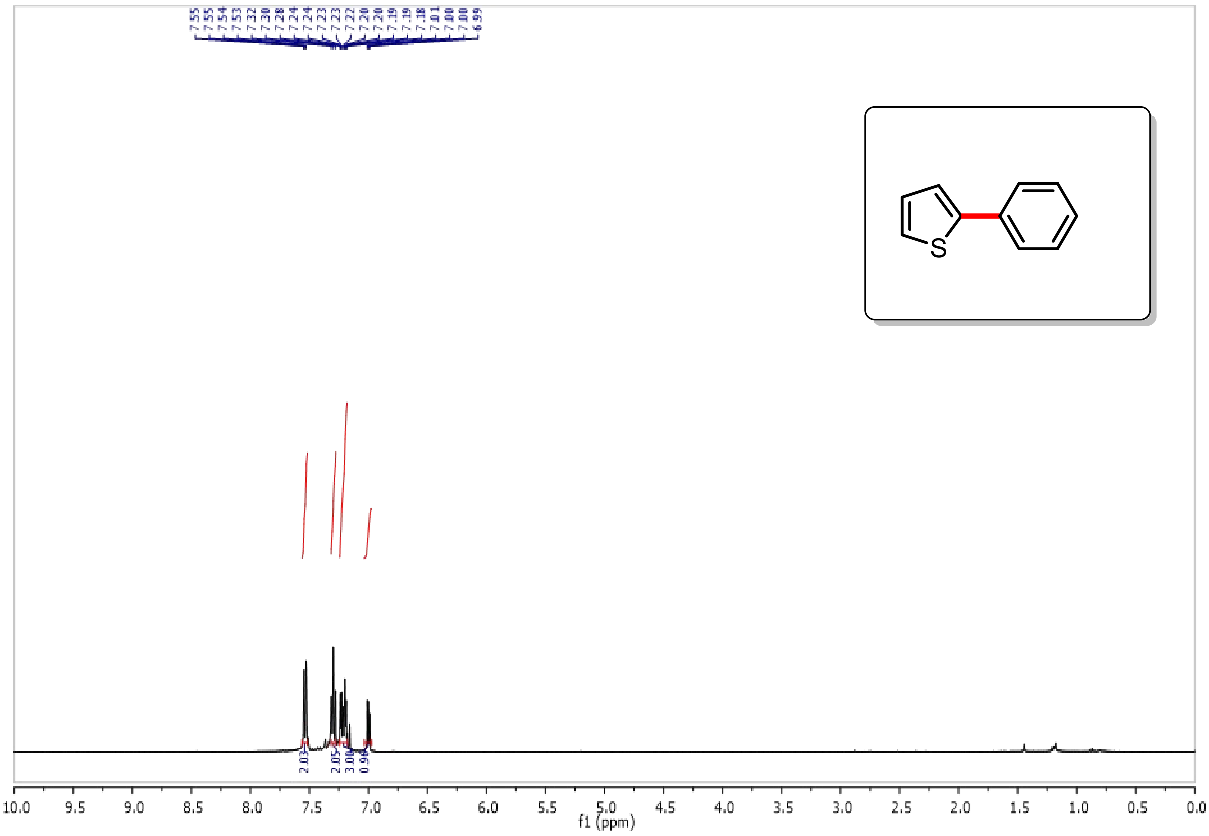

7.55
7.55
7.54
7.53
7.32
7.30
7.28
7.24
7.24
7.23
7.23
7.22
7.20
7.20
7.19
7.19
7.18
7.01
7.00
7.00
6.99
2.03
2.05
3.00
0.96
10.0 9.5 9.0 8.5 8.0 7.5 7.0 6.5 6.0 5.5 5.0 4.5 4.0 3.5 3.0 2.5 2.0 1.5 1.0 0.5 0.0
f1 (ppm)
S

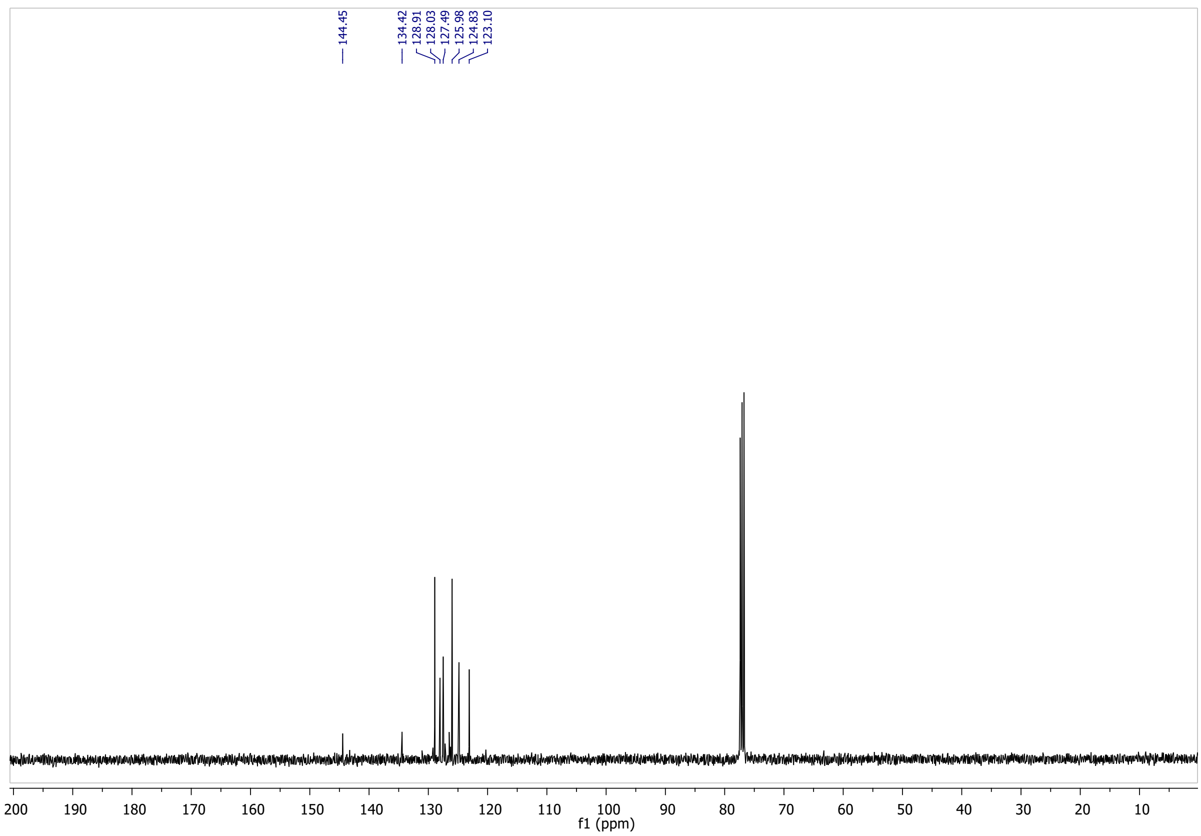

144.45
134.42
128.91
128.03
127.49
125.98
124.83
123.10
200 190 180 170 160 150 140 130 120 110 100 90 80 70 60 50 40 30 20 10
f1 (ppm)

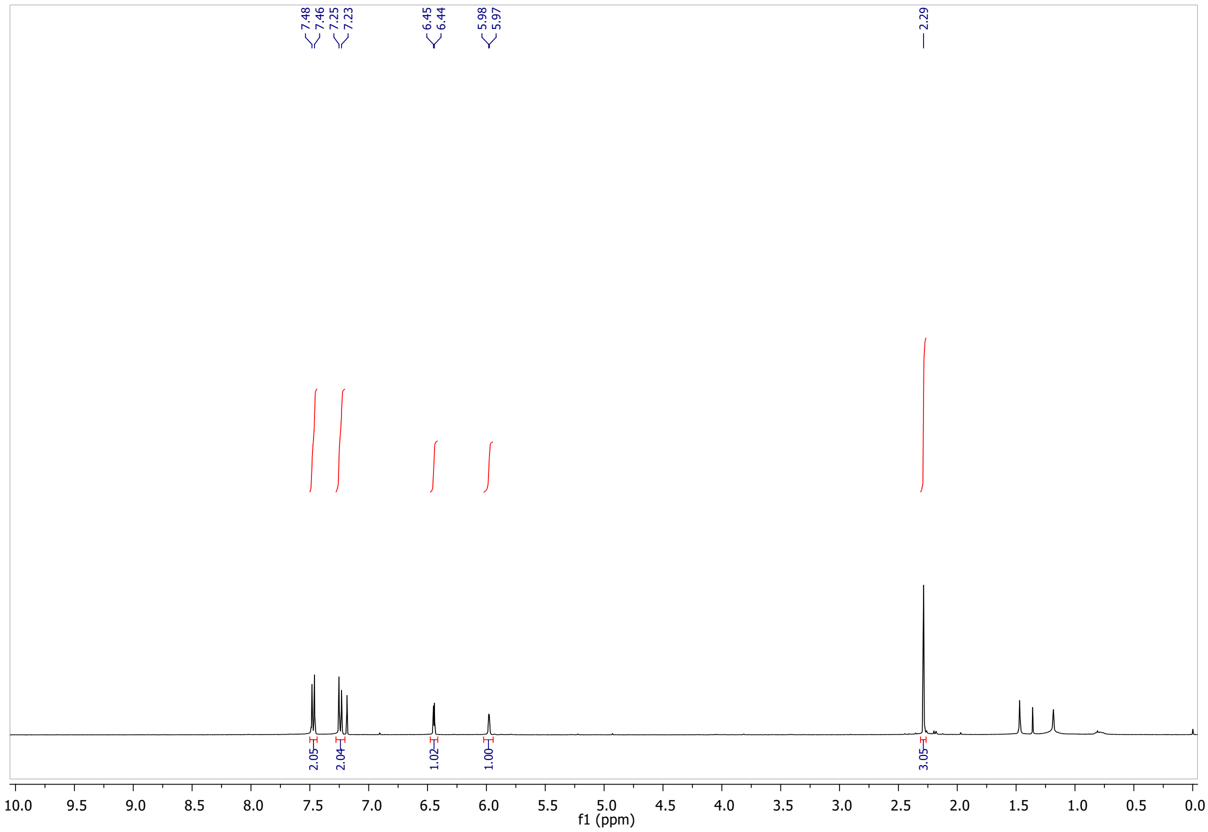
7.48
7.46
7.25
7.23
6.45
6.44
5.98
5.97
2.29
2.05
2.04
1.02
1.00
3.05
f1 (ppm)

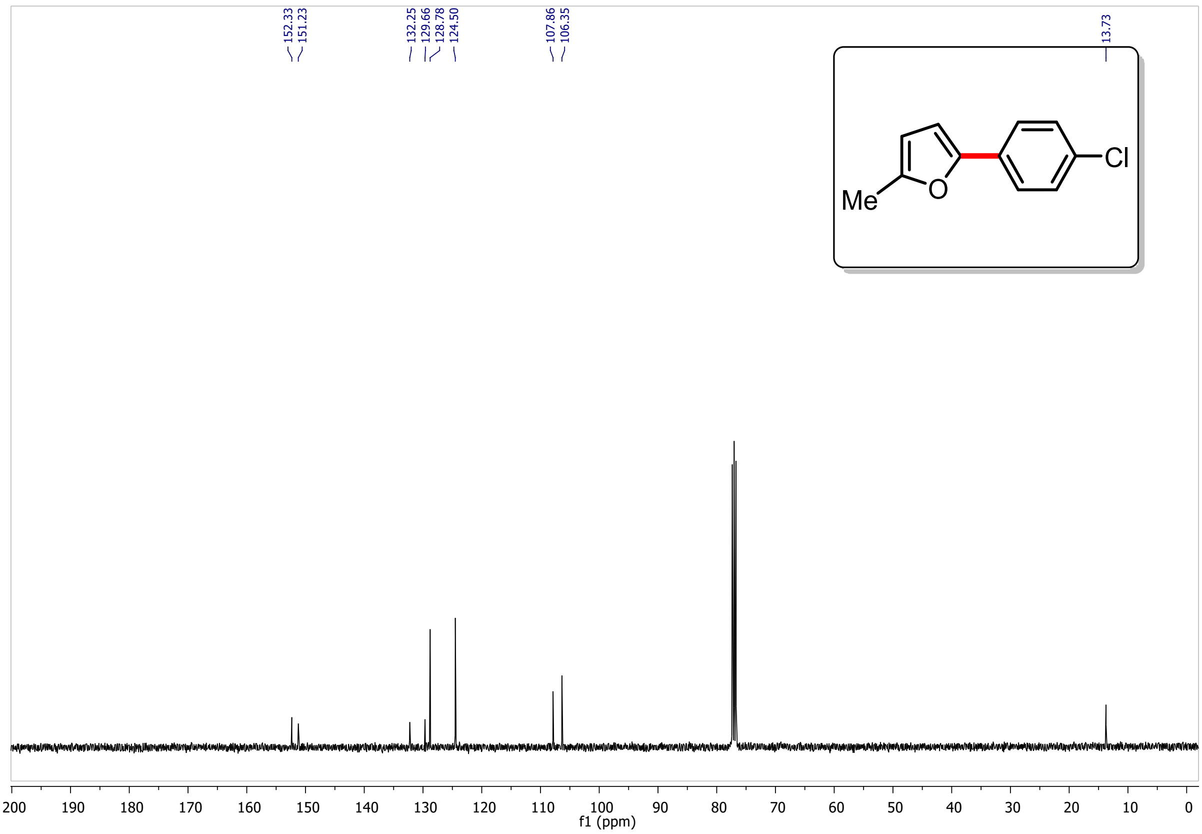
152.33
151.23
132.25
129.66
128.78
124.50
107.86
106.35
13.73
Me
O
Cl
f1 (ppm)

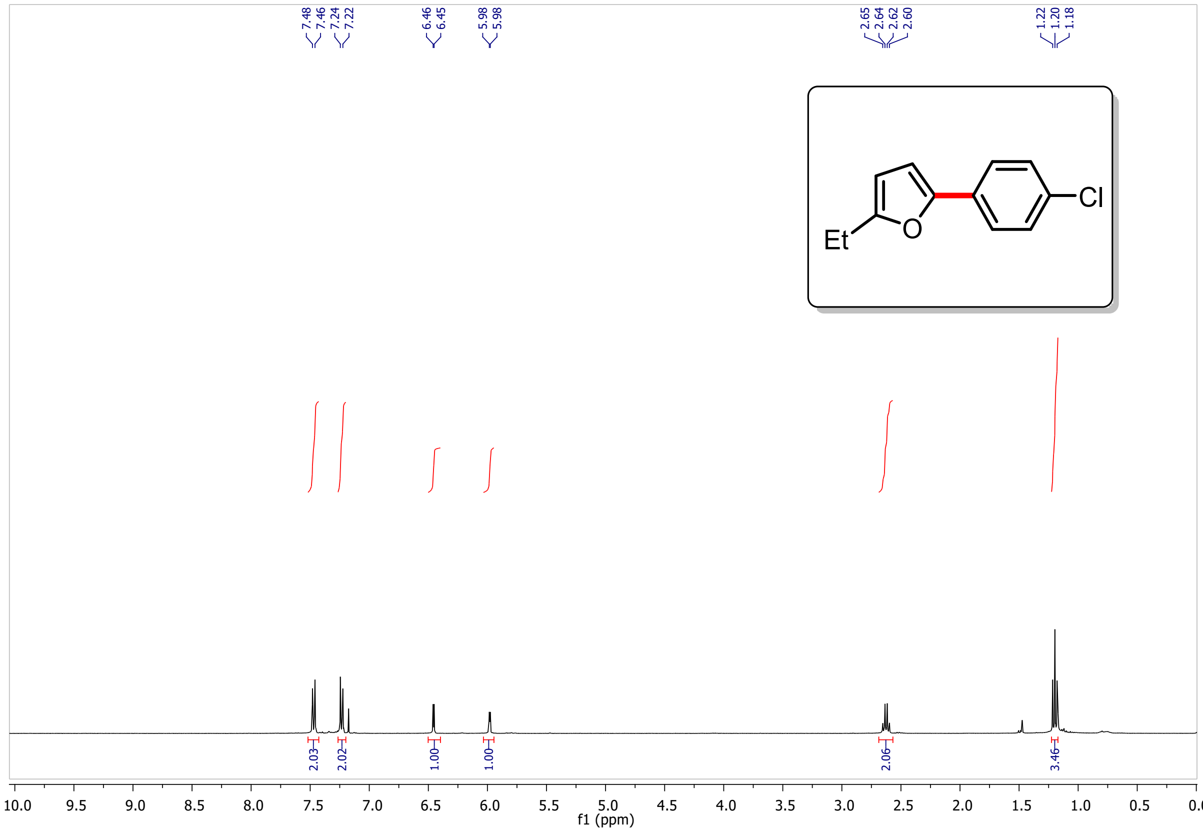

7.48
7.46
7.24
7.22
6.46
6.45
5.98
5.98
2.65
2.64
2.62
2.60
1.22
1.20
1.18
Et
O
Cl
2.03
2.02
1.00
1.00
2.06
3.46
10.0 9.5 9.0 8.5 8.0 7.5 7.0 6.5 6.0 5.5 5.0 4.5 4.0 3.5 3.0 2.5 2.0 1.5 1.0 0.5 0.0
f1 (ppm)

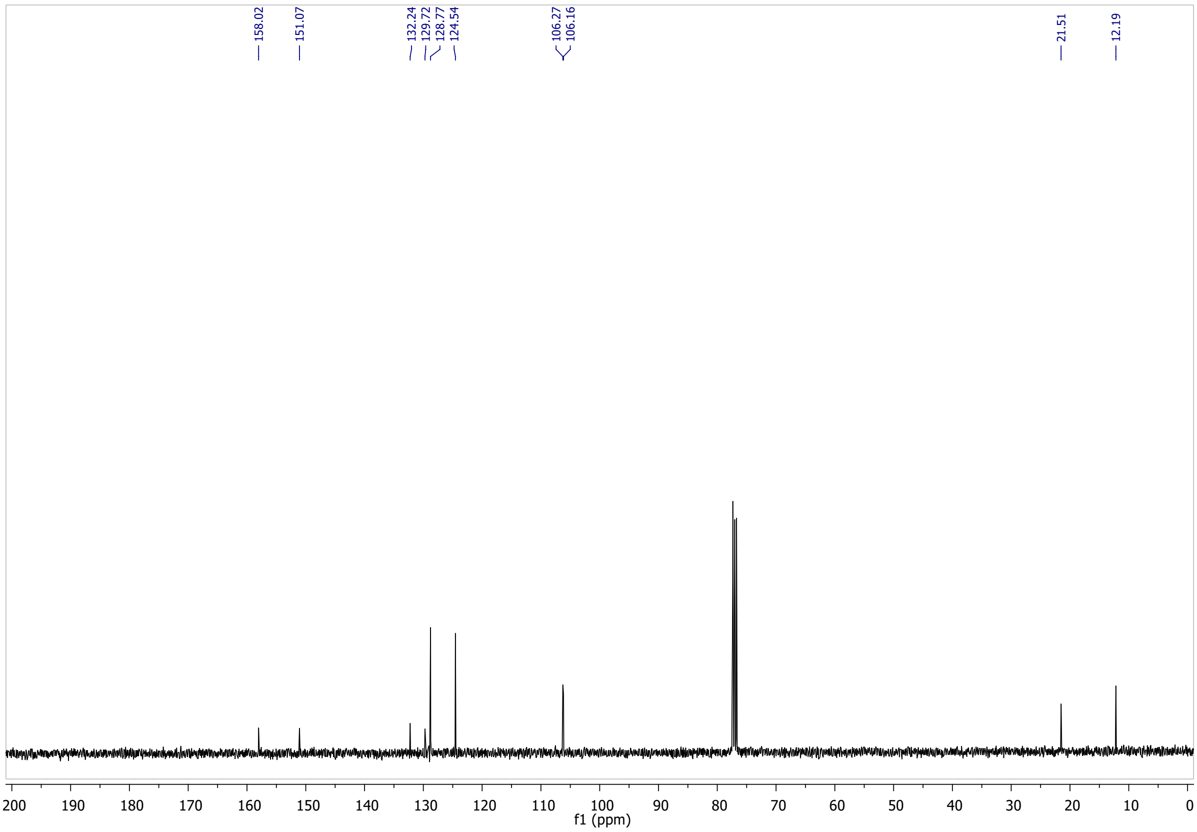
158.02
151.07
132.24
129.72
128.77
124.54
106.27
106.16
21.51
12.19
200 190 180 170 160 150 140 130 120 110 100 90 80 70 60 50 40 30 20 10 0
f1 (ppm)

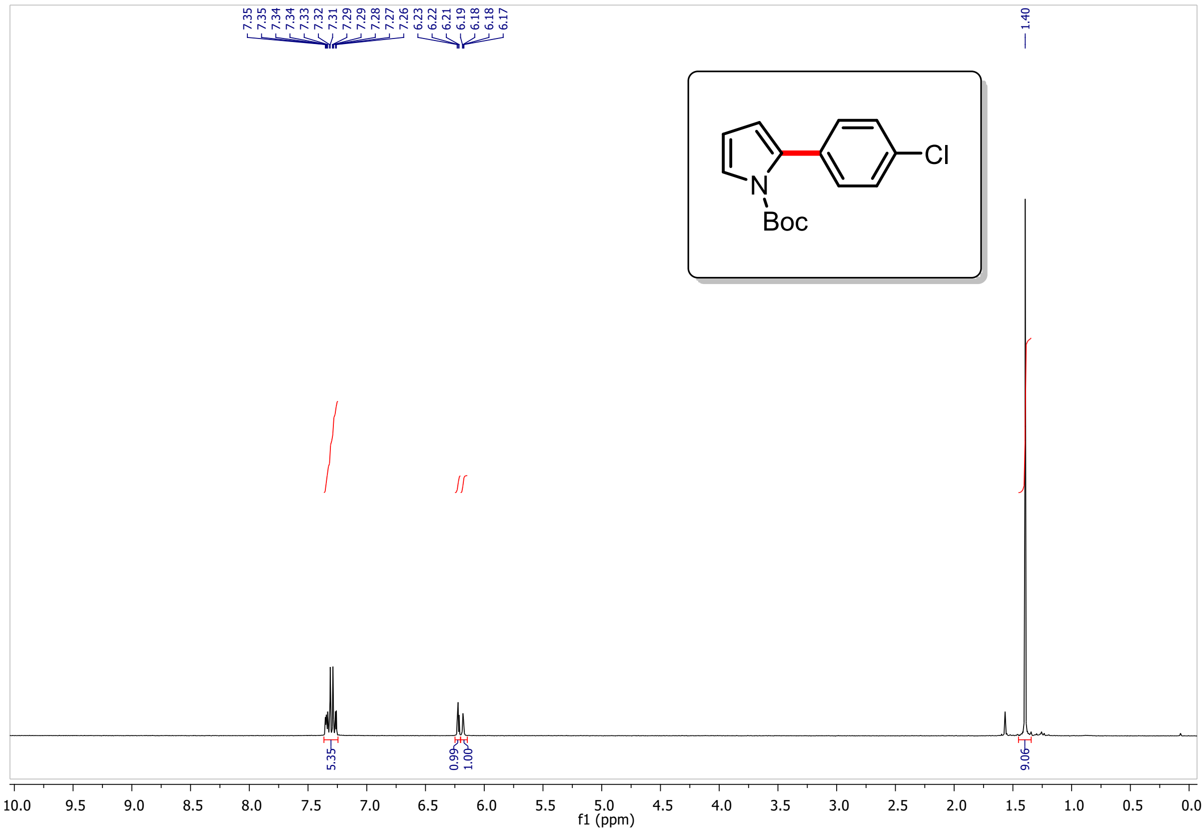
7.35
7.35
7.34
7.34
7.33
7.32
7.31
7.29
7.29
7.28
7.27
7.26
6.23
6.22
6.21
6.19
6.18
6.18
6.17
1.40
N
Boc
Cl
5.35
0.99
1.00
9.06
10.0
9.5
9.0
8.5
8.0
7.5
7.0
6.5
6.0
5.5
5.0
4.5
4.0
3.5
3.0
2.5
2.0
1.5
1.0
0.5
0.0
f1 (ppm)

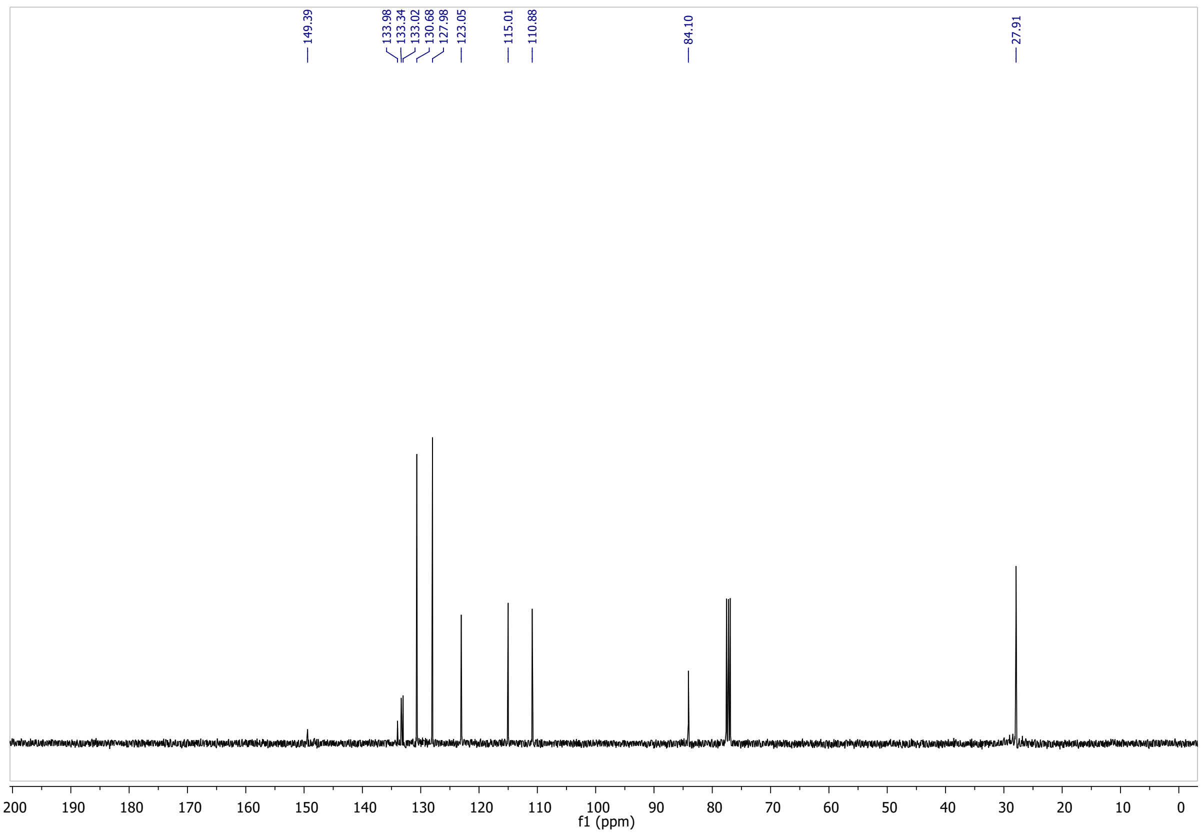
149.39
133.98
133.34
133.02
130.68
127.98
123.05
115.01
110.88
84.10
27.91
200
190
180
170
160
150
140
130
120
110
100
90
80
70
60
50
40
30
20
10
0
f1 (ppm)

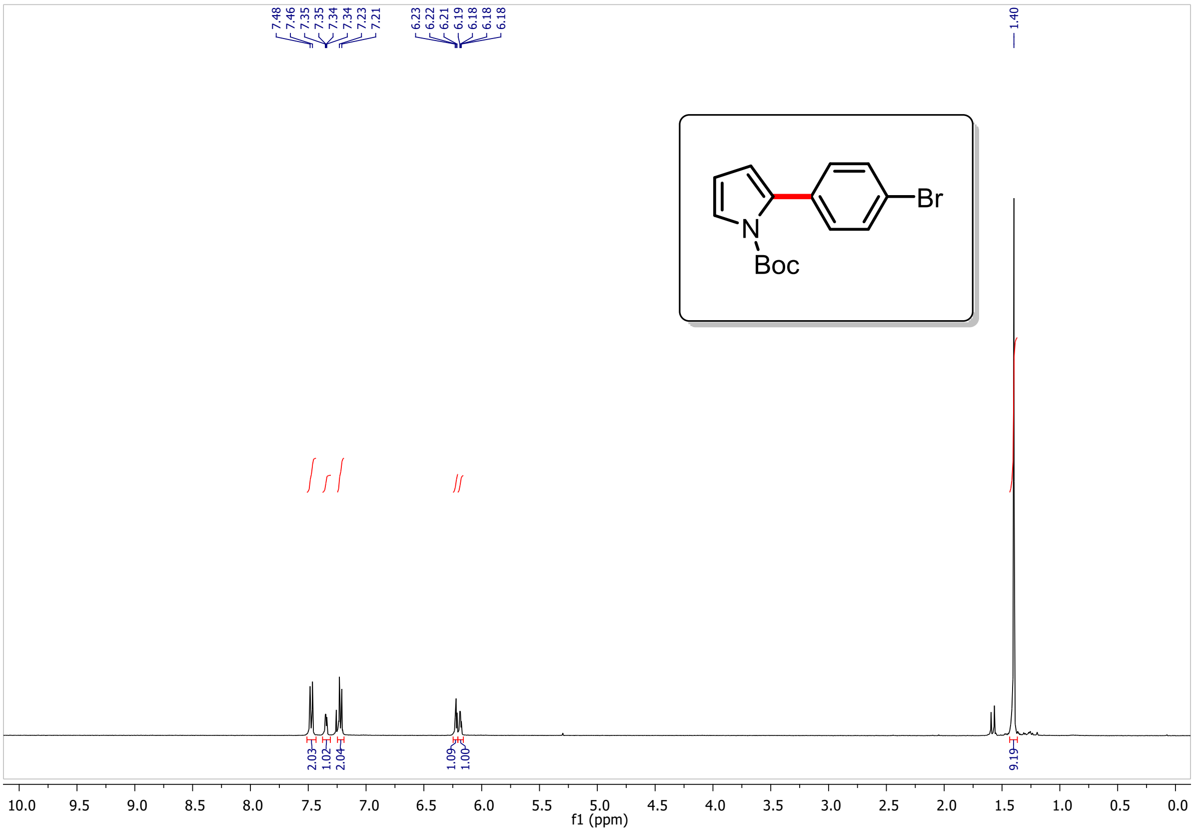
7.48
7.46
7.35
7.35
7.34
7.34
7.23
7.21
6.23
6.22
6.21
6.19
6.18
6.18
6.18
1.40
N
Boc
Br
2.03
1.02
2.04
1.09
1.00
9.19
10.0
9.5
9.0
8.5
8.0
7.5
7.0
6.5
6.0
5.5
5.0
4.5
4.0
3.5
3.0
2.5
2.0
1.5
1.0
0.5
0.0
f1 (ppm)

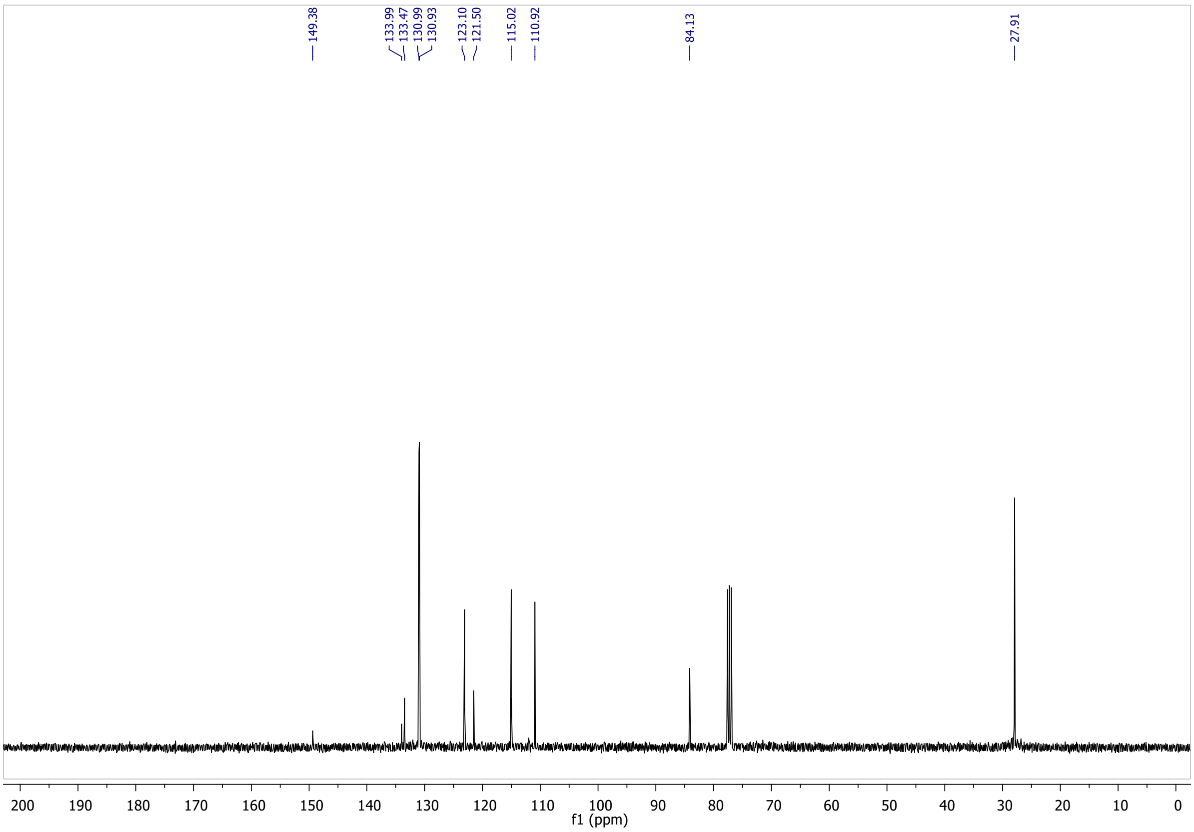
149.38
133.99
133.47
130.99
130.93
123.10
121.50
115.02
110.92
84.13
27.91
200
190
180
170
160
150
140
130
120
110
100
90
80
70
60
50
40
30
20
10
0
f1 (ppm)

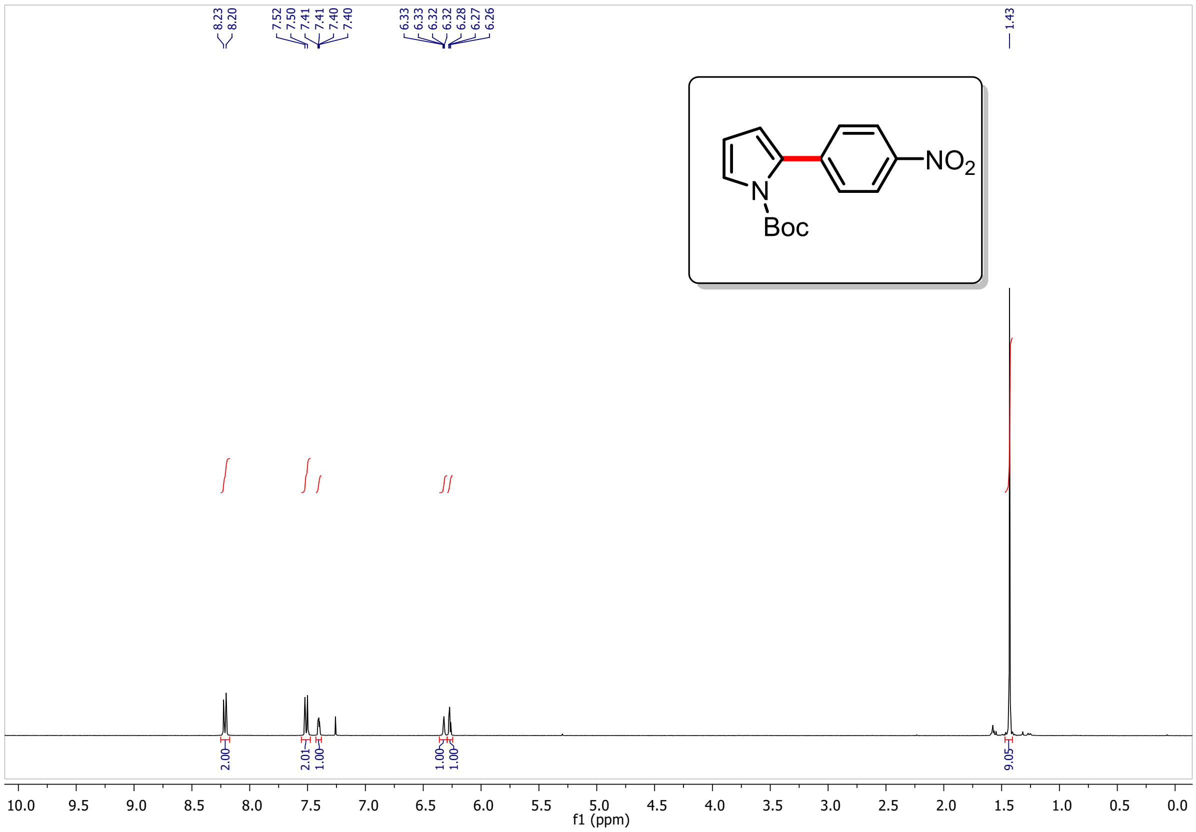

8.23
8.20
7.52
7.50
7.41
7.41
7.40
7.40
6.33
6.33
6.32
6.32
6.28
6.27
6.26
1.43
NO2
N
Boc
2.00
2.01
1.00
1.00
1.00
9.05
10.0 9.5 9.0 8.5 8.0 7.5 7.0 6.5 6.0 5.5 5.0 4.5 4.0 3.5 3.0 2.5 2.0 1.5 1.0 0.5 0.0
f1 (ppm)

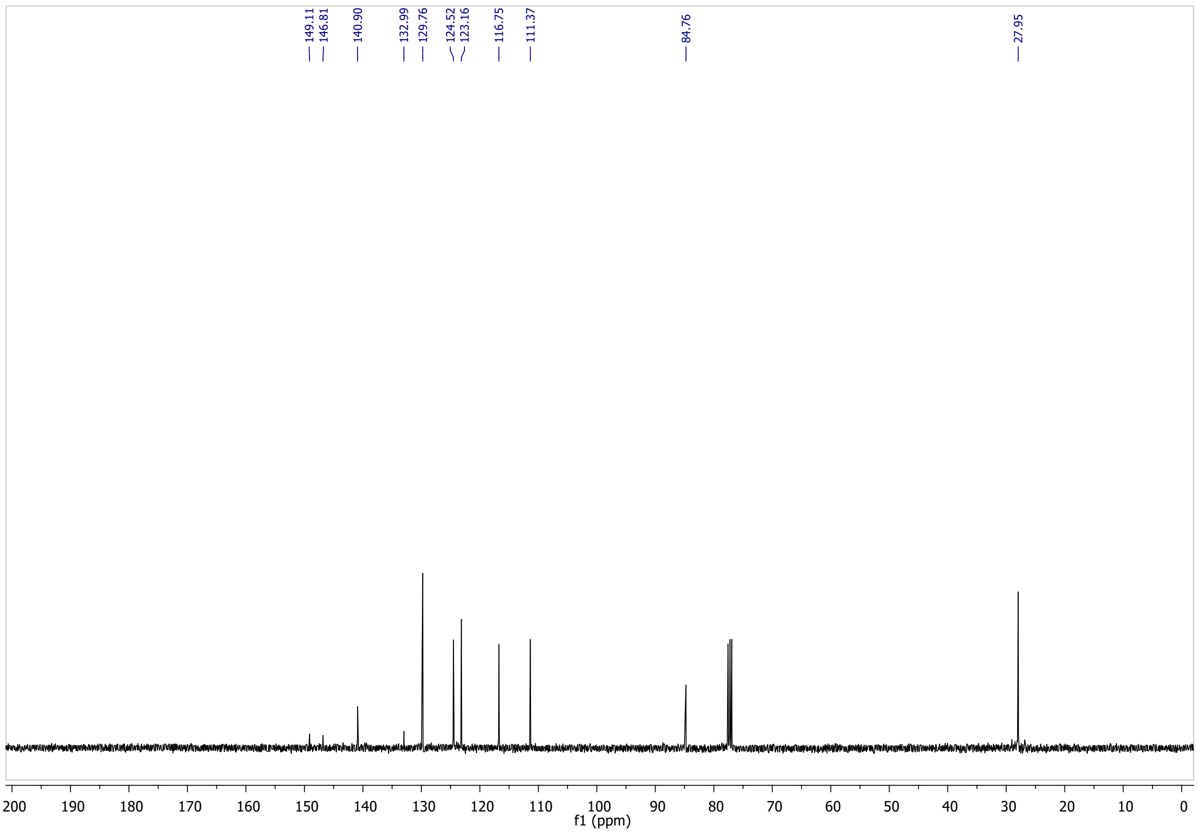

149.11
146.81
140.90
132.99
129.76
124.52
123.16
116.75
111.37
84.76
27.95
200 190 180 170 160 150 140 130 120 110 100 90 80 70 60 50 40 30 20 10 0
f1 (ppm)

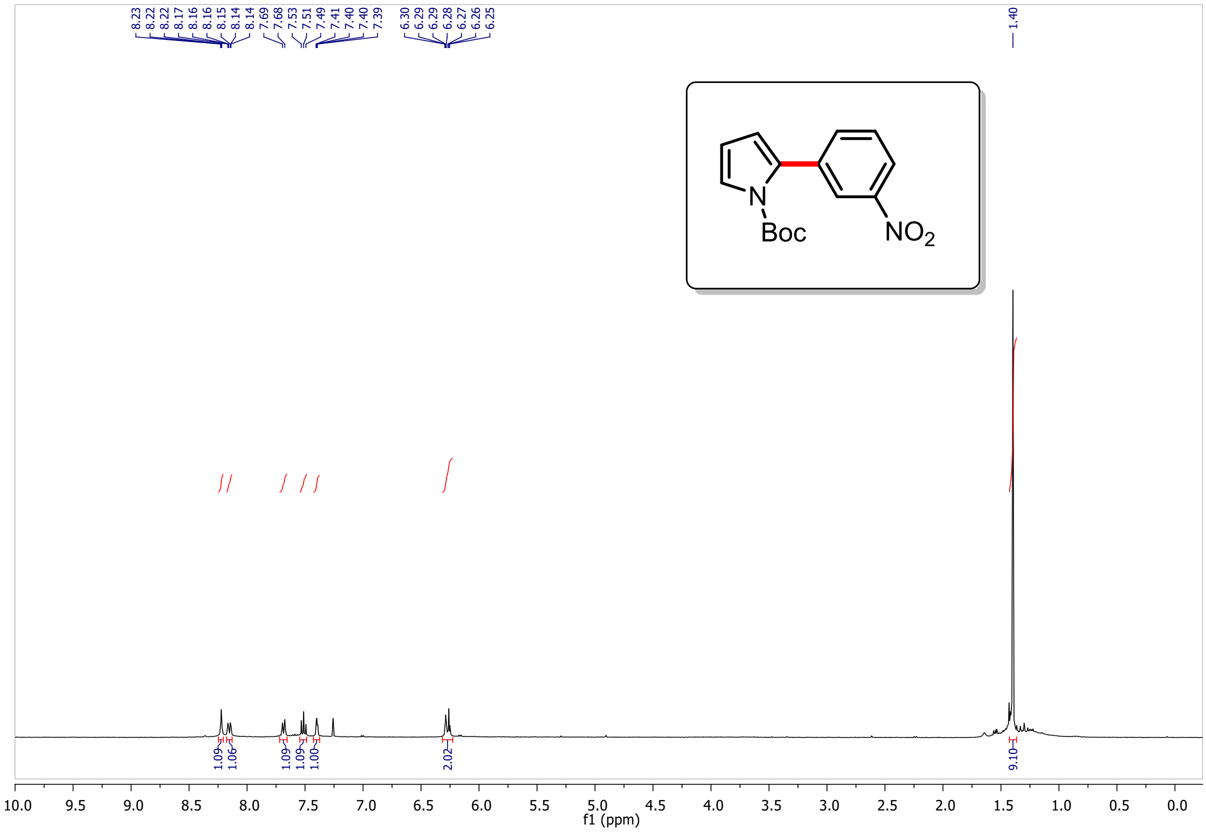

8.23
8.22
8.22
8.17
8.16
8.16
8.15
8.14
8.14
7.69
7.68
7.53
7.51
7.49
7.41
7.40
7.40
7.39
6.30
6.29
6.29
6.28
6.27
6.26
6.25
1.40
N
Boc
NO2
1.09
1.06
1.09
1.09
1.00
2.02
9.10
f1 (ppm)

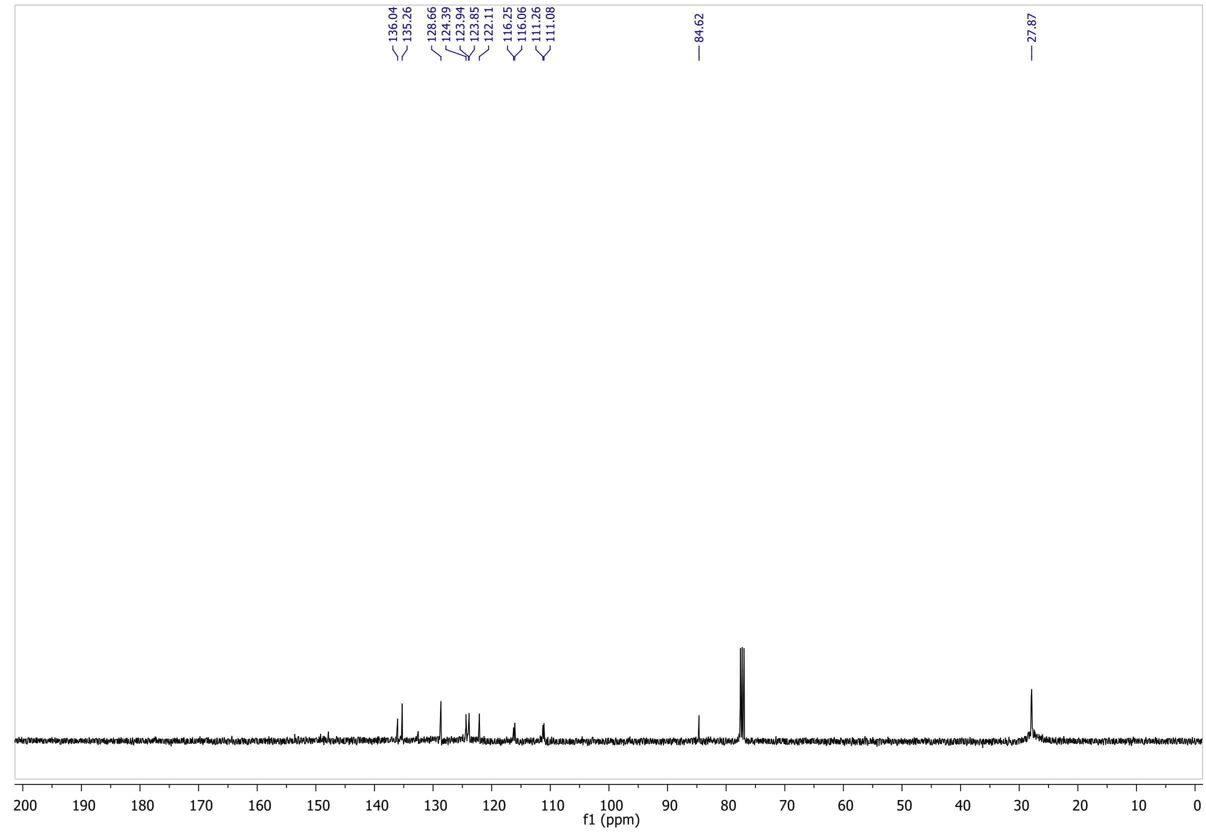

136.04
135.26
128.66
124.39
123.94
123.85
122.11
116.25
116.06
111.26
111.08
84.62
27.87
f1 (ppm)

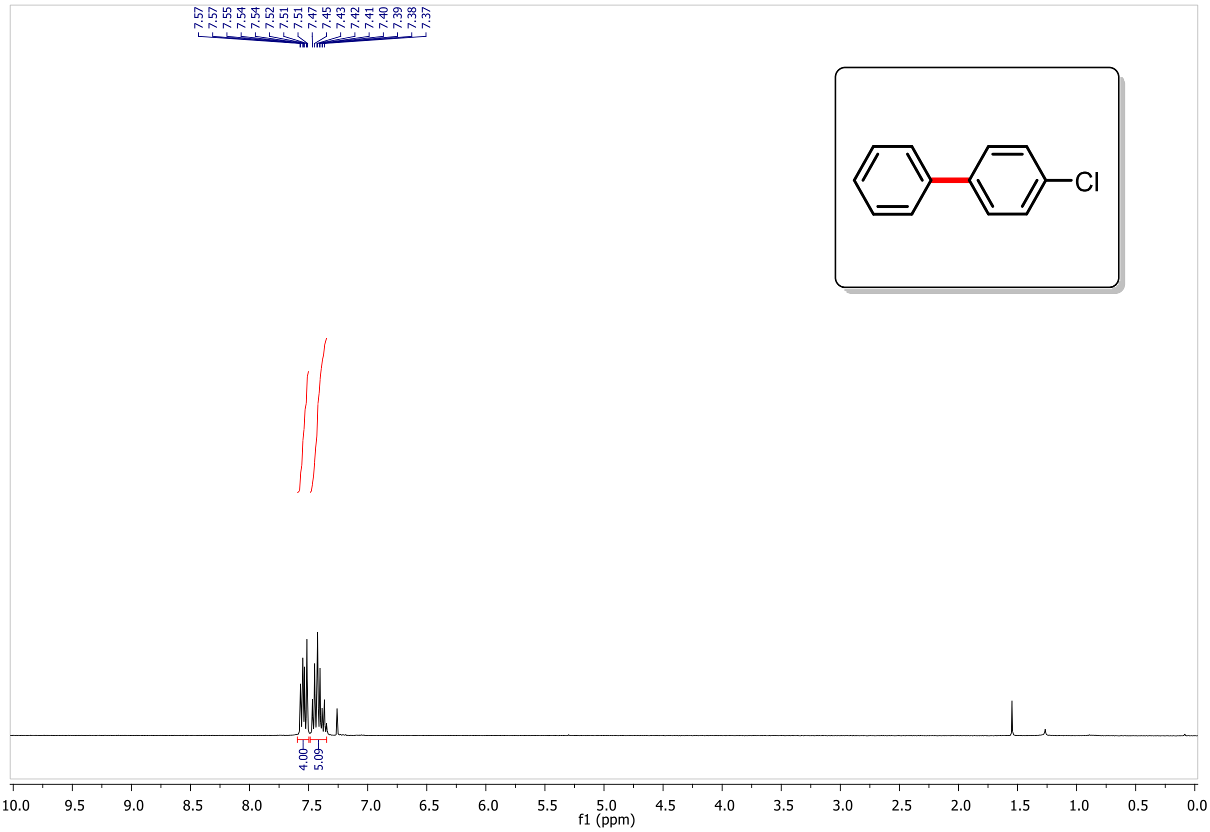
7.57
7.57
7.55
7.54
7.54
7.52
7.51
7.51
7.47
7.45
7.43
7.42
7.41
7.40
7.39
7.38
7.37
Cl
4.00
5.09
f1 (ppm)

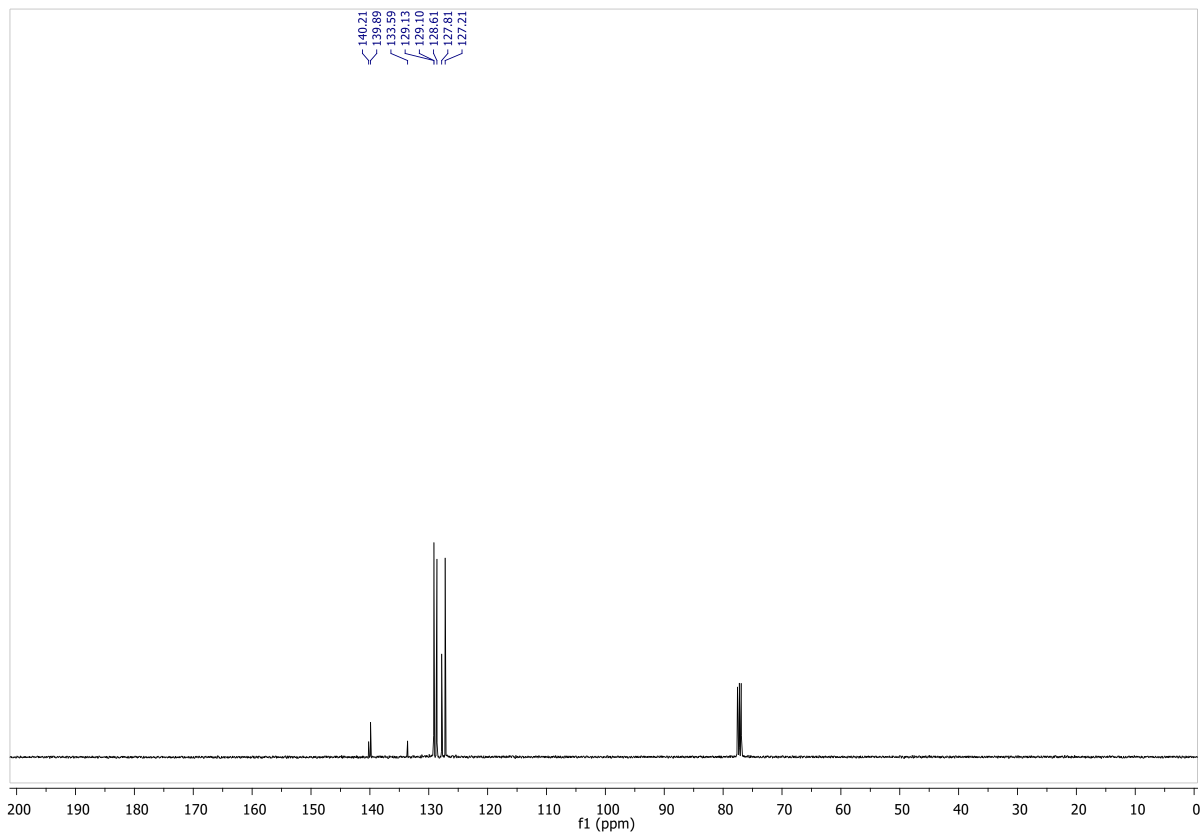
140.21
139.89
133.59
129.13
129.10
128.61
127.81
127.21
f1 (ppm)

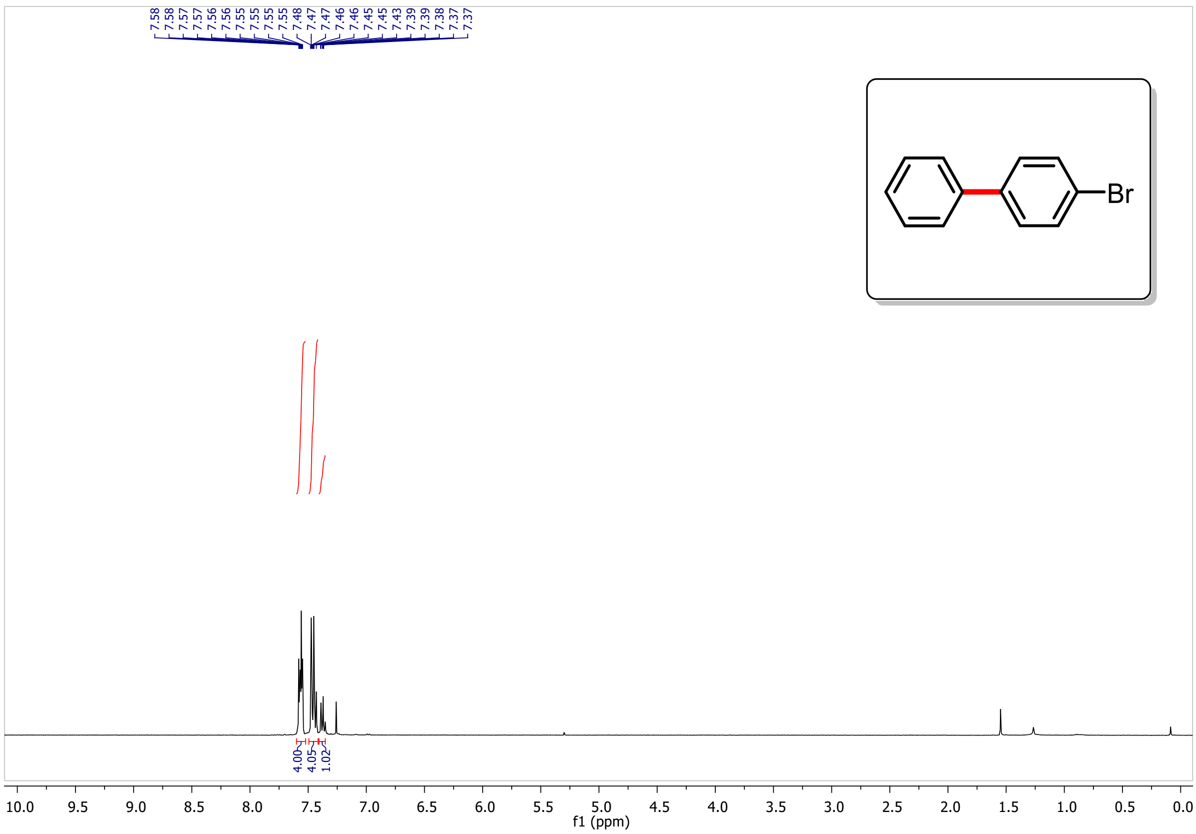

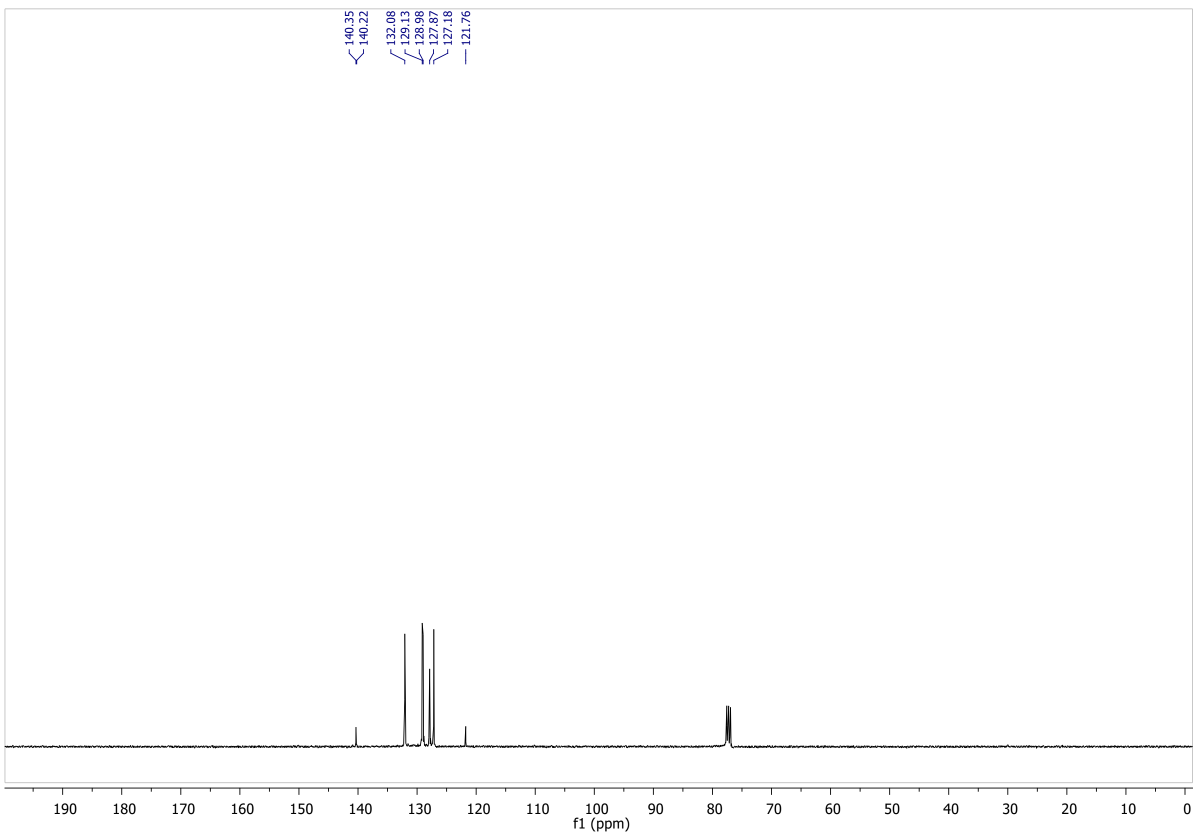

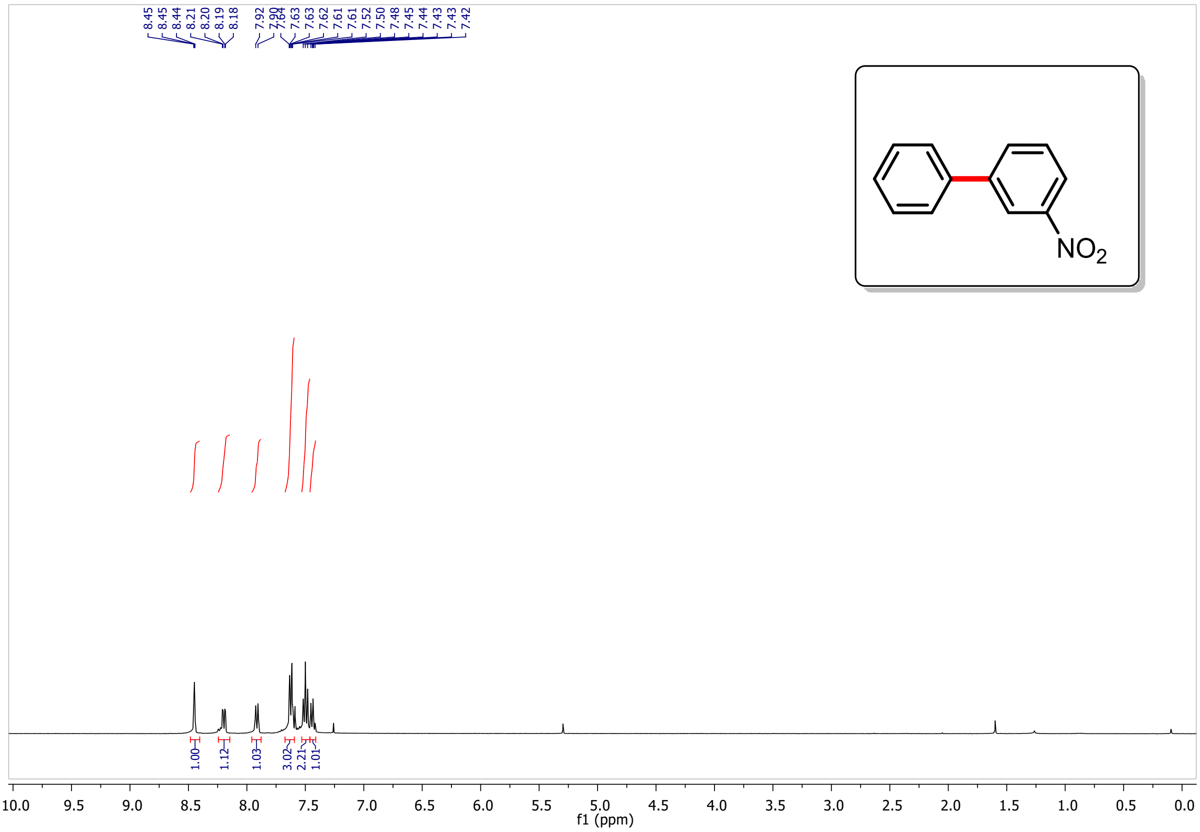
8.45
8.45
8.44
8.21
8.20
8.19
8.18
7.92
7.90
7.64
7.63
7.63
7.62
7.61
7.61
7.52
7.50
7.48
7.45
7.44
7.43
7.43
7.42
NO2
1.00
1.12
1.03
3.02
2.21
1.01
f1 (ppm)

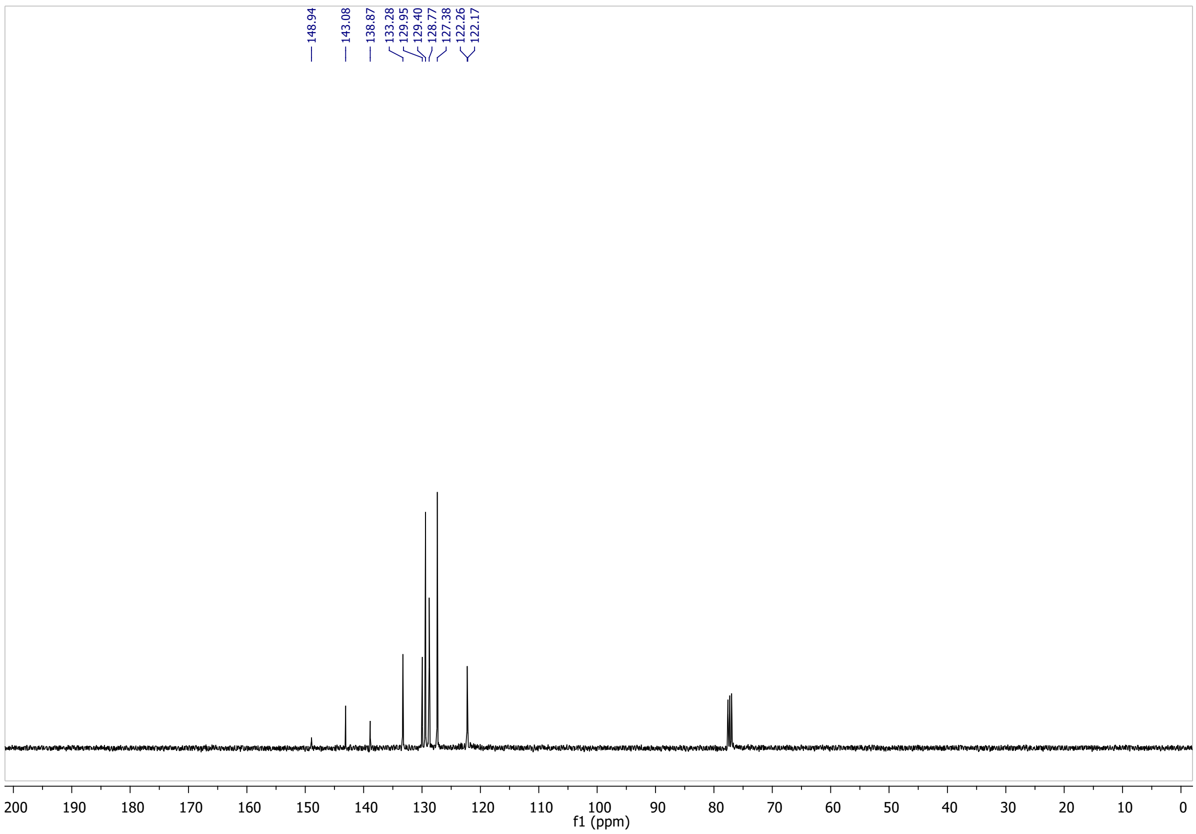
148.94
143.08
138.87
133.28
129.95
129.40
128.77
127.38
122.26
122.17
f1 (ppm)

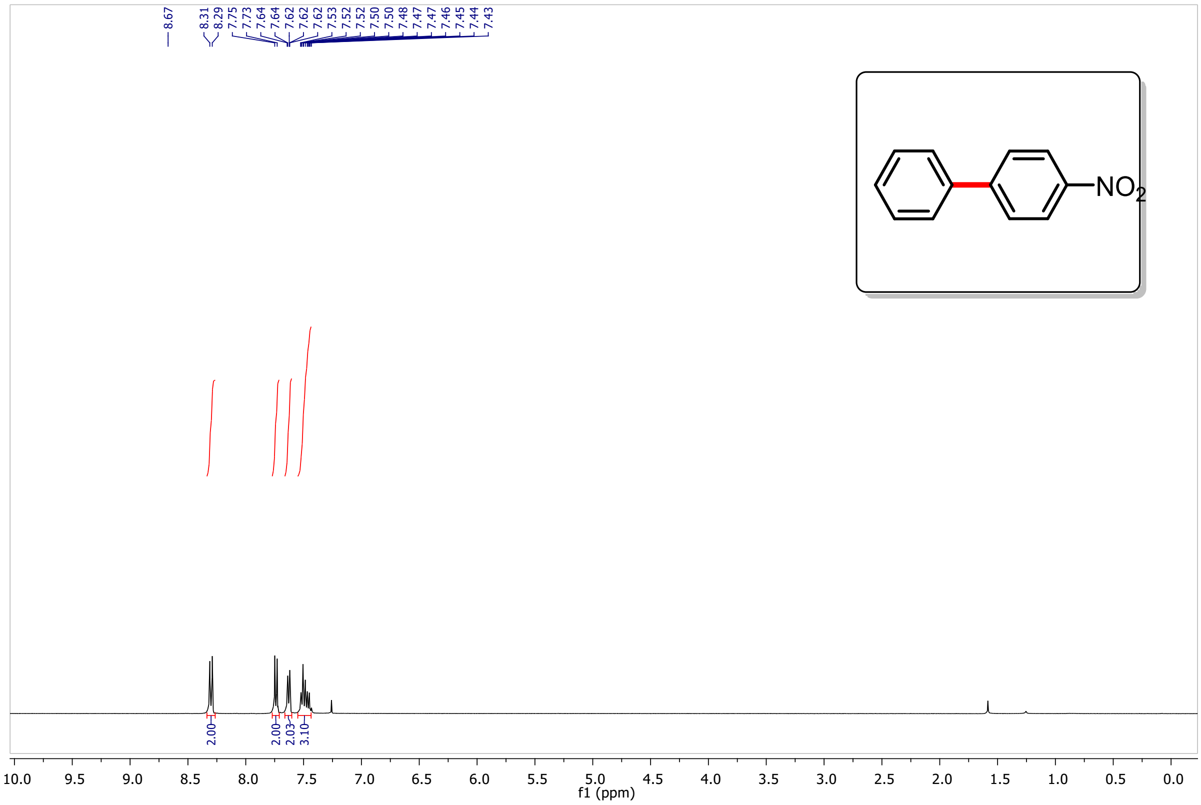
8.67
8.31
8.29
7.75
7.73
7.64
7.62
7.62
7.62
7.53
7.52
7.52
7.50
7.50
7.48
7.47
7.47
7.46
7.45
7.44
7.43
NO_2
2.00
2.00
2.03
3.10
10.0
9.5
9.0
8.5
8.0
7.5
7.0
6.5
6.0
5.5
5.0
4.5
4.0
3.5
3.0
2.5
2.0
1.5
1.0
0.5
0.0
f1 (ppm)

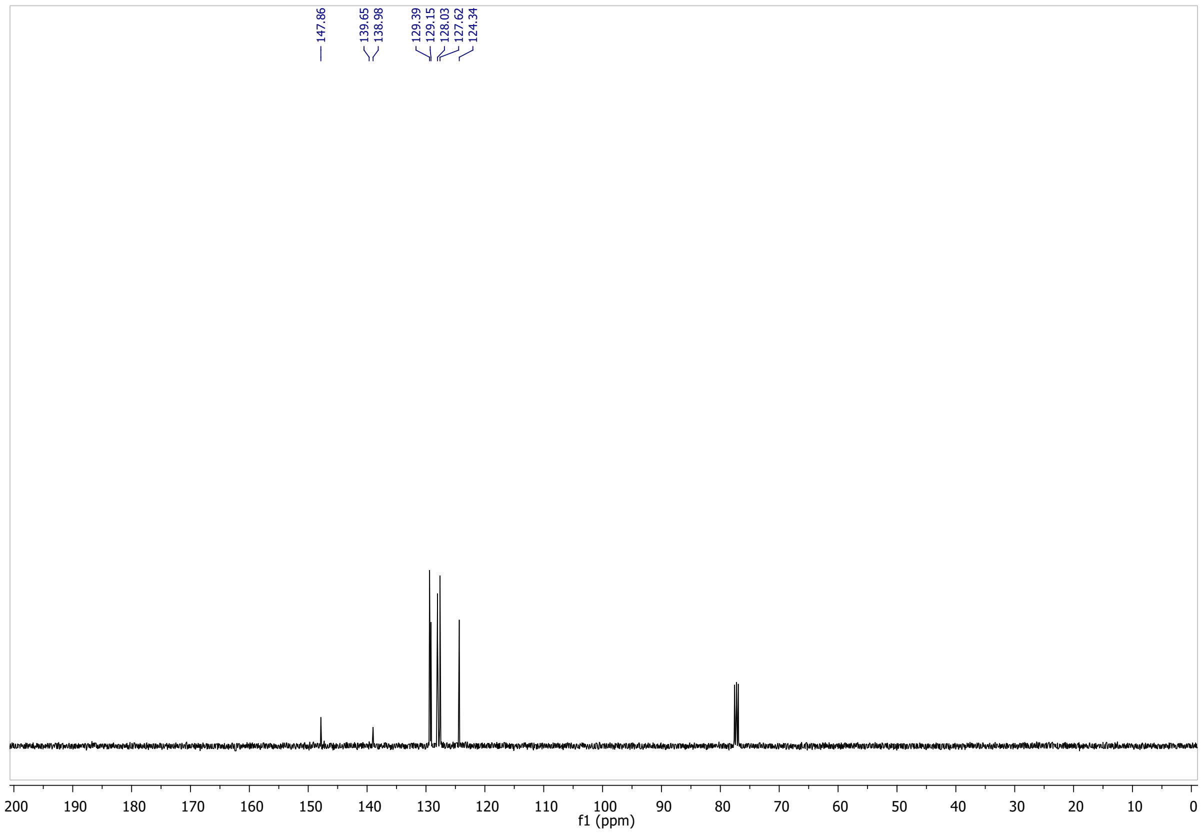
147.86
139.65
138.98
129.39
129.15
128.03
127.62
124.34
200
190
180
170
160
150
140
130
120
110
100
90
80
70
60
50
40
30
20
10
0
f1 (ppm)

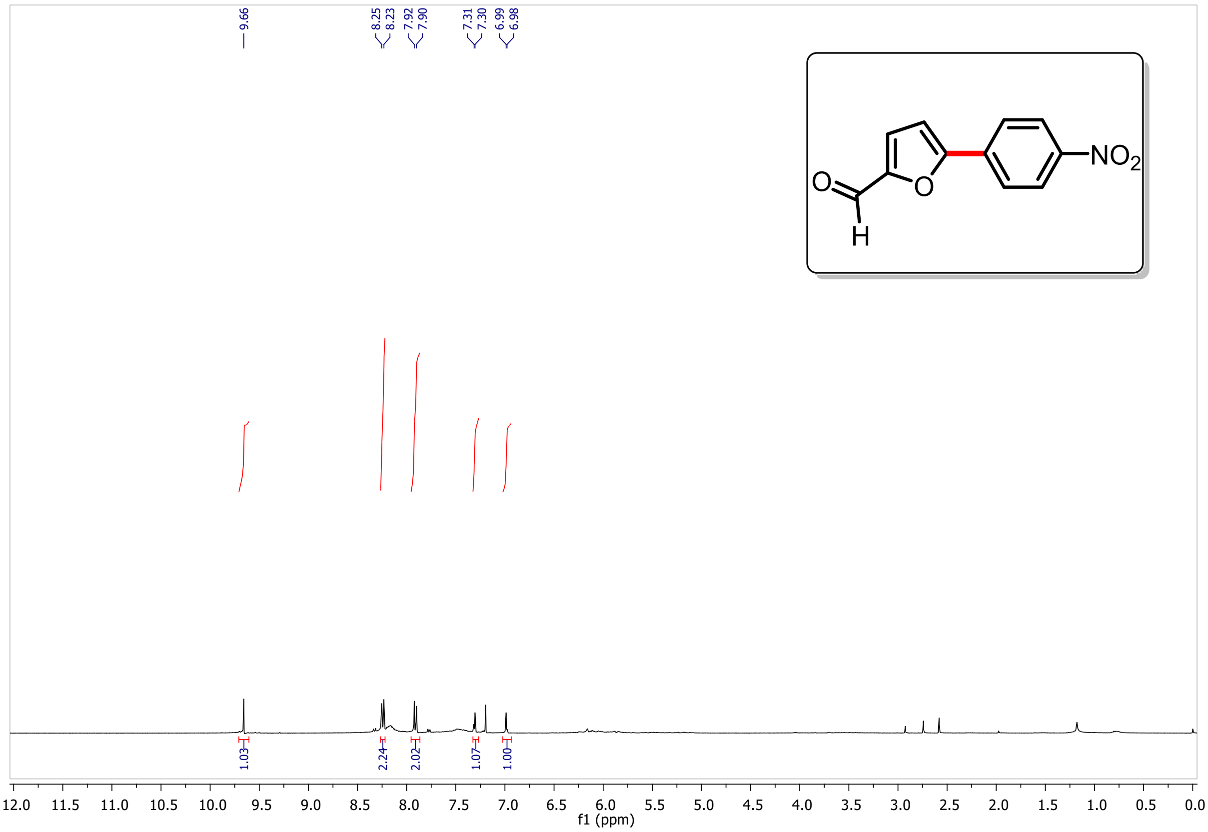
9.66
8.25
8.23
7.92
7.90
7.31
7.30
6.99
6.98
NO2
O
O
H
1.03
2.24
2.02
1.07
1.00
12.0 11.5 11.0 10.5 10.0 9.5 9.0 8.5 8.0 7.5 7.0 6.5 6.0 5.5 5.0 4.5 4.0 3.5 3.0 2.5 2.0 1.5 1.0 0.5 0.0
f1 (ppm)

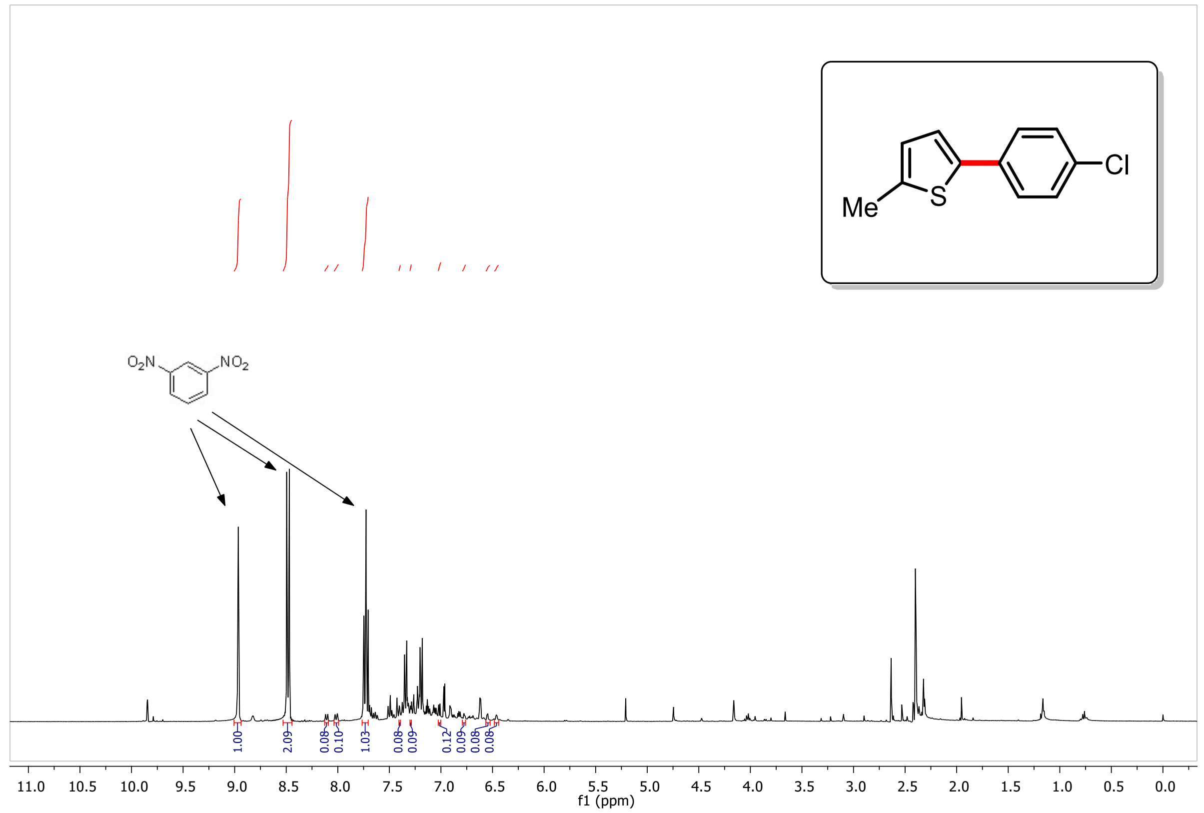
Cl
S
Me
O2N
NO2
1.00
2.09
0.08
0.10
1.03
0.08
0.09
0.12
0.09
0.08
0.08
11.0 10.5 10.0 9.5 9.0 8.5 8.0 7.5 7.0 6.5 6.0 5.5 5.0 4.5 4.0 3.5 3.0 2.5 2.0 1.5 1.0 0.5 0.0
f1 (ppm)

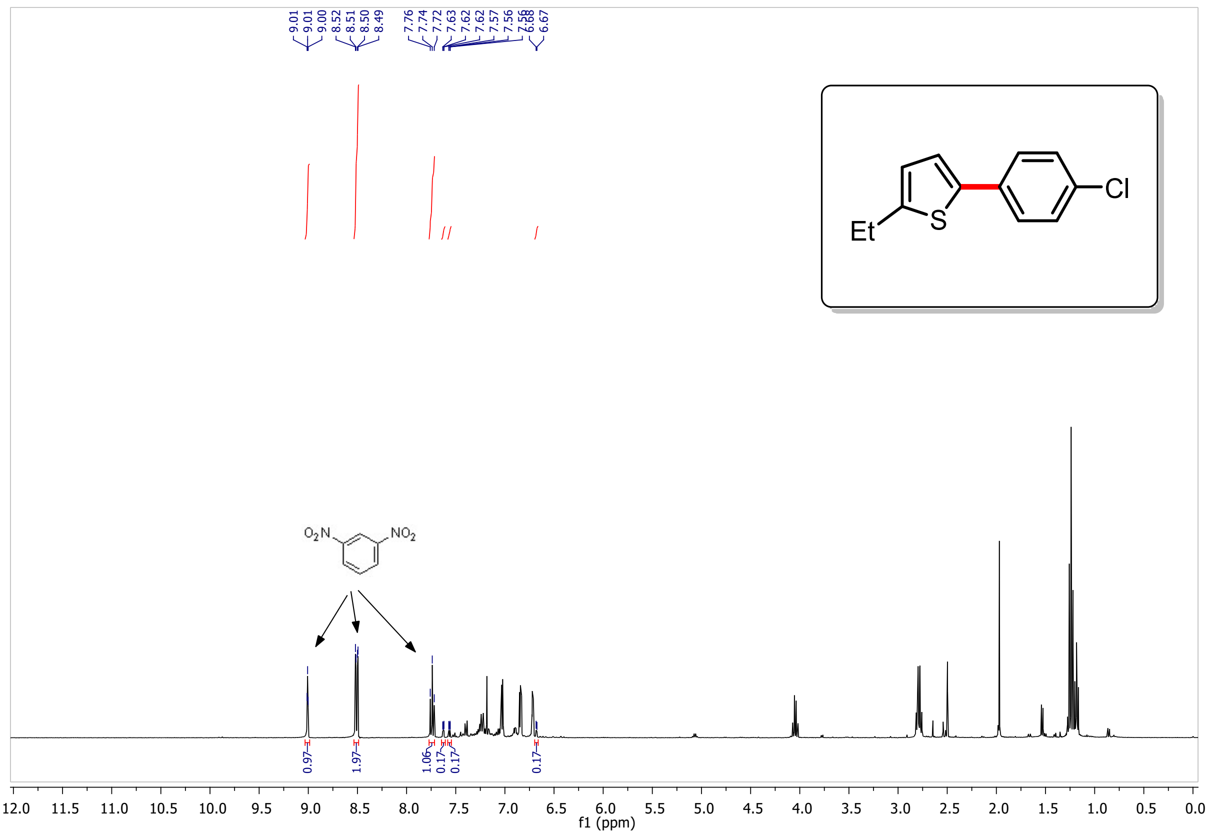

9.01
9.01
9.00
8.52
8.51
8.50
8.49
7.76
7.74
7.72
7.63
7.62
7.62
7.57
7.56
6.68
6.67
Et
S
Cl
O2N
NO2
0.97
1.97
1.06
0.17
0.17
0.17
12.0 11.5 11.0 10.5 10.0 9.5 9.0 8.5 8.0 7.5 7.0 6.5 6.0 5.5 5.0 4.5 4.0 3.5 3.0 2.5 2.0 1.5 1.0 0.5 0.0
f1 (ppm)

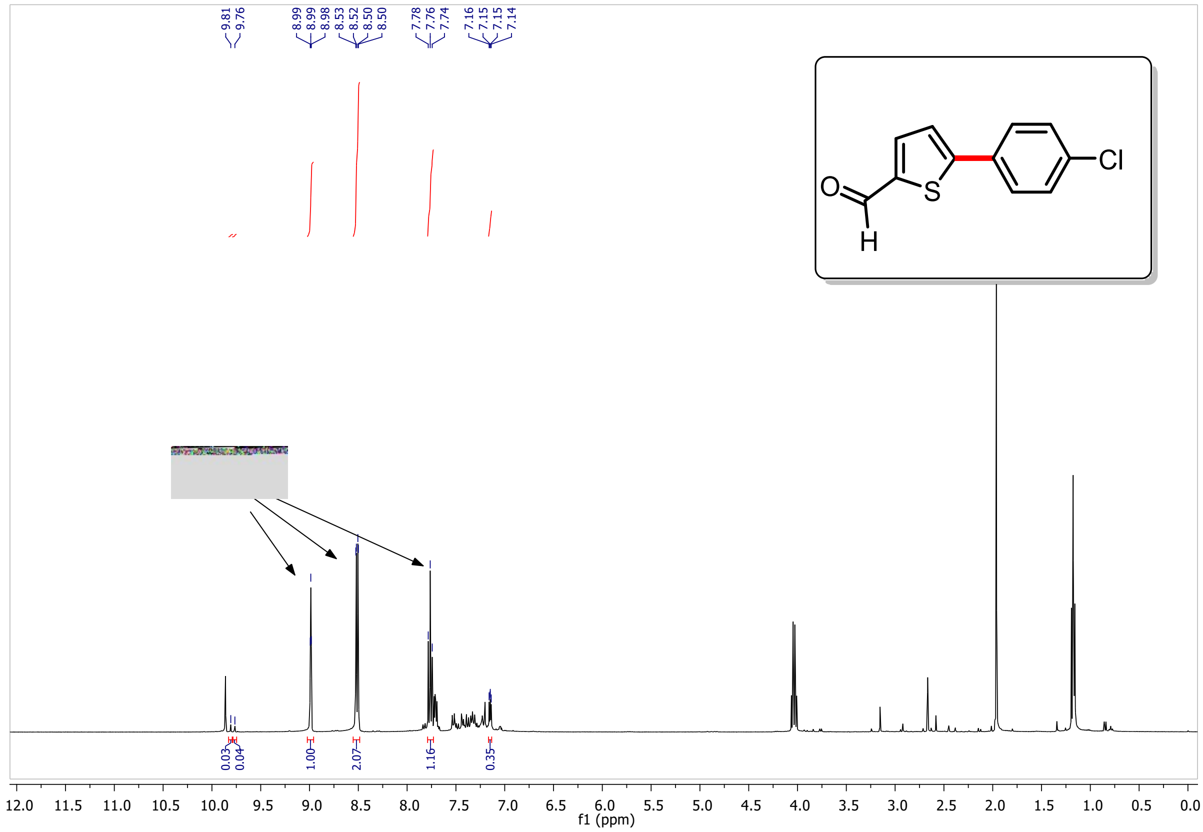

References

1. D. P. Hari, P. Schroll and B. König, Metal-free, visible-light-mediated direct C–H arylation of heteroarenes with aryl diazonium salts, *J. Am. Chem. Soc.*, 2012, **134**, 2958-2961.
2. O. Turbedaroglu, T. Kubanaliev, S. Alemdar, Z. Eroglu, H. Kilic and O. Metin, Reduced Graphene Oxide/Few-Layer Phosphorene Binary Heterojunctions as Metal-Free Photocatalysts for the Sustainable Photoredox C–H Arylation of Heteroarenes, *ACS Sustainable Chem. Eng.,* 2024, **12**, 3659-3670.
3. X. Cai, H. Liu, L. Zhi, H. Wen, A. Yu, L. Li, F. Chen and B. Wang, A g-C_3N_4/rGO nanocomposite as a highly efficient metal-free photocatalyst for direct C–H arylation under visible light irradiation, *RSC Adv.*, 2017, **7**, 46132-46138.
4. J. Haner, K. Jack, M. L. Menard, J. Howell, J. Nagireddy, M. A. Raheem and W. Tam, Synthesis of C1-Substituted Oxabenzonorbornadienes, *Synthesis*, 2012, **44**, 2713-2722.
5. S. Zhang, Z. Tang, W. Bao, J. Li, B. Guo, S. Huang, Y. Zhang and Y. Rao, Perylenequinonoid-catalyzed photoredox activation for the direct arylation of (het)arenes with sunlight, *Org. Biomol. Chem.*, 2019, **17**, 4364-4369.
6. E. T. Nadres, A. Lazareva and O. Daugulis, Palladium-catalyzed indole, pyrrole, and furan arylation by aryl chlorides, *J. Org. Chem.*, 2011, **76**, 471-483.
7. D. C. Fabry, Y. A. Ho, R. Zapf, W. Tremel, M. Panthöfer, M. Rueping and T. H. Rehm, Blue light mediated C–H arylation of heteroarenes using TiO_2 as an immobilized photocatalyst in a continuous-flow microreactor, *Green Chem.*, 2017, **19**, 1911-1918.

8. I. Karakaya, Amphiphilic Polypyridyl Ruthenium Catalyzed, Photoredox-Mediated C−H Arylation of Heteroarenes with Aryl Diazonium Salts, *ChemistrySelect*, 2021, **6**, 11551-11556.
9. E. B. Pinxterhuis, M. Giannerini, V. Hornillos and B. L. Feringa, Fast, greener and scalable direct coupling of organolithium compounds with no additional solvents, *Nat. Commun.*, 2016, **7**, 11698.
10. A. Xia, X. Qi, X. Mao, X. Wu, X. Yang, R. Zhang, Z. Xiang, Z. Lian, Y. Chen and S. Yang, Metal-free aerobic oxidative selective C–C bond cleavage in heteroaryl-containing primary and secondary alcohols, *Org. Lett.*, 2019, **21**, 3028-3033.
11. A. Lerchen, T. Knecht, M. Koy, J. B. Ernst, K. Bergander, C. G. Daniliuc and F. Glorius, Non-Directed Cross-Dehydrogenative (Hetero)arylation of Allylic $C(sp^3)$−H bonds enabled by C−H Activation, *Angew. Chem., Int. Ed.*, 2018, **57**, 15248–15252.
12. N. Frank, M. Leutzsch and B. List, Bronsted Acid-Catalyzed Reduction of Furans, *J. Am. Chem. Soc.,* 2025, **147**, 7932-7938.
13. Y. Liang, R. Steinbock, L. Yang and L. Ackermann, Continuous Visible-Light Photoflow Approach for a Manganese-Catalyzed (Het) Arene C− H Arylation, *Angew. Chem.*, 2018, **130**, 10785–10789.
14. M. Kumar, S. Sharma, P. Sil, M. Kushwaha, S. Mayor, R. A. Vishwakarma and P. P. Singh, C–H Arylation of N-Heteroarenes under Metal-Free Conditions and its Application towards the Synthesis of Pentabromo- and Pentachloropseudilins, *Eur. J. Org. Chem.*, 2019, **2019**, 3591–3598.
15. Z. Li, L. Chen, D. Rong, L. Yuan and Y. Xie, Photochemical acridone-mediated direct arylation of (hetero) arenes with aryl diazonium salts, *Org. Biomol. Chem.,* 2023, **21**, 8739–8743.
16 A. Basak, M. S. Ozer, Z. Eroglu, K. Sun and O. Metin, Bridging Gaps in the Synthesis of g-CN/WO_3–x for Photocatalytic H_2O_2 Generation: Insights into S-Scheme Heterojunction and Plasmon-Induced Hot Electrons, *Langmuir*, 2025, **41**, 13381–13394.
17. P. Du, J. Schneider, G. Luo, W. W. Brennessel and R. Eisenberg, Visible light-driven hydrogen production from aqueous protons catalyzed by molecular cobaloxime catalysts, *Inorg. Chem.,* 2009, **48**, 4952–4962.
18. J. Bisquert and V. S. Vikhrenko, Interpretation of the Time Constants Measured by Kinetic Techniques in Nanostructured Semiconductor Electrodes and Dye-Sensitized Solar Cells, *J. Phys. Chem. B.*, 2004, **108**, 2313–2322.
19. A. Lerchen, T. Knecht, M. Koy, J. B. Ernst, K. Bergander, C. G. Daniliuc and F. Glorius, Non-Directed Cross-Dehydrogenative (Hetero)arylation of Allylic C(sp3)−H bonds enabled by C−H Activation, *Angew. Chem. Int. Ed.*, 2018, **57**, 15248–15252.
20. L. Chen, Y. Du, X.-P. Zeng, T.-D. Shi, F. Zhou and J. Zhou, Successively Recycle Waste as Catalyst: A One-Pot Wittig/1,4-Reduction/Paal–Knorr Sequence for Modular Synthesis of Substituted Furans, *Organic Letters*, 2015, **17**, 1557–1560.
21. B.-T. Luo, H. Liu, Z.-J. Lin, J. Jiang, D.-S. Shen, R.-Z. Liu, Z. Ke and F.-S. Liu, Aerobic and Efficient Direct Arylation of Five-Membered Heteroarenes and their Benzocondensed Derivatives with Aryl Bromides by Bulky α-Hydroxyimine Palladium Complexes, *Organometallics*, 2015, **34**, 4881–4894.
22. D.-Z. Zheng, D.-H. Li, H. Liu, Y. Shao, Z. Ke and F.-S. Liu, Bis(imino)acenaphthene (BIAN)-Supported N-Heterocyclic Carbene Palladium Complexes with Ancillary Ligands: Readily Activated Precatalysts for Direct C–H Arylation of Thiophenes, *Organometallics,* 2022, **41**, 948–961.

23. M. Bu, G. Lu, J. Jiang and C. Cai, Merging visible-light photoredox and micellar catalysis: arylation reactions with anilines nitrosated in situ, *Catalysis Sci. Technol*, 2018, **8**, 3728–3732.
24. L. Wang, J. Shen, S. Yang, W. Liu, Q. Chen and M. He, C–H arylation reactions through aniline activation catalysed by a PANI-gC_3N_4-TiO_2 composite under visible light in aqueous medium, *Green Chemistry*, 2018, **20**, 1290–1296.
25. L. Buglioni, P. Riente, E. Palomares and M. A. Pericàs, Visible-light-promoted arylation reactions photocatalyzed by bismuth (III) oxide, *Eur. J. Org. Chem.*, 2017, **2017**, 6986–6990.
26. S. Zhang, Z. Tang, W. Bao, J. Li, B. Guo, S. Huang, Y. Zhang and Y. Rao, Perylenequinonoid-catalyzed photoredox activation for the direct arylation of (het) arenes with sunlight *Org. Biomol. Chem.*, 2019, **17**, 4364–4369.
27. Z. Huang, J. Zhu, Q. Dong, Q. Huang, M. Wang, Y. Zhu, W. Huang and Y. Zi, Photoredox CH arylation of heteroarenes by high-efficiency bismuth quantum dots, *Tetrahedron Lett*, 2023, **127**, 154667.
28. S. Rossi, F. Herbrik, S. Resta and A. Puglisi, Supported Eosin Y as a photocatalyst for CH arylation of furan in batch and flow, *Molecules*, 2022, **27**, 5096.
29. Y. Liang, R. Steinbock, L. Yang and L. Ackermann, Continuous Visible-Light Photoflow Approach for a Manganese-Catalyzed (Het) Arene C− H Arylation, *Angew. Chem. Int. Ed.*, 2018, **130**, 10785–10789.
30. R. Rajmohan, P. Nisha and P. Vairaprakash, 5-Hydroxymethylfurfural-Derived Boron-Dipyrromethene Immobilized on Resin Support as a Sustainable Catalyst for C–H Arylation of Heterocycles, *ACS Omega*, 2019, **4**, 14458–14465.
31. D. P. Hari, P. Schroll and B. König, Metal-free, visible-light-mediated direct C–H arylation of heteroarenes with aryl diazonium salts, *J. Am. Chem. Soc.,* 2012, **134**, 2958–2961.
32. T. A. Demircioglu, Z. Eroglu, M. S. Ozer, B. Sundu, Z. Canbulat and O. Metin, Mesoporous Black Arsenic: Wet-Chemical Synthesis and Its Photo-Enhanced Activity in the C–H Arylation of Heteroarenes under Red Light Illumination, *ACS Appl. Mater. Interfaces*, 2026, **18**, 6712–6722.
33. Y.-S. Feng, X.-S. Bu, B. Huang, C. Rong, J.-J. Dai, J. Xu and H.-J. Xu, NADH coenzyme model compound as photocatalyst for the direct arylation of (hetero) arenes, *Tetrahedron Lett.*, 2017, **58**, 1939–1942.
34. L. Zhi, H. Zhang, Z. Yang, W. Liu and B. Wang, Interface coassembly of mesoporous MoS2 based-frameworks for enhanced near-infrared light driven photocatalysis, *Chem. Commun*., 2016, **52**, 6431–6434.
35. K. Paramanik, N. Bandopadhyay, S. K. Agrawalla, C. S. Purohit, B. Biswas and H. S. Das, Highly efficient phenalenyl–copper bifunctional photoredox catalyst for direct C–H bond arylation of arenes and heteroarenes, *Catal. Sci. Technol.*, 2025, **15**, 3325–3331.
36. Q.-H. Liu, S.-L. Kang, Z.-S. Cui, Y.-H. Liu, M. Zhang and Z.-H. Zhang, Visible light-driven C–H arylation of heteroarenes with aryl diazonium salts in water catalyzed by a Z-scheme CuInS2/KC_3N_4 heterojunction, *Green Chem.*, 2024, **26**, 4803–4810.